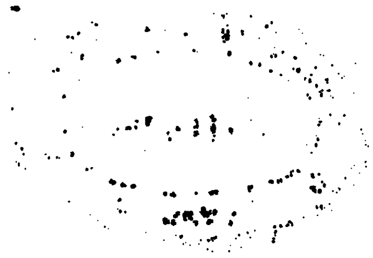


THEORY, DESIGN, CONSTRUCTION AND TESTING

OF

A FRACTIONAL-HORSEPOWER, SINGLE-PHASE, CAPACITOR-START

INDUCTION MOTOR.

BY

A. SHANMUGASUNDARAM.

SUBMITTED IN PARTIAL FULFILMENT OF THE REQUIREMENTS

FOR

M.Sc., DEGREE IN ELECTRICAL MACHINE DESIGN

OF THE

UNIVERSITY OF MADRAS.

DEPARTMENT OF ELECTRICAL MACHINE DESIGN

COLLEGE OF ENGINEERING

GUINDY, MADRAS-25.

1957-'58.

***

ACKNOWLEDGMENT.

The author wishes to acknowledge with deep gratitude and sincere thanks the valuable guidance and constructive criticism of Prof. A. Srinivasan, B.E., M.Sc., M.S.E.E., (Illinois), Mem.A.I.E.E., Mem.C.I.G.R.E, M.I.E.(Ind.). The help given by Mr. K.M.A. Mohamed Sulaiman, B.E., M.E.E., A.M.A.I.E.E., and Mr. P.C.Chandrasekaran, B.E., had been of immense benefit during the preparation of this paper.

Thanks are also due to the Staff of the Electrical Engineering Laboratory and the attached Workshop for the incalculable help rendered by them in constructing the meter and testing it.

S C O P E.

This paper deals with the theory, design, construction and testing of a 3/8 horsepower, single-phase, capacitor-start induction motor. The project has been undertaken in partial fulfilment of the requirements for the Degree of Master of Science in Electrical Machine Design of the University of Madras. The size of the Machine and construction are controlled by the availability of material and limited workshop facilities, and so they are not of the commercial standard.

The performance characteristics of the machine are predetermined from the design data and compared with those obtained from actual tests. The discrepancy between the predetermined and the actual characteristics is attempted to be explained.

The project serves to develop a better and fuller appreciation of the influence of the various factors which determine the design constants and the machine performance, and thus helps the student to gain greater confidence in the design and construction of single-phase, capacitor-start induction motors.

S U M M A R Y.

As contrasted with its three phase counterpart, a good many varieties of single-phase induction motors are available. This necessitates a short review of the various types of single-phase induction motors. While the single-phase induction motor is simpler in construction than the three phase one, its theoretical analysis is comparatively complicated. The different theories explaining the operation of single-phase induction motors have been presented in the second chapter. The single-phase induction motor by its very nature poses certain special problems which are also dealt with briefly. The windings usually employed for single-phase induction motors, are markedly different from those usually employed for other rotating electrical machinery. The usual windings of single-phase induction motors are explained in the fourth chapter. The actual design of the machine with the features taken into account explained then and there, the predetermination of the characteristics of the machine, the tests conducted on the machine and their results follow.

C O N T E N T S.

LIST OF SYMBOLS.

A

A	number of parallel paths.
A_{er}	Current density in the end-ring.
A_r	Current density in the rotor copper.
A_s	Current density in stator copper.
A_{sm}	Current density in stator main winding.
A_1	amplitude of the fundamental wave.
a	$\frac{\text{effective starting winding turns}}{\text{effective main winding turns}}$
a_r	amplitude of the r^{th} harmonic of the mmf. wave.

B

B_g	flux density in the air gap.
B_{tr}	flux density in rotor teeth (parallel teeth).
B_{ts}	flux density in stator teeth (parallel teeth).

B_{ts_1} Flux density in stator teeth at air-gap surface.

B_{yr} flux density in rotor yoke.

B_{ys} flux density in stator yoke.

B_{δ} flux density at any point in the air gap and at any pointstant.

C

C output constant.

C_w winding constant.

C_{wa} Winding constant, auxiliary winding.

C_{wm} Winding constant, main winding.

D

D inside diameter of stator.

d_s slot depth.

d_{yr} double radial depth of rotor yoke.

d_{ys} double radial depth of stator yoke.

E

E Total counter emf. in the main winding due to the backward and forward field components.

E_{av} average value of voltage induced.

E_{eff} effective value of voltage induced.

E_{fo} Voltage impressed on the forward field at no load.

E_m counter emf. in the main winding.

E_s counter emf. in the starting winding.

E_t terminal voltage.

e_B rotor voltage due to the backward field component cutting rotor conductors.

e_F rotor voltage due to the forward field component cutting rotor conductors.

e_b e_B reflected on the stator main winding.

e_f e_F reflected on to stator main winding.

F

F_s saturation factor.

F_{sr} rotor slot leakage factor.

F_{ss} stator slot leakage factor.

f frequency, cycles per second.

f_d field form distribution factor.

G

G_{ct} weight of core in teeth.

G_{cy} weight of core in yoke.

I

I effective value of current.

I_b effective value of current in rotor bars.

I_m current in the main winding.

I_{max} maximum value of current in rotor bars.

I_o no-load current.

I_s current in the starting winding.

I_s' capacitor winding current in main winding terms with 90° backward phase shift.

$= - j\, a\, I_s$.

I_{sa} locked-rotor current in the auxiliary winding.

I_{sm} locked-rotor current in the main winding.

I_{st} locked-rotor current with both the windings in parallel.

I_x rotor current in the start axis referred to and reflected on to the starting winding.

$I_x{}^*$ rotor current in the cross axis referred to the main winding but not reflected on to it.

I_y $I_y{}^*$ reflected on to the main winding

$= - I_y{}^*$.

$I_y{}^*$ rotor current in the main axis referred to main winding.

I_ϕ Magnetising current (of the main winding).

I_{2b} backward rotor current.

I_{2f} forward rotor current.

$I_2{}'b$ I_{2b} referred to and reflected on to the main winding.

$I_2{}'f$ I_{2f} referred to and reflected on to the main winding.

Length of rotor [illegible]

K

K	any integer.
K_d	winding distribution factor.
K_f	form factor.
K_p	pitch factor.
K_p	} leakage flux factors.
K_r	}
K_p	$\sqrt{K_r}$
K_r	$\frac{X_o - X_{lm}}{X_o}$
k	air-gap coefficient.

L

L_{ya}	Length of half mean-turn, auxiliary winding.
L_{sm}	Length of half mean-turn, main winding.
l	length of stator core.
l_b	length of rotor bar.

M

M	order of stator tooth harmonics .
M_1	mmf. to produce flux ϕ_1
M_2	mmf. to produce flux ϕ_2
M_r	mmf. to produce flux ϕ_r.
m	number of phases.
m_s	number of phases in stator winding.

N

N	order of stator tooth harmonics.
N	number of conductors in series per phase.
N	actual.rpm.
N_a	number of conductors in series, auxiliary winding.
N_b	Number of rotor bars.
N_c	conductors per slot or number of turns per coil.
N_m	number of conductors in series, main winding.
N_s	synchronous rpm.

n   number of teeth per pole.

P

P   number of poles.

Q

Q   ampere conductors per inch of stator gap circumference.

R

R   order of rotor teeth harmonies.

R   virtual load resistance.

$$= \frac{s r_2}{1 - s^2} .$$

R_a total auxiliary winding resistance.

$$= r_{1a} + a^2 r_2 .$$

R_b apparent resistance of the 'backward revolving rotor'

R_c capacitor resistance.

R_f apparent resistance of the 'forward revolving rotor'

R_M — real component of total impedance of main phase at stand still.

R_m — total main winding resistance,

$= r_{1m} + r_2$.

R_s — real component of total impedance of start phase at stand still.

R_T — resistance at temperature T deg. Centigrade.

R_2 — resistance of rotor.

r — 0.692 for 25° C .

r_a — resistance of the auxiliary winding including the capacitor.

r_c — core loss resistance in parallel with x'_m .

r'_m — core loss resistance in series with x'_m .

r_t — resistance at temperature t° C .

r_1' — $(r_{1m} / 2)$.

r_{1m} — resistance of the stator main winding.

r_2 — resistance of the rotor referred to the stator main winding.

r_2' — $(r_2 / 2)$.

S

S per unit synchronous speed

$$= \frac{\text{actual speed}}{\text{synchronous speed}}.$$

S_b section area of each rotor bar.

S_{cr} total rotor copper section area.

S_{cs} total stator copper section area.

S_r number of rotor slots.

S_s number of stator slots.

S_{tr} total rotor teeth section area.

S_{ts} total stator teeth section area.

s slip.

s_b slip with respect to the backward revolving field.

s_f slip with respect to the forward revolving field.

s_0 no-load slip.

s_m section area of main winding conductor.

T

T	torque.
T	order of rotor tooth harmonics.
T	periodic time in seconds.
T	temperature - degrees centigrade.
T_{bb}	torque due to the inter-action of backward revolving flux and I_{2b}' .
T_{bf}	torque due to the inter-action of backward revolving flux and I_{2f}' .
T_{fb}	torque due to the interaction of forward revolving flux and I_{2b}' .
T_{ff}	torque due to the interaction of forward revolving flux and I_{2f}' .
T_{ph}	tuns per phase.
T_1	torque due to the interaction of I_y and ϕ_c .
T_2	torque due to the interaction of I_2' and $(\phi_g - \phi_2)$
T_{2w}	double frequency pulsating torque.
t	~~time in seconds.~~ [illegible]

t	temperature - degrees centigrade.
t_p	turns per pole.
t_{1r}	rotor tooth pitch at air-gap surface.
t_{1s}	stator tooth pitch at air-gap surface.

V

V	terminal or applied voltage.
v	peripherial velocity, feet per minute.

W

W_c	core loss.
W_{ct}	core loss in teeth due to fundamental frequency flux.
W_{cy}	core loss in yoke due to fundamental frequency flux.
W_{fw}	bearing friction and windage losses.
W_{1b}	fundamental backward field component of stator wave.
W_{1f}	fundamental forward field component of stator wave.

W_{2b}	fundamental backward field component of rotor wave.
W_{2f}	fundamental forward field component of rotor wave.
w_{tr}	width of rotor tooth.
w_{tr_1}	width of rotor tooth at air-gap surface.
w_{ts}	width of stator tooth.
w_{ts_1}	width of stator tooth at air-gap surface.

X

X	ideal short circuit reactance of motor $\simeq X_{dm}$
X_B	rotor reactance at frequency (2-s) f
	$= (2 - s) X_2$.
X_b	apparent reactance of the 'backward revolving rotor'
X_c	reactance of the capacitor.
X_F	rotor reactance at frequency sf . $= s X_2$
X_f	apparent reactance of the 'forward revolving rotor'
X_{1a}	total leakage reactance, auxiliary winding.
X_{1m}	total leakage reactance, main winding.

X_M j component of the total impedance of the main phase at standstill.

X_o Open circuit reactance of motor.

X_s j component of the total impedance of the start phase at standstill.

X_2 leakage reactance of rotor (at frequency f).

X distance.

x distance on stator periphery.

x_e end-connection leakage reactance.

x_m magnetising reactance of the main axis.

x_m' magnetising reactance of either of the forward and backward revolving fields.

$= x_m / 2$.

x_s slot leakage reactance.

x_{sk} skew leakage reactance.

x_z zigzag leakage reactance.

x_{lm} leakage reactance of the main winding.

x_{ls} leakage reactance of the start winding.

x_1' half of the leakage reactance of the main winding.

$= \frac{x_{1m}}{2}$

x_2 distance on rotor periphery.

x_2 leakage reactance of the rotor referred to the stator main winding.

x_2' half of x_2

Y

y_b admittance of the 'backward revolving rotor'.

$= \frac{1}{Z_b}$

y_f admittance of the 'forward revolving rotor'

$= \frac{1}{Z_f}$

y_m admittance of the magnetising circuit, main axis.

y_s admittance of the magnetising circuit, start axis.

Z

Z_{ac} total impedance of the auxiliary winding with capacitor at standstill.

Z_B rotor impedance at frequency (2-s)f

$R_2 + j\ (2 - s)\ X_2$

Z_b apparent impedance of the 'backward revolving rotor'

Z_c impedance of the capacitor.

× Z_F rotor impedance at frequency sf.

× Z_f apparent impedance of the 'forward revolving rotor'

Z_{1m} total main winding locked-rotor impedance

$\sqrt{R_m^2 + x_{1m}^2}$

× Z_M TOTAL impedance of the main phase at standstill

$R_M + j\ X_M$

× Z_m magnetising impedance of the main axis.

× Z_s magnetising impedance of the start axis.

× Z_{ac} total impedance of the auxiliary winding with capacitor at standstill.

Z_{1m} impedance of the main winding $r_{1m} + j\ x_{1m}$.

Z_{1s}	impedance of the starting winding.
Z_2	impedance of the rotor referred to main wdg.
	$= r_2 + j\,x_2$
Z_2'	$= \dfrac{r_2}{1 + s} + j\,x_2$
	$\simeq 0.55\, r_2 + j\,x_2$

GREEK LETTERS.

α	initial angle of coil when ϕ_M is zero.
δ	length of air gap.
θ	angular position of coil of Fig. (2.3.1) at any instant.
	$= S\,wt + \alpha$
θ	time phase difference between ϕ_1 and ϕ_2
θ_{sk}	rotor skew angle - radians
λ	angle which ϕ_P makes with the horizontal.
ν	order of the stator space harmonics.
τ	pole pitch

Φ_M	maximum value of flux in the main axis.
Φ_1	maximum value of ϕ_1
Φ_2	maximum value of ϕ_2
ϕ	power factor angle.
ϕ	angle between I_s and I_m .
ϕ	flux per pole.
ϕ_B	backward rotating flux component.
ϕ_c	cross-axis flux.
ϕ_{c1}	flux through the coil of Fig. (2.3.1)
ϕ_F	forward rotating flux component.
ϕ_M	flux in the main axis.
	$= \Phi_M \sin wt$
ϕ_m	power factor angle of I_m
ϕ_r	resultant field of ϕ_1 and ϕ_2
ϕ_t	hypothetical total flux.
ϕ_1	primary leakage flux.

ϕ_2	secondary leakage flux.
ϕ_1 and ϕ_2	an arbitrary system of two fluxes with time displacement and space displacement.
ψ	space displacement between ϕ_1 and ϕ_2
ω	electrical angular velocity at synchronous speed.
ω_o	electrical angular velocity at any speed S.

C H A P T E R - I.

INTRODUCTION.

In 1888 Nikola Tesla demonstrated the production of rotating field by two alternating fields displaced both in space and time, and the induction motor action of a rotating field on a squirrel cage rotor (88.01). But the field produced by a single-phase winding alone would be an alternating or pulsating field and not a rotating field. Hence the single-phase motor with only one winding, cannot produce a starting torque by induction. Supposing that the rotor begins to rotate in a particular direction, then it can develop torque in that direction and continue to rotate, the reason being the fact, as Steinmetz puts it (97.01) that "In a single-phase motor the one of the two superimposed magnetic quadrature fields is excited by the primary electric circuit, the other by the induced secondary (or armature) currents carried into quadrature position by the rotation of the secondary". So then it now remains to start the motor which would continue to rotate afterwards. A number of methods are available for starting single-phase induction motors on which basis they are classified. A brief [illegible] (2.1).

survey of the different types of single-phase induction motors is made in the following paragraphs. **

1.01. Split-phase Induction Motors:

The split-phase motor is one of the oldest types of single-phase motors ever built for commercial use. Even to-day, it is one of the most important and most widely used of all types of single-phase motors. It is used for such applications as washing machines, oil burners, blowers, centrifugal pumps, wood-working tools, business machines, grinders and a host of other applications. It is most widely used in the ratings from 1/20 to 1/3 h.p.

The American Standards Association formally defines a split-phase motor as follows:

"A split-phase motor is a single-phase induction motor equipped with an auxiliary winding, displaced in magnetic position from, and connected in parallel with, the main winding.

Note: Unless otherwise specified, the auxiliary circuit is assumed to be opened when the motor has attained

---

** Most of the material in this Chapter from hereon is taken from (R.1).

a predetermined speed. The term split-phase motor, used without qualification, describes a motor to be used without impedance, other than that offered by the motor windings themselves, other types being separately defined.*

The essential components are shown in Fig.(1.1). Ordinarily the two windings are spaced 90 electrical degrees apart; i.e., the centre of each pole group of the auxiliary

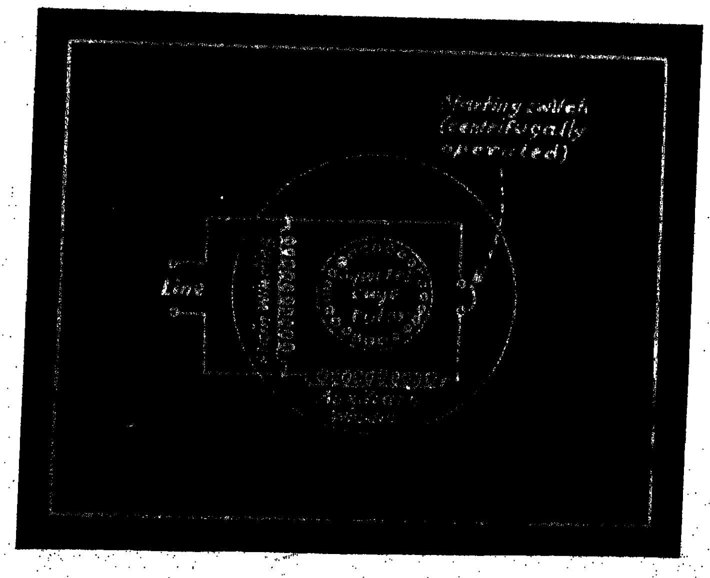


Figure (1.1).

winding is spaced half-way between the centres of two pole groups of the main winding. The rotor is usually of the squirrel-cage construction. While starting, both the main

and the auxiliary windings are in parallel across the lines. At approximately 75 to 80 percent of synchronous speed the centrifugal switch in series with the auxiliary winding opens out the auxiliary winding circuit.

Sometimes resistance or reactance other than those inherently present in the winding is used to 'split' the phase in which case the motor is known as a resistance-start or reactor-start split-phase motor. While starting, if resistance is used it is usually connected in series with the auxiliary winding and if a reactor is used, with the main winding.

1.02 Capacitor-start Motors:

The principle of using a capacitor in the auxiliary winding to 'split' the phase was known even in 1890's . But the capacitors to give the necessary capacitance required by single-phase motors were so unwieldy in size and costly that the capacitor motor was not a commercial feasibility then. Great strides have been made in the design and development of the capacitor motor
by 1936 it became the accepted motor for use
frigeration machines and many other domestic
(27.01 & 2.2). Also it made obsolete the
motor which was its immediate competitor in

then. This great development in the design and manufacture of capacitor motors was mainly due to the development of electrolytic capacitors which would be dealt with in detail under 'Special Problems'.

There are now three different recognised types of capacitor motors, the characteristics of which are distinctly different from each other. They are the following:

1. Capacitor-start Motor.
   A capacitor-start motor is one in which the capacitor phase is in circuit only during the starting period.

2. Permanent-split Capacitor Motor.
   A permanent-split capacitor motor is one having the same value of capacitance for both starting and running conditions.

3. Two-value Capacitor Motor.
   A two-value Capacitor motor is a capacitor motor using different values of effective capacitance for the starting and running connections.

By the use of capacitor in the auxiliary winding the angle between the main phase current and the auxiliary phase current can be made as great as even 90 degrees.

Hence for the same current in the two windings the locked-rotor torque in the capacitor-start motor can be made much higher than in a split-phase motor. Further, whereas in a split-phase motor, the line current almost equals the algebric sum of the currents in the two windings, in the case of a capacitor motor, it is much less because the two currents are almost in quadrature. Thirdly, in the auxiliary winding of a split-phase motor, the leakage reactance has to be kept small in order that the locked-rotor current may be nearly in phase with the voltage. Because the leakage reactance varies as the square of the number of turns, only a few turns can be used. In the capacitor-start motor, the reactance of the auxiliary winding is more than compensated by the capacitor, so that more turns can be used than in the auxiliary winding of a split-phase motor. Then the same current sets up more ampere-turns and hence more flux and more torque. Finally, the flux conditions in a capacitor motor at standstill are similar to the flux conditions of a two-phase motor and this also accounts for its greater effectiveness of starting.

The capacitor-start motor is the most popular type of single-phase motor for general-purpose heavy-duty applications requiring high locked-rotor and running torques.

This type of motor is built in all fractional horse-power sizes from 1/8 h.p. upward.

Fig. (1.2) shows the essential parts of a capacitor-start motor schematically. It can be easily noted that it very much resembles Fig. (1.1) -- the similar sketch for a split-phase motor -- except for the addition of the capacitor

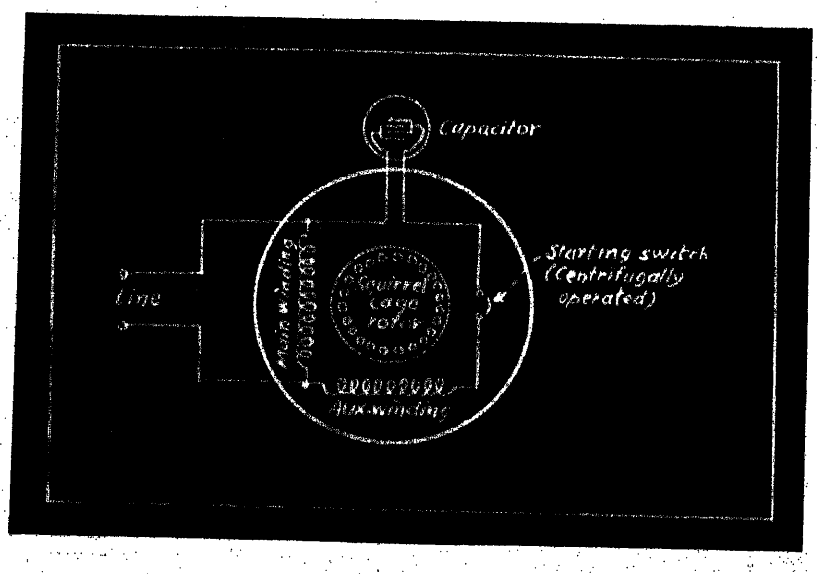


Figure (1.2).

in the auxiliary phase. But it is not to be forgotten that the auxiliary phase of a capac... ...
designed and proportioned an...
not merely split-phase motor...

1.03 Two-value Capacitor Motors:

The two-value capacitor motor was po...

After the development of capacitor motor. But it subsequently lost its place to the capacitor-start motor. Its field of application consisted of applications requiring high locked-rotor torque and high running torque.

In a two-value capacitor motor the effective value of a capacitance in series with the auxiliary winding

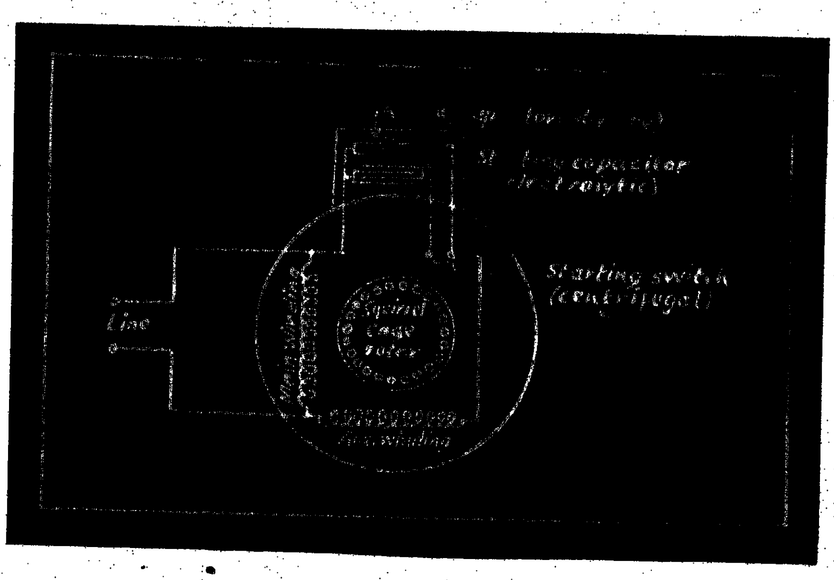


Figure (1.3).

while running is different from that during starting. This does not mean that two capacitors are always used. The effective value of the capacitance can be changed by the use of a capacitor-transformer unit. These two discussed briefly:

a) Motor using Two Capacitors:

citor motor using two separate capacitors is illustrated diagrammatically in Fig. (1.3). The running capacitor is permanently connected in series with auxiliary winding. This capacitor is of low capacity and is of the usual paper-spaced oil-filled continuous rated type. The starting capacitor which is connected in parallel with the running

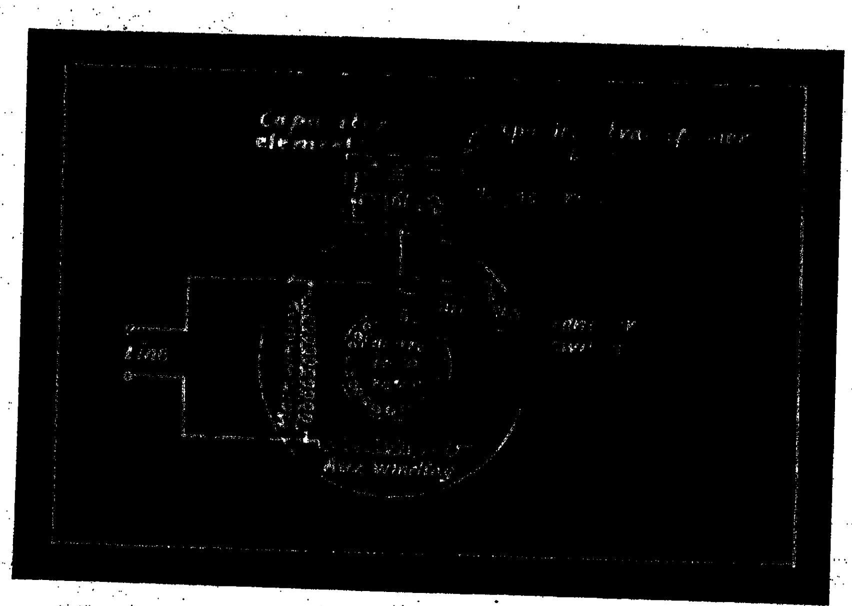


Figure (1.4).

capacitor of higher capacity. It is of the electrolytic type and will be dealt with in greater detail under 'Special Problems'. The starting capacitor is thrown out of circuit at the optimum speed by a centrifugal switch.

b) Motor using a Capacitor-Transformer Unit: Fig.(1.4) shows schematically a two-value capacitor motor using a capaci-

tor-transformer unit. The diagram needs little explanation. While the centrifugal switches used with other capacitor motors are of the single-pole, single-throw type, here it is a transfer switch, that is a single-pole, double-throw one. The effective value of capacitance in series with the auxiliary winding is kept high during starting by impressing a higher voltage to the capacitor during starting by the use of the transformer. At the optimum speed the centrifugal switch changes over to the other tap so that a smaller voltage is applied to the capacitor thus keeping the effective capacitance low while running.

The two-value capacitor motor is simply a capacitor-start motor with a 'running capacitor' permanently connected in series with the auxiliary winding. Considering any given motor, this addition improves the characteristics of the motor. Firstly, it improves the full-load efficiency and power factor. This may be briefly explained as follows: At the outset of this Chapter, it has been pointed out that the rotating field of a single-phase induction motor may be considered as comprised of two component pulsating fields, a main field and a cross-field spaced 90 electrical degrees apart and differing in time phase by 90 degrees. The main field component is set up directly by the main winding and the cross-

field by the rotor. When the auxiliary winding is connected across the line in series with a running capacitor of propoer value, the current drawn by it differs from that drawn by the main winding by almost 90 degrees in time phase. The net result is that the auxiliary winding sets up a part or all of the cross-field, thereby reducing or eliminating the magnetizing currents in the rotor and the accompanying copper losses.

Another effect of the running capacitor is to give 5 to 30 percent more breakdown torque. Still another effect is the reduction of the double-frequency torque pulsations normally inherent in single-phase motors and the consequent reduction in noise. In short, the effect of the running capacitor is to make the motor perform more nearly like a two-phase motor, particularly at one value of load.

1.04 <u>Permanent-Split Capacitor Motors</u>:

Permanent-split capacitor motors are also called as permanent-split-phase motors because the split-phase action continues during running also, and as single-value capacitor motors, because the same value of capacitance is in series with the auxiliary winding while starting as well as running. These motors are generally used for general purpose applications. Continuous-duty motors of this type

have low inherent locked-rotor torque; they are used principally for unit heaters and for other shaft-mounted fans or blowers. They are especially suited for fans because of the relative ease with which their speed can be controlled when driving fans. Intermittent-duty motors of this type can be designed for high locked-rotor torque; a popular use for such motors is for plug-reversing control motors for operating induction regulators, rheostats, dampers etc.

The permanent-split capacitor motor can be diagrammatically represented by Fig. (1.2) itself but for the fact that there is no starting switch in series with the auxiliary winding and the capacitors, and that the auxiliary winding is permanently in circuit. However, this does not mean that any capacitor-start motor can be converted into a permanent-split capacitor motor simply by short-circuiting the centrifugal switch in the auxiliary circuit. For, the auxiliary winding of a capacitor-start motor is usually [illegible] short-time operation and if permanently conn[illegible] the winding may be burnt out.

Remarkable adaptability [illegible] single-value capacitor motors. They [illegible] number of ways and can be used with or withou[illegible] and the direction of rotation can be [illegible]

case. The simple arrangement of reversing control shown in Fig. (1.5) may not be out of place here. Here a novel arrangement of windings and capacitor is employed. When the reversing switch is in the 'up' position, winding 'A' becomes the main winding, and 'B' becomes the auxiliary winding; when the switch is in the 'down' position, 'A' becomes the auxiliary winding and 'B' becomes the main winding.

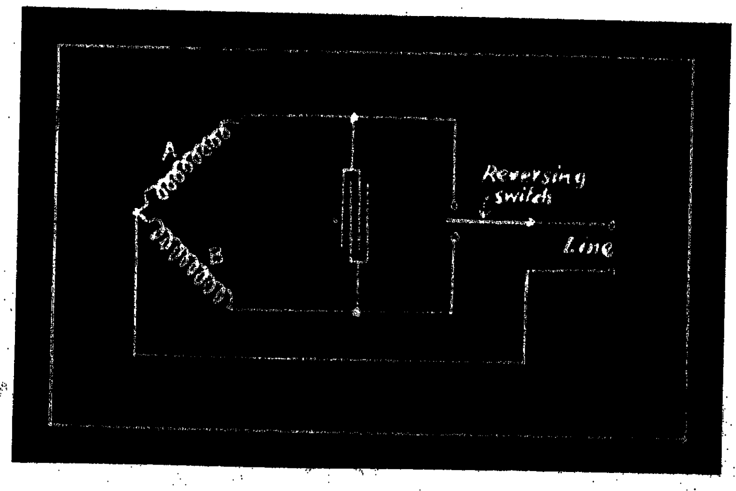


Figure (1.5)

Since in a capacitor motor the direction of rotation is always from the auxiliary winding toward the main winding, it follows that interchanging main and auxiliary winding reverses the direction of rotation. The single-pole double-throw switch is both an 'on and off' and a reversing switch. A simpler control could scarcely be devised.

Motors of this sort are widely used for operating valves, arc-welding control etc. They are built in all common horse-power ratings from 1/20 to 3/4, for four-, six- and eight-pole speeds.

1.05 Repulsion-Start Induction Motors:

The repulsion-start induction motor is, perhaps, the first type of single-phase induction motor that gained widespread commercial acceptance. Invented by Dr. Engelbert Arnold, it was used commercially in America as early as 1896. Although widely popular and until the middle thirties, it has now been generally supplanted for new applications by capacitor-start and two-value capacitor motors.

The repulsion-start induction motor is sometimes erroneously called a repulsion induction motor or simply a repulsion motor. The A.S.A. defines them as follows:

" A repulsion-start induction motor is a single-phase motor having the same winding as a repulsion motor but at a predetermined speed, the rotor winding is short-circuited or otherwise connected to give the equivalent of a squirrel-cage winding. This type of motor starts as a repulsion motor but operates as an induction motor with constant speed characteristics.

" A repulsion motor is a single-phase motor which has a stator winding arranged for connection to the source of power and a rotor winding connected to a commutator. Brushes on the commutator are short-circuited and are so placed that the magnetic axis of the rotor winding is inclined to the magnetic axis of the stator winding. This type of motor has a varying speed characteristics.

" A repulsion-induction motor is a form of repulsion motor which has a squirrel-cage winding in the rotor in addition to the repulsion motor winding. A motor of this type may have either a constant-speed or varying-speed characteristic."

Fig.(1.6) shows a cutway view of a repulsion-start induction motor showing clearly the essential and necessary parts:

a. The stator winding usually is a single, concentric winding. Because of the fact that there is only one winding, all the stator slots may not be wound. Some manufacturers use the empty slots for ventilating ducts to keep the motor cool. The empty slots are visible in this photograph. The stator core is laminated because it is

excited with alternating currents.

b. The rotor is slotted and wound just as if it were a d.c.-armature. The core is, of course, laminated.

c,d. Commutator and Brushes:

e. The brushes are mounted on a rocker ring or

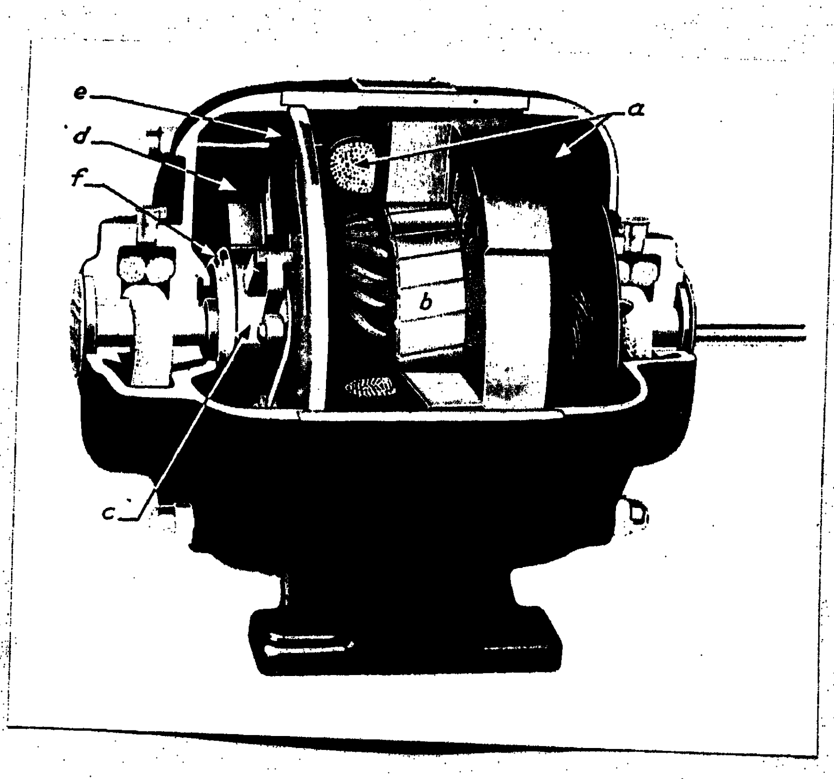


Figure (1.6)

brush yoke, which can be shifted circumferentially to reverse the direction of rotation.

f. A centrifugally operated short-circuiter short-

circuits all the commutator bars, making the armature, in effect, a squirrel-cage rotor.

1.06 Shaded-Pole Induction Motors:

Shaded-pole motors are used for nearly all applications requiring an induction motor of 1/20 h.p. or less. In the subfractional range-- horse-power ratings below 1/20 -- it is the standard general-purpose constant-speed a.c. motor. It is simple in construction, low in cost, and extremely rugged and reliable because it employs no commutator, switch, collector rings, brushes, governor, sliding or make-and-break contacts of any sort. It is low in efficiency, but this factor is not usually important because power inputs are low; however, the characteristically low efficiency does keep it from being built and used in the large horsepower ratings. It is used for such applications as advertising devices, damper controllers, fans and others.

The following is a definition of the shaded-pole motor by the A.S.A:

" A shaded-pole motor is a single-phase induction motor provided with an auxiliary short-circuited winding or windings displaced in magnetic position

from the main winding".

In the usual form of construction, salient poles are used, and the 'auxiliary short-circuited winding' consists of a single turn placed around a portion of the main pole. This coil is known as a 'shading coil'

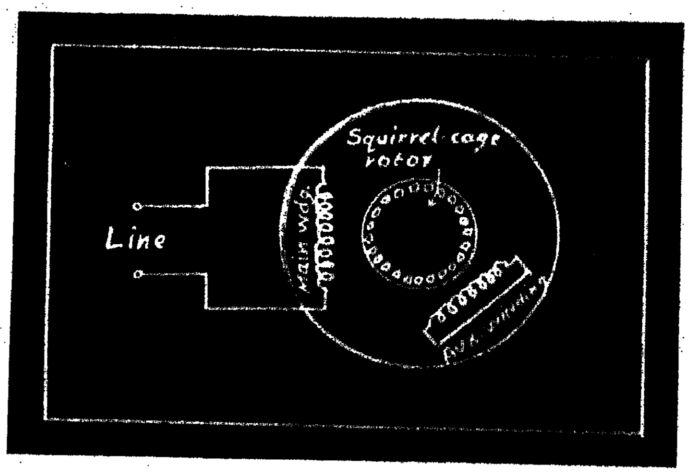


Figure (1.7)

because it causes the flux in that portion of the pole surrounded by it to lag behind the flux in the rest of the pole.

Fig.(1.7) gives a schematic representation of a simple shaded-pole motor. There is but a single winding, which is connected to the line, a second winding permanently short-circuited upon itself, and a squirrel-cage rotor,.

The short-circuited winding is displaced from the main winding by an angle which can never be 90 electrical degrees. It has to be shifted by a definite amount in order to set up a field along an axis in space different from that of the main winding; Furthermore, this shift has to be less than 90 degrees so that a voltage can be induced in the short-circuited winding by transformer action of the main winding. In analysing this motor four circuits have to be considered; primary, shading coil, and two rotor phases. These have been analyzed and the performance characteristics of a shaded-pole motor are discussed by P.H.Triskey. (36.01).

Construction of the shaded-pole motor may be varied very widely. Some of the typical constructions are shown in Fig. (1.8). Fig.(1.8 a) shows a most typical construction. The stator is composed of single-piece identical laminations held together by rivets near the periphery. The main winding consists of coils wound on a form and then slid on over the pole. The shading winding is simply 4 coils of one turn each of bare copper strap, each coil short-circuited on itself.

Fig.(1.8 b) shows a similar construction except that iron wedges bridge the pole tips. As a general rule the increased leakage flux of the shaded pole results in a motor of more desirable characteristics.

Since the magnetic wedges are so often desirable, advantage is sometimes taken to construct the wedge as a part of the pole as shown in Fig.(1.8 c). The stator core is made in two parts, an outside ring and an inner spider, each built up of laminations and riveted. The main coils are very easily slipped over the spider, and then the ring pressed on over it. Its simplicity of winding is so great that for small sizes this type is very popular. It has the disadvantages of a spongy core, of having to complete the shading coils after putting them on the core, and of a slight air gap at the joint between the two parts of the core.

Fig.(1.8 d) shows to what extent the shaping of field structure may be varied. The primary laminations in this case have only one joint, but alternate punchings are reversed, and stacked in the coil in the same manner as in small transformers.

C H A P T E R - II.

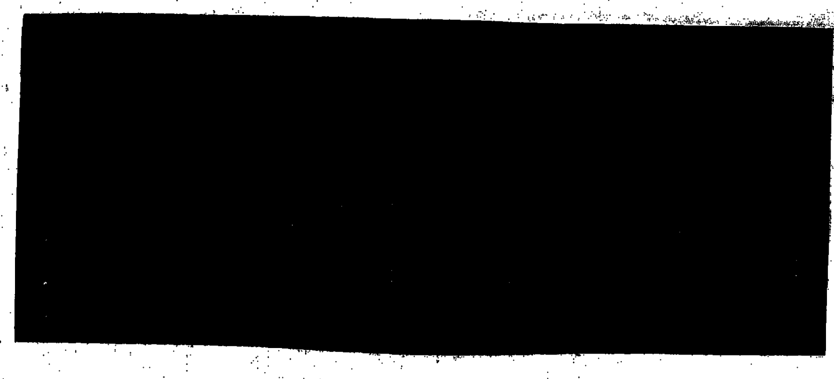
THEORIES OF OPERATION.

Two theories are used to explain the action of the single-phase induction motor; the double revolving field theory and the cross-field theory. Both involve various simplifying assumptions which have some effect on their accuracy (B.3). Other methods of analysing the single-phase induction motor are more in the nature of procedures to the solution of single-phase-induction-motor performance characteristics rather than explaining how the single-phase induction motor runs at all.

2.1 Double Revolving Field Theory:

The windings of the single-phase induction motor are usually distributed to produce a nearly sinusoidal field. But, for analysis we shall consider a single-turn single-phase winding. Fig.(2.1.1) shows a single-phase full-pitch winding having one slot per pole (B.4). The directions of current are shown for a single instant of time. The air-gap is assumed to be uniform. The [illegible]

directions of lines of force are shown in the Figure and the only lines of force possible are those linking with only one coil. No lines of force are possible which are linked with two coils at the same time because the mmf. of such force lines is zero. The mmf. of all lines of force is constant and has a maximum value of $\sqrt{2}$ I M_s . Since every line of force consists of two symmetrical parts taking opposite directions in the air-gap and in the teeth, the



Figure

mmf. is divided into two pa
crossing of the gap; the
having a maximum height of
tained as the mmf. curve of
one slot per pole.

The maximum value of the magnetomotive force appears when the current is at its maximum value. If the current is decreased, the height of the rectangle is also decreased, and it will be zero when the current is zero. If the direction of current is reversed, the rectangle appears on the other side of the axis and reaches its maximum value when the current is a maximum. Thus the mmf. produced by a single-phase winding is pulsating in space. Since we have assumed the air-gap to be uniform the flux density at every point is directly proportional to the mmf. at that point. Hence the mmf. curve represents the field distribution also to a different scale and the flux also is, therefore, pulsating but fixed in space. Since the flux entering the armature must be equal to the flux leaving the armature, it follows that the positive area in Fig.(2.1.1) must be equal to the negative area.

The rectangular curve of Fig.(2.1.1) can now be reduced to its fundamental and harmonics. If the co-ordinate axis is taken through the centre of the pole, $f(-x) = f(x)$ and only cosine terms are present. Further, since $f(x+\pi) = -f(x)$, only odd harmonics are present.

[illegible]

Consequently,

$$f(x) = \sum_{\nu=1}^{\nu=\infty} a_\nu \, Cos \, \nu \frac{\pi}{\tau} x \quad .. \quad (2.1.1)$$

where ν is odd.

Further,

$$a_\nu = \frac{1}{\tau} \int_0^{2\tau} f(x) \, Cos \, \nu \frac{\pi}{\tau} x \, dx$$

$$= \frac{\sqrt{2}}{2} \, I \, N_s \, Sin \, \omega t \left(\frac{4}{\pi} \frac{1}{\nu} \, Sin \, \nu \frac{\pi}{2} \right) \quad .. \quad (2.1.2)$$

Therefore,

$$f(x) = \frac{\sqrt{2}}{2} \, I \, N_s \, Sin \, \omega t \; x \; \frac{4}{\pi} \sum \frac{1}{\nu} \, Sin \, \nu \frac{\pi}{2} \, Cos \, \nu \frac{\pi}{\tau} x$$

Since,

$$Sin \, \nu \frac{\pi}{2} = \pm 1$$

$$f(x) = 0.9 \, I \, N_s \, Sin \, \omega t \left[Cos \frac{\pi}{\tau} x - \frac{1}{3} Cos \, 3 \frac{\pi}{\tau} x + \frac{1}{5} Cos \, 5 \frac{\pi}{\tau} x - \, . \, . \, . \, . \, . \right] \quad (2.1.3)$$

Anything that holds good for the fundamental holds good for the harmonics as well. Hence considering the fundamental alone

$$f(x) = 0.9 \, I \, N_s \, \text{Sin} \, \omega t \, \text{Cos} \, \frac{\pi}{\tau} x$$

$$= \frac{0.9}{2} I \, N_s \, \text{Sin} \left(t - \frac{\pi}{\tau} x \right)$$

$$+ \frac{0.9}{2} I \, N_s \, \text{Sin} \left(t + \frac{\pi}{\tau} x \right) \quad .. \quad (2.1.4)$$

The two parts of the right hand side of eq. (2.1.4) are easily identified as expressions for forward travelling wave and backward travelling wave. Thus the alternating field has been resolved into two revolving fields which travel in opposite directions and whose amplitudes are each half of the amplitude of the alternating field.

Let us now assume that the motor is running at a speed ω_e. Then the slips with respect to the forward and backward fields are,

$$s_f = \frac{\omega - \omega_0}{\omega} = 1 - \frac{\omega_0}{\omega} = s \qquad (2.1.5)$$

$$s_b = \frac{\omega - (-\omega_0)}{\omega} = 1 + \frac{\omega_0}{\omega} = 2 - s \qquad (2.1.6)$$

It is convenient to consider a the single-phase motor as two superimposed 2-phase motors (B.6),

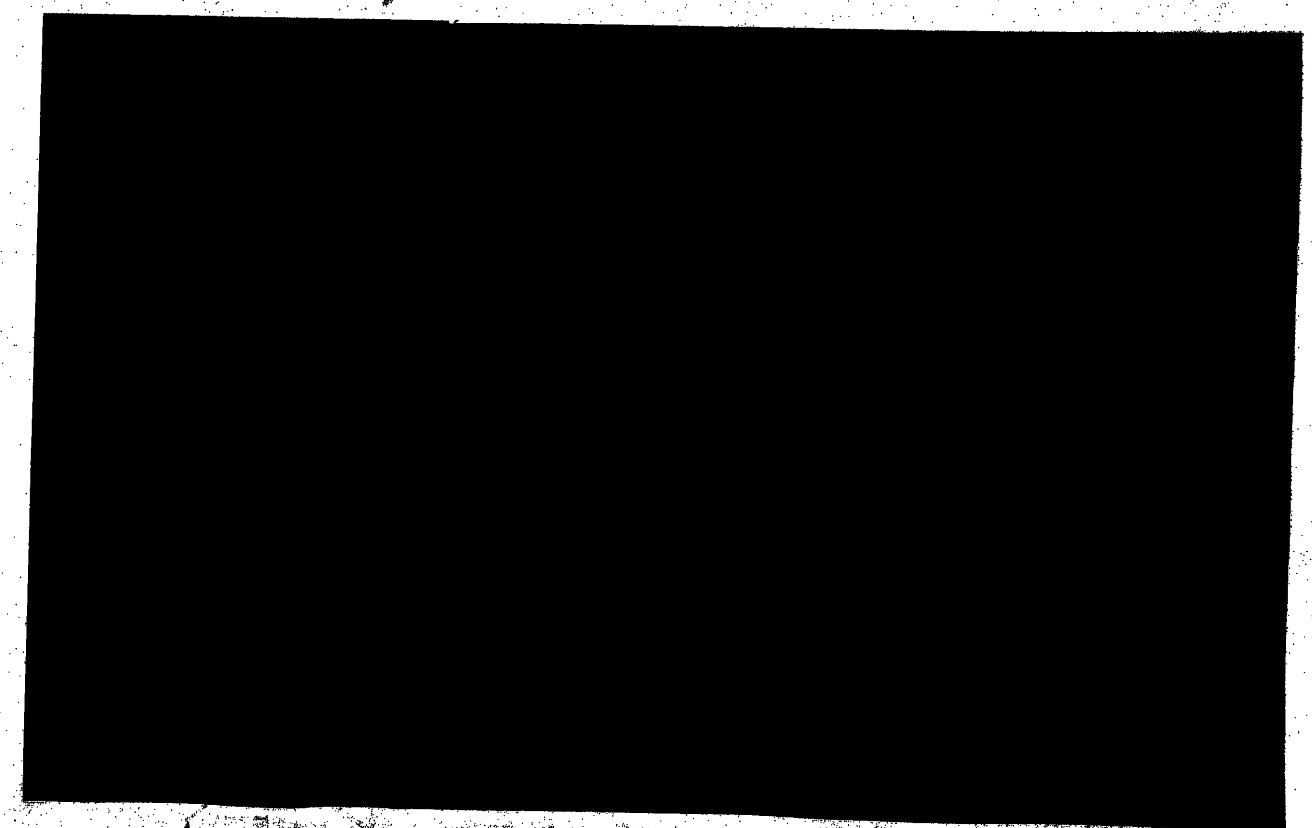


Figure (2.1.2).

having forward and backward rotating fields respectively,

as indicated in Fig.(2.1.2). The actual stator winding of T_m turns contributes $(T_m/2)$ turns to each 2-phase motor, and the stator current are the same in each, so that the phase-1 ampere-turns balance is

$$\frac{T_m I_m}{2} + \frac{T_m I_m}{2} = T_m I_m$$

But the currents in the phase-2 coils must be opposed in order to develop rotating fields of opposite direction, and their superimposed ampere-turns, therefore, cancel. Thus the two fictitious polyphase machines superimpose to form the actual single-phase motor.

Each 2-phase motor has a stator resistance of r_1' ohms per phase and a reactance of x_1' ohms per phase, and since the stators are in series, there must be $2\,r_1' = r_{1m}$ and $2\,x_1' = x_{1m}$, to satisfy the single-phase stator impedance.

But it must be borne in mind that this representation of a single-phase induction motor by two two-phase motors connected as shown, is not true to the facts, but holds good only in certain respects, for in a polyphase

machine, the torque is a constant torque, whereas in the single-phase machine, the torque is a pulsating one (B.6).

We shall next proceed to set up the various voltage equations and derive, therefrom, an equivalent circuit for the single-phase induction motor based on the above principles. We know that in a 3-phase induction motor the following to be the voltage equation of the stator:

$$\bar{V} = (r_1 + jx_1)\,\bar{I}_1 + j\,x_m\,(\bar{I}_1 + \bar{I}_2')$$

Hence the voltage equation of the stator for a single-phase induction motor becomes,

$$\bar{V} = (r_{1m} + jx_{1m})\,\bar{I}_m + jx_m'\,(\bar{I}_m + \bar{I}_{2f}') + jx_m'\,(\bar{I}_m + \bar{I}_{2b}') \quad .. \quad (2.1.7)$$

$(\bar{I}_m + \bar{I}_{2f}')$ represents the resultant mmf. of the forward rotating field and $(\bar{I}_m + \bar{I}_{2b}')$ represents that of the backward rotating field.

If the rotor has a slip 's' with respect

to the forward rotating field and a slip (2 - s) with respect to the backward rotating field, then the frequency of the rotor current due to the forward rotating field is 'sf'

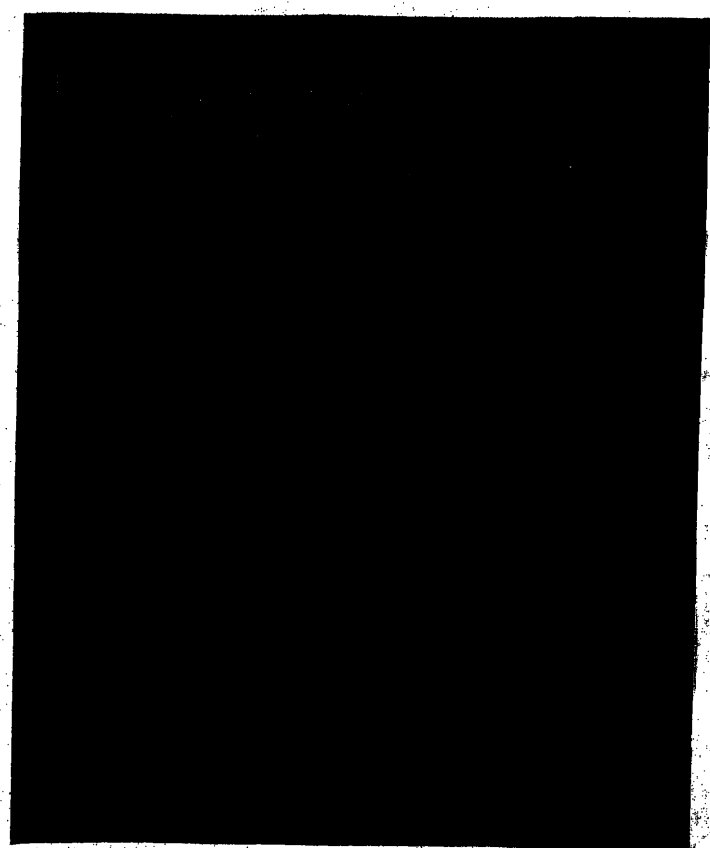


Figure (2.1.2).

and that due to the backward rotating field is (2 - s)f. Since the rotor currents have different frequencies, two different voltage equations are necessary for the rotor. Therefore the voltage equations of the rotor are,

$$0 = \left(\frac{r_2'}{s} + jx_2' \right) \bar{I}_{2f}' + jx_m' \left(\bar{I}_m + \bar{I}_{2f}' \right) \quad .. \; (2.1.8)$$

$$0 = \left(\frac{r_2'}{2 - s} + jx_2' \right) \bar{I}_{2b}' + jx_m' \left(\bar{I}_m + \bar{I}_{2b}' \right) \quad .. \; (2.1.9)$$

Inspection of equations (2.1.7), (2.1.8) and (2.1.9) shows that the equivalent circuit for the single-phase induction motor is as shown in Fig. (2.1.3).



Figure (2.1.4).

So far we have neglected the iron losses in

the core and the teeth due to the main flux. The simplest way to treat them is to lump them into one equivalent resistance connected across the motor terminals (B.2) as

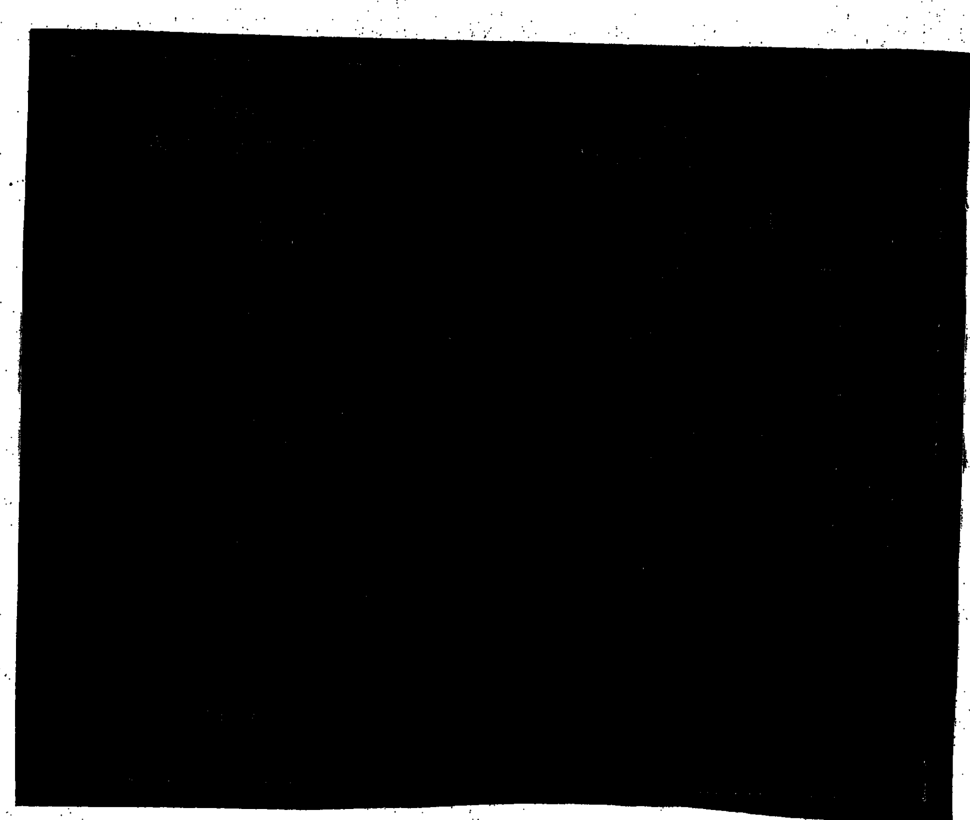


Figure (2.1.5).

shown in Fig. (2.1.4). This results in an- in-phase addition to the current and a constancy for these losses at all loads. The connection of the equivalent resistance beyond the stator impedance, as shown in dotted lines, causes a reduction in losses with the counter emf. which

also reduces with increase in load.

The equivalent resistance for considering core losses may also be grouped with the magnetising reactance, either in parallel or by replacement with a new equivalent series impedance. This is shown in Figs. (2.1.5) (a) and (b).

The simultaneous equations (2.1.7),(2.1.8) and (2.1.9) can be solved toget the value of I_m and the equivalent circuit itself can be solved toget the characteristics of the motor at any particular slip. This will be dealt with in greater detail under "Performance Calculation".

Before leaving the topic of double revolving field theory, the similarity between the analyses by this theory and symmetrical components has to be brought out. As T.C.Lloyd puts it " This (double revolving field theory) approach to motor analysis is very closely allied to that developed by the symmetrical components method." (B.3). F.W.Suhr has presented a paper (45.01) showing the applications of symmetrical components in calculating the performance of the single-phase induction motor analytically. But R.R.Lawrence (B.7) does not make any difference between the double revolving field theory and the symmetrical components method of treating the single-phase induction motor.

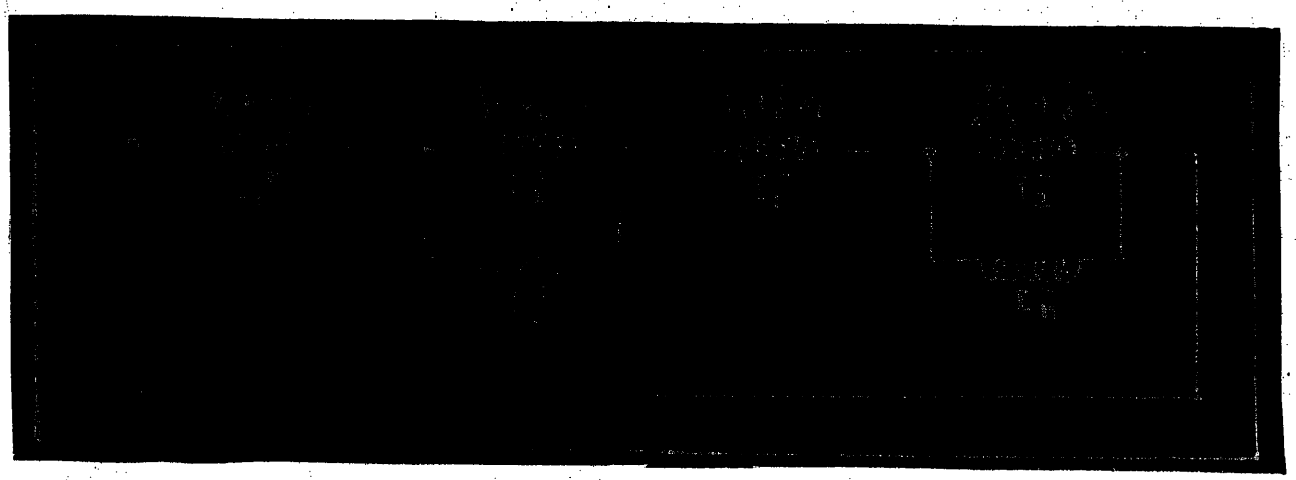


FIGURE (2.1.6).

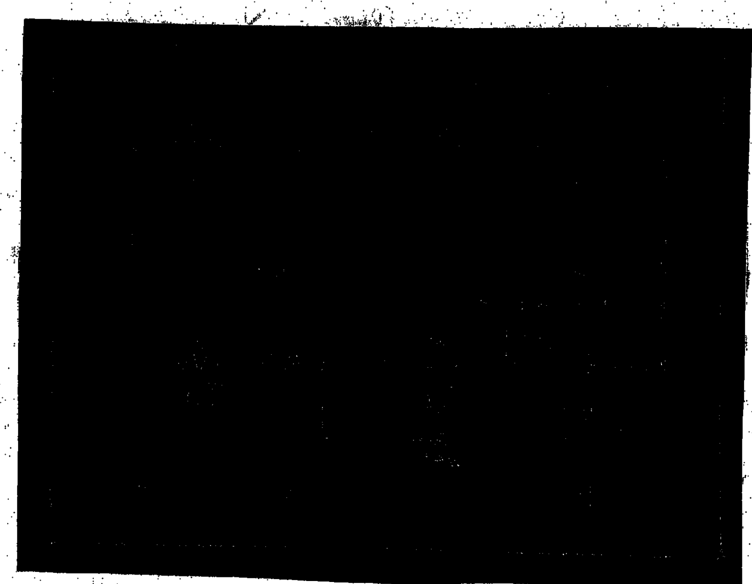


FIGURE (2.1.7).

He considers the symmetrical components method and the cross-field theory as the two chief methods of calculating the performance of single-phase induction motors. Equivalent circuits based on symmetrical components have been derived by Lawrence and, Wagner and Evans (B.8) which are given in Figs. (2.1.6) and (2.1.7). It can be readily seen that these circuits are identical with the one given in Fig. (2.1.3). However there is a school of thought which considers fluxes and mmf's as follows: " A magnetic flux represents energy while a magnetomotive force represents force only. Fluxes therefore, follow the laws of energy while magnetomotive forces follow the laws of force. Magnetomotive forces being forces combine vectorially into a resultant that depends on the space angle at which the components act. Fluxes, on the other hand, being energies combine arithmetically irrespective of the space angle at which the components merge." (45.02). According to this, it is wrong to conceive of the alternating flux produced by a single-phase winding as equivalent to two rotary fluxes rotating in opposite directions. In that case, however, resort may be made to the symmetrical components method which leads to the same equivalent circuit and consequently same procedure to calculate the performance of the motor from the equivalent circuit.

2.2 <u>Cross-Field Theory:</u>

The cross-field theory of the operation of single-phase induction motors was first put forward by C.P. Steinmetz (98.01) in the year 1898. Steinmetz was of the opinion that the double revolving field theory had to be completely given up for the following reasons: At stand-still the magnetic field of the single-phase induction motor is undoubtedly alternating, and can be resolved into two equal and oppositely revolving fields. At speed, however and especilly at synchronism, one component has disappeared altogether and the other component is of full intensity, that is, the field is a uniformly revolving field. Secondly according to him, the current while running light should be equal to the sum of the exciting current of a polyphase motor of half impressed emf. plus the current taken by a polyphase motor of half impressed emf. when driven backward at full speed, which should evidently be high. But the actual current taken by a single-phase induction motor at synchronism is much less than this.

As for his first objection to the double revolving field theory, as was pointed out by Dr. Kennelly (98.02), Steinmetz did not take into account the field produced by the rotor currents. As for his second objec-

tion, Steinmetz might have wrongly conceived the "forward revolving rotor" and the "backward revolving rotor" to be in parallel while actually they should be in series as had already been shown while dealing with double revolving field theory.

Four years after the enunciation of the cross-field theory by Steinmetz, Branson (12.01) presented a complete analysis of the single-phase induction motor based on cross-field theory. Later it was developed by West (26.01), Perkins (25.01), Puchstein & Lloyd (41.01), and Chang (47.01).

2.2.1 Development of the Complete Vector Diagram of the various components of flux, voltage and current:

To identify the various components of flux, voltage and current, a rather complex system of subscripts will be used. Subscripts 'S' and 'T' will indicate the primary cause of a voltage as speed or transformer action, respectively. With two flux system, we will show whether the emf. originates from the main - or the cross-axis flux by the second subscript 'M' or 'C', respectively. If the emf. is instrumental in producing a current and an mmf. which affect the winding of the main (or 'y') axis or the

cross (or 'x') axis, the third subscript will so indicate by 'y' or 'x', respectively (5.2).

The single-phase induction motor with a squirrel-cage rotor can be represented schematically as

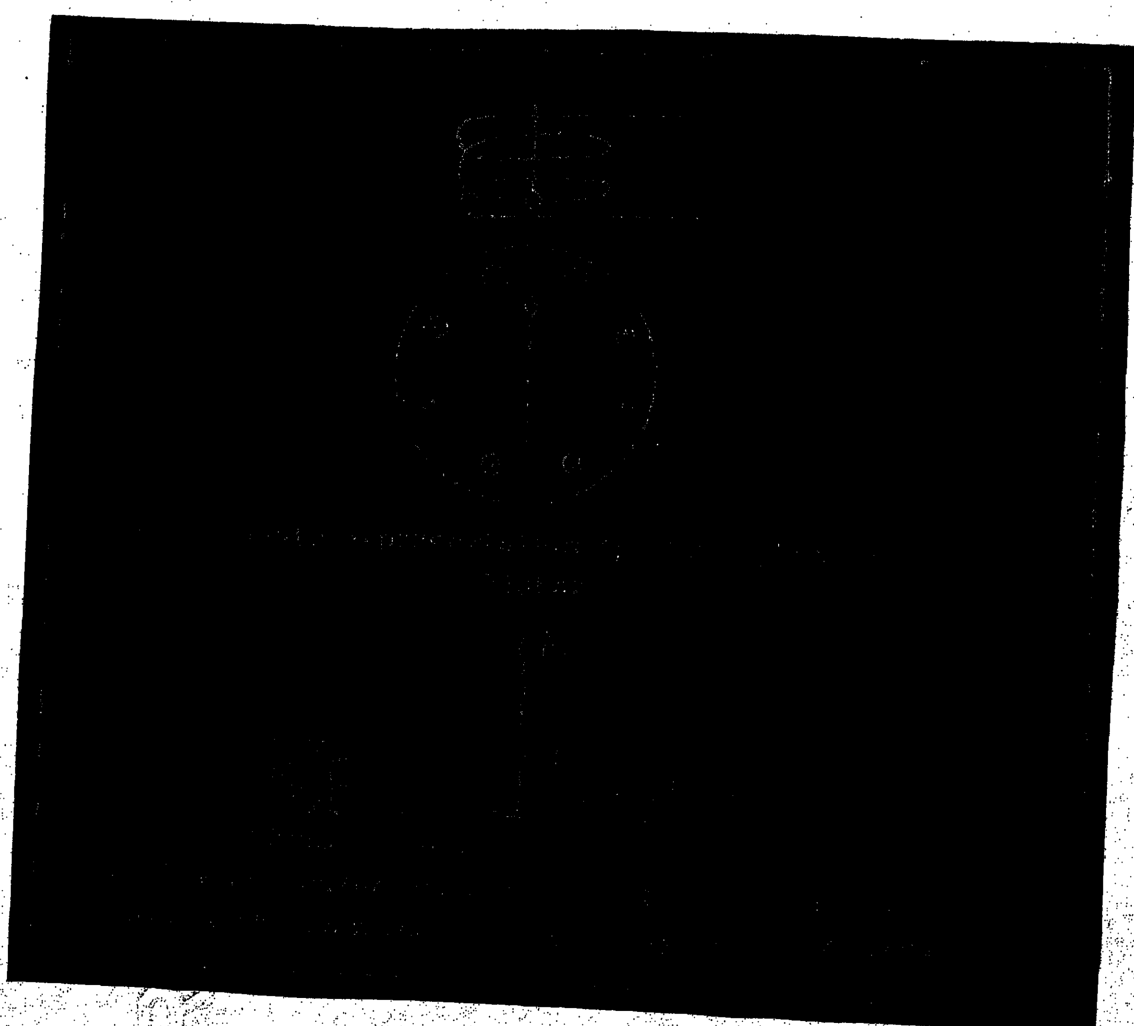


Figure (2.2.1)

shown in Fig. (2.2.1)(a). Although the stator winding is actually distributed, it is equivalent electromagnetically

to the concentrated stator coil. Exciting the stator with an alternating emf. causes the alternating flux along the main axis. This will be designated ϕ_M.

The voltage induced in the rotor winding is E_{TMy}, and from transformer fundamental it is in lagging quadrature with the flux causing it. This will be equal and opposite to the counter emf. - E_{TMY} induced in the stator winding. These facts enable us to draw the partial vector diagram of Fig. (2.2.1)(b). The core loss component of the magnetising current is neglected. The stator winding is assumed to have the usual resistance and leakage reactance drops, $I_\phi r_{1m}$ and $I_\phi x_{1m}$ respectively.

Rotation of the rotor bars through ϕ_M produced a generated emf., E_{GMx} as shown in Fig.(2.2.2)(a). Evidently ϕ_M and E_{GMx} are in time phase. A speed voltage will be considered positive and drawn in a positive direction, if it ultimately results in a positive flux. For the conditions shown both E_{GMx} and ϕ_S are positive.

E_{GMx} will cause a current to flow thro' the current bars, which act like turns centred on the horizontal axis. The resulting mmf. has no stator winding to act upon. Hence the cross-axis of the rotor acts

like a reactance coil; the flux ϕ_c gives the winding a large reactance. Therefore the cross-axis current I_x' lags behind E_{Mx} almost by 90 degrees in time. These relationships are shown in Fig. (2.2.2)(c). The flux of the cross-axis will be a maximum when the current causing it is a maximum and hence we can draw ϕ_c in time phase with I_x' . The axis of the flux ϕ_c is horizontal [Fig. (2.2.2)(b)] . while that of the main flux ϕ_M is vertical; that is these two flux systems are in space quadrature. So now, we have produced two flux systems in the air gap of a single-phase induction motor, in time and space quadrature, somewhat similar to those which would result in a two-phase motor.

Numerically,

$$E_{Mx} = S\, E_{My} \qquad .. \quad (2.2.1)$$

where

$$S = \frac{N}{N_s} = \frac{\text{Actual rpm.}}{\text{Synchronous rpm.}} \qquad .. \quad (2.2.2)$$

The permeance of the cross-axis flux path is the same as that for the mutual flux of the main axis. Hence, since the fictitious rotor winding turns

of the two axes are equal, reactance of the rotor windings are practically the same in each axis and the mutual flux of the cross-axis induces a rotor emf., $I_x'' x_M$.

The cross-axis flux ϕ_c induces, in turn, a voltage E_{TCx} in the rotor by transformer action. Then E_{TCx} is equal to $I_x'' x_M$. In addition, the current I_x'' , flowing through the rotor conductors, builds up a small leakage-flux system which gives a leakage-reactance drop. The rotor windings also possess a resistance r_2 All these elements can be combined as follows:

E_{SMx} can be considered as the voltage "applied" to a reactance coil. The voltage is used up in overcoming (i) the reactance drop of the mutual reactance, (ii) drop caused by the leakage reactance of the winding and (iii) the resistance drop of the winding. These quantities are represented by the rotor vector diagram of Fig. (2.2.3) .

This whole system of vectors [Fig.(2.2.3)] arises from speed. As the speed changes, the diagram "expands" or "contracts" accordingly. At zero speed, all these vectors reduced to zero. No energy required by this axis can come directly from the stator winding

because there is no magnetic link between them. But, since these cross-axis losses result from the generated voltage E_{sMx} , the cross-axis forms a generator load on the motor, exerting a negative torque which must be overcome.

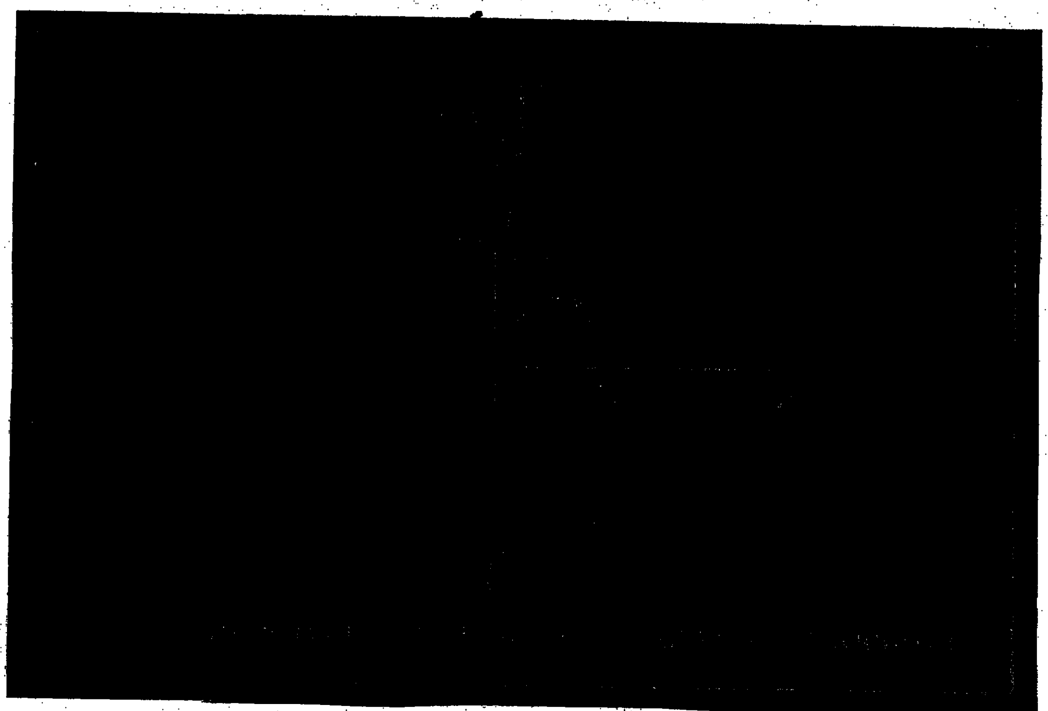


Figure (2.2.3)

The only remaining component of voltage to be discussed is the voltage, E_{sCy} caused by the speed action from the cross-axis flux. E_{sCy} will be in time phase with, or in phase opposition to, ϕ_c since they reach their respective maxima at the same instant.

E_{SC_y} combines with E_{TM_y} to produce a current (I_y") active in the y-axis of the rotor. In a sense, E_{SC_y}, depending as it does on speed action, is a generated counter emf. which together with the rotor impedance drop of y-axis "uses up" the voltage "applied" to the rotor, ie., E_{TM_y} [Fig. (2.2.4)] .

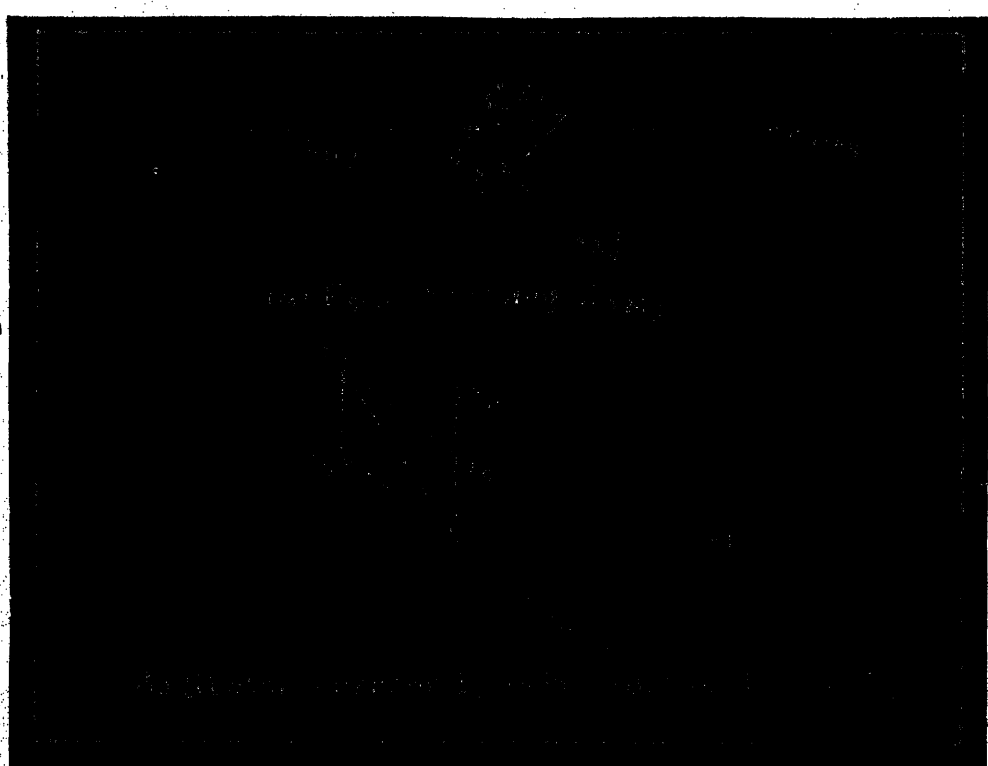


Figure (2.2.4).

The rotor current, I_y" requires a balancing component in the primary, equal and opposite (for an assumed

ratio, stator to rotor, of unity). This stator current will be designated by I_y. Then

$$I_y = - I_y' \qquad .. \quad (2.2.3)$$

Together with the magnetising component of the stator current, they combine to form the total current taken by the motor. Vectorially,

$$I_y + I_\phi = I_m \qquad .. \quad (2.2.4)$$

Summarising all, the final vector diagrams of the various components of current and voltage are given by Figs. (2.2.5)(a), (b), and (c).

We shall now try to establish certain equations connecting the various impedances, currents and emfs. Equation (2.2.4) can be rewritten as,

$$I_\phi = I_m - I_y$$

Also a counter emf. by transformer action is numerically equal to the product of the magnetising current and magnetising reactance. Hence,

$$I_{\phi} \; x_m \quad = \quad E_{TMy} \qquad .. \quad (2.2.5)$$

As vectors:

$$-j \; x_m \; (I_m - I_y) \quad = \quad E_{TMy} \qquad .. \quad (2.2.6)$$

The Kirchoff Law equation for the stator is then,

$$V \; = I_m \; Z_{1m} + j \; x_m \; (I_m - I_y) \qquad .. \quad (2.2.7)$$

The vector diagram corresponding to the equation (2.2.7) is shown in Fig. (2.2.6)(a).

Equation No. (2.2.1) can be written as

$$E_{SMx} \quad = \quad S \; x_m \; (I_m - I_y) \qquad .. \quad (2.2.8)$$

Further, $\quad E_{TGx} \; = \; - \; j \; x_m \; I_x'' \qquad .. \quad (2.2.9)$

hence,

$$S \; x_m \; (I_m - I_y) - j \; x_m \; I_x'' \; = \; I_x'' \; Z_2 \; .. \quad (2.2.10)$$

We shall take the view point, following Arnold, West, Puchstein, and Lloyd, that speed voltages result from cutting not only the mutual flux, as Steinmetz has assumed, but the rotor leakage fluxes as well. Then

a speed voltage from the leakage flux would be 'S' times as large as the leakage-reactance drop caused by that flux. The sign of the speed voltage from such a source will be the same of the sign af the speed voltages from the mutual flux.

Adding this speed voltage to equation (2.2.10), the final equation for the cross-axis becomes,

$$I_x' Z_2 = S x_m (I_m - I_y) - j x_m I_x' - S I_y x_2 \qquad .. \quad (2.2.11)$$

This vector diagram is given in Fig. (2.2.6)(b).

For the main axis (Fig. (2.2.5)(b)

$$E_{MY} = - j x_m (I_m - I_y) \qquad .. \quad (2.2.12)$$

$$E_{SQY} = - S x_m I_x' \qquad .. \quad (2.2.13)$$

Then,

$$-j x_m (I_m - I_y) - S x_m I_x' = I_y' Z_2 \qquad .. \quad (2.2.14)$$

Reversing I_y' to obtain the reflection of the rotor current in the stator, [illegible]

[illegible]

$$-j\,x_m\,(I_m - I_y) - S\,x_m\,I_x' \;=\; -\,I_y\,Z_2 \qquad .. \quad (2.2.15)$$

The speed voltage arising from the leakage flux is $S\,I_x'\,x_2$, which takes its sign from the corresponding speed voltage of the mutual cross-axis flux. Then for the final equation of the main axis,

$$I_y\,Z_2 \;=\; j\,x_m\,(I_m - I_y) + S\,I_x'\,(x_m + x_2) \qquad .. \quad (2.2.16)$$

The vector diagram corresponding to this condition is shown in Fig. (2.2.6)(c).

2.2.2 The Equivalent Circuit:

The problem taken for study is that of a single-phase capacitor-start induction motor. During the time between starting and the opening of the centrifugal switch the motor will run as a capacitor motor. Therefore to study the starting characteristics of the motor taken for investigation, we must know how to determine the characteristics of a capacitor motor also. Hence before developing an equivalent circuit for the plain single-phase motor, that for a capacitor motor will be developed. Once we develop the equivalent circuit for the capacitor motor that for a plain motor can be easily got by making X_c tend to infinity.

Equations (2.2.7), (2.2.11) and (2.2.16) will form the basis for further analyses. But till now we had not considered any iron loss and the stator had no circuit in the quadrature axis. Taking into account that we now have a circuit (called start winding) in the quadrature axis, the fundamental relations can be briefly stated as follows: (41.01).

1. The voltage applied to the main winding overcomes a local stator impedance drop and the counter-emf. built up by the mutual flux of the main winding.

2. The stator current is the resultant of a load component reflected by transformer action from the rotor and a main-axis magnetising current which may or may not contain an iron loss component.

3. The voltage applied to the start winding overcomes the local stator impedance drop of that winding, the reactance or impedance drop of the capacitor in series with the winding, and the counter emf. built up by the mutual flux of the cross-axis.

4. The stator current of the cross-axis is the resultant of a load component reflected by transformer action from the rotor, and a start or cross-axis

magnetising current similar to that of the main winding, but usually differing in magnitude.

5. In the rotor, the main or 'y' axis current results from two emf's;

a) The transformer voltage, opposite in phase to the stator counter emf. but of the same magnitude if the rotor constants are all considered in main winding terms.

b) A speed voltage, resulting from the rotor conductors cutting the cross-axis mutual flux and the leakage flux of the rotor as well. By Kirchhoff's law the vector sum of these voltages and the rotor impedance drop caused by the main axis current, equals zero.

6. In the start or 'x' axis of the rotor, two emf's, similar to those listed above are present;

a) A transformer voltage opposite in phase to the cross-axis counter emf. but different in magnitude by the ratio of transformation between start winding and rotor, or start and main windings.

b) A speed voltage resulting from cutting the main winding mutual and rotor leakage fluxes. The vector sum of these voltages and the rotor impedance drop

of the cross-axis rotor current equals zero.

Based on these principles, equation (2.2.7) of the stator main axis is modified (47.01) as,

$$E_m + I_m Z_{1m} = V \qquad .. \quad (2.2.17)$$

where,

$$E_m = Z_m \; (I_m - I_y) \qquad .. \quad (2.2.18)$$

Whereas we had no equation for the stator quadrature axis, previously, we now get it as,

$$E_s + I_s \, (Z_{1s} + Z_s) = V \qquad .. \quad (2.2.19)$$

where,

$$E_s = Z_s \, (I_s - I_x) \qquad .. \quad (2.2.20)$$

The rotor equation (2.2.11) in the 'x' axis is modified as,

$$\frac{E_s}{s} + j \, S \, (-E_m + j \, I_y \, x_2) = s \, Z_2 \, I_x \qquad .. \quad (2.2.21)$$

The rotor equation (2.2.15) in the 'y' axis is modified as,

$$- E_m + j S \left(- \frac{E_s}{a} + j\, a\, I_x\, x_2 \right) = - I_y\, Z_2 \quad .. \; (2.2.22)$$

Torque in synchronous watts being given by the product of the emf. and the current, and the sine of the angle between them, the expression for the torque becomes,

$$T = a\, E_m\, I_x \operatorname{Sin}(E_m, I_x) + \frac{E_s}{a} I_y \operatorname{Sin}(I_y, E_s) \quad .. \; (2.2.23)$$

Equation (2.2.23) is a scalar expression of the torque. In vector form it becomes,

$$T = \text{Real part of } \left[-j \left(a\, I_x \operatorname{conj} E_m - I_y \operatorname{conj} \frac{E_s}{a} \right) \right] \quad .. \; (2.2.24)$$

E_m , I_y, Z_{1m} , Z_m , Z_2 are in main winding terms.

Z_s , E_s , I_x , Z_{1s} are in starting winding terms.

Equations (2.2.21) and (2.2.22) can be solved for E_s and E_m and yield,

$$\frac{E_s}{a} = \frac{j\, S\, r_2}{1 - S^2} I_y + j\, a\, x_2\, I_x + \frac{r_2}{1 - S^2} a\, I_x \quad .. \; (2.2.25)$$

$$E_m = \frac{-j\ S\ r_2}{1 - S^2}\ a\ I_x + j\ x_2\ I_y + \frac{r_2}{1 - S^2}\ I_y \quad .. \ (2.2.26)$$

The following symbols will now be introduced:

$$R = \frac{S\ r_2}{1 - S^2}$$

$$Z_2' = \frac{r_2}{1 - S} + j\ x_2$$

$$E_s' = - \frac{j\ E_s}{a}$$

$$I_x' = - j\ a\ I_x \quad \text{and}$$

$$I_s' = - j\ a\ I_s$$

The expression for $\frac{E_s}{a}$ and E_m can now be written as ,

$$E_s' = (Z_2' + R)\ I_x' + R\ I_y \quad .. \ (2.2.27)$$

$$E_m = (Z_2' + R)\ I_y + R\ I_x' \quad .. \ (2.2.28)$$

Equations (2.2.27) and (2.2.28) are recognised readily as the mesh equations of the circuit shown in Fig. (2.2.7).

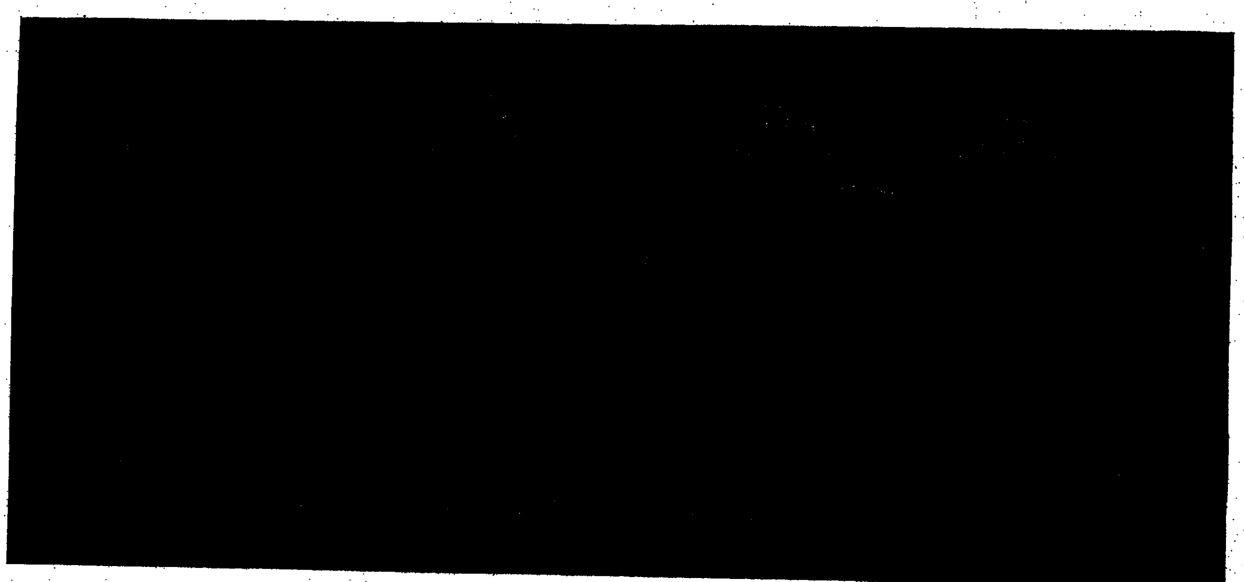


Figure (2.2.7).

Equation (2.2.24) in terms of the new notation E_s' , I_x' , becomes,

$$T = \text{Real Part of } \left[I_x' \text{ conj } E_m + I_y \text{ conj } E_s' \right] \quad ..(2.2.29)$$

where $\quad \text{conj } E_s' = \dfrac{j \text{ conj } E_s}{a}$

Substituting in equation (2.2.29) for E_s' and E_m from equations (2.2.27) and (2.2.28),

$$T = \text{Real Part of } \Big[I_y (\text{conj } Z_2' + R) \text{ conj } I_x'$$

$$+ R\, I_y \text{ conj } I_y + I_x' (\text{conj } Z_2' + R) \text{ conj } I_y$$

$$+ R\, I_x' \text{ conj } I_x' \Big]$$

$$= \text{Real Part of } \Big[\text{conj } Z_2' (I_y \text{ conj } I_x' + I_x' \text{ conj } I_y)$$

$$+ R\, (I_y \text{ conj } I_y + I_y \text{ conj } I_x' + I_x' \text{ conj } I_y$$

$$+ I_x' \text{ conj } I_x') \Big]$$

$$= \text{Real part of } \Big[\text{conj } Z_2' (I_y \text{ conj } I_x' + I_x' \text{ conj } I_y)$$

$$+ R\, (I_y + I_x') \text{ conj } (I_y + I_x') \qquad .. \quad (2.2.30)$$

From vector geometry, we know that I_y conj I_x' $+ I_x'$ conj I_y $= 2\, I_x'\, I_y \text{ Cos } (I_x', I_y)$. Then equating the real part of the expression on the left of equation (2.2.30) to T, we get,

$$T = \frac{2\ r_2}{1\ \ s}\ I_x'\ I_y\ \cos\ (I_x',\ I_y)$$

$$+ R\ \left| I_x' + I_y \right|^2 \qquad .. \quad (2.2.31)$$

Multiplying equations (2.2.19) and (2.2.20)

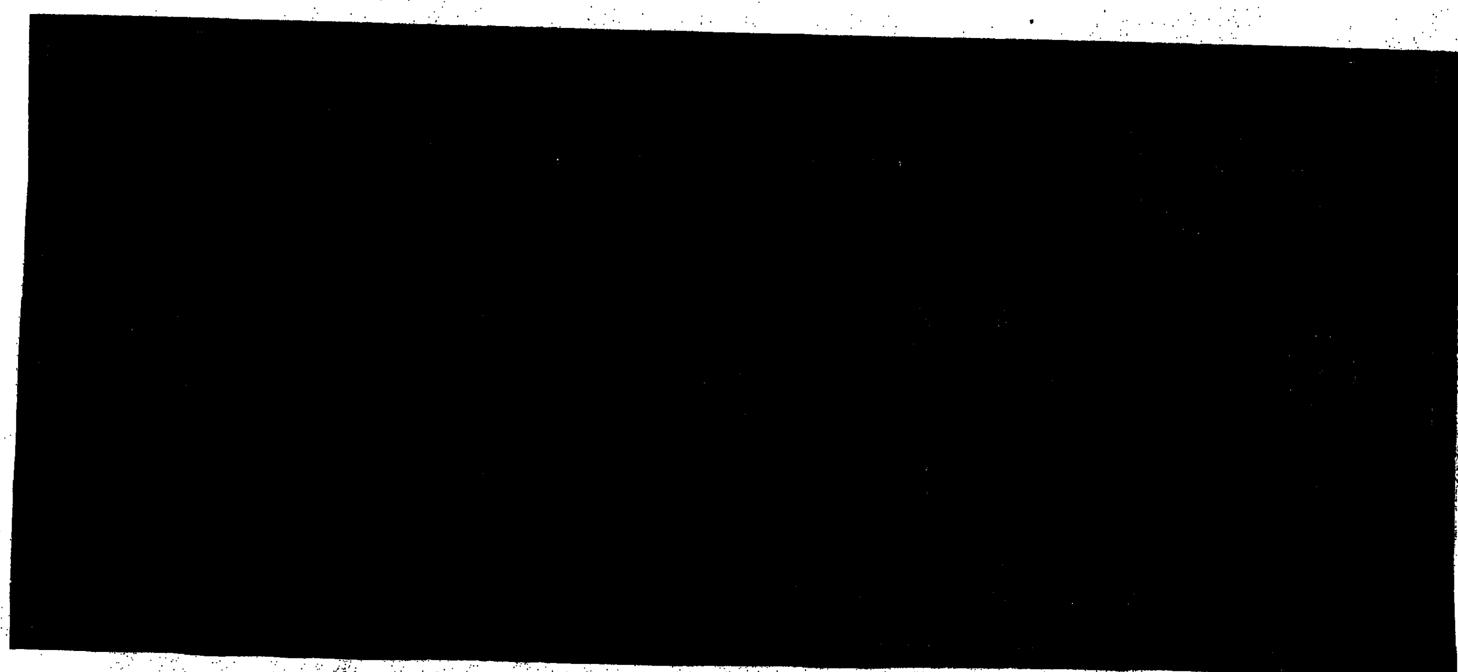


Figure (2.2.8)

by $-j/a$ we find that,

$$E_s' + I_s' \left(\frac{Z_{1s}}{a^2} + \frac{Z_s}{a^2} \right) = \frac{-j\ V}{a} \qquad .. \quad (2.2.32)$$

and $\quad E_s' \quad \frac{Z_s}{a^2}(I_s' - I_x') \quad .. \quad (2.2.33)$

Equations (2.2.32), (2.2.33), (2.2.17) and (2.2.18) can be used to add stator parameters to the rotor circuit of Fig. (2.2.7). The result is Fig. (2.2.8). This is the equivalent circuit of a

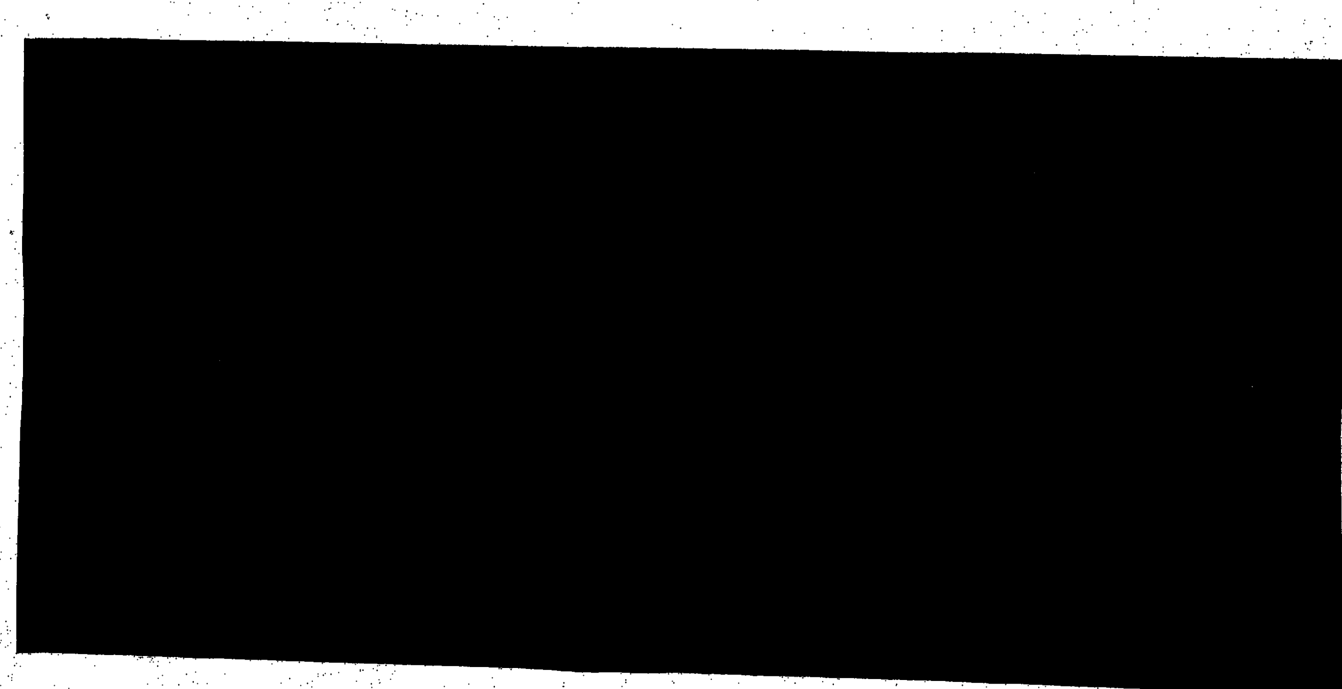


Figure (2.2.8)

capacitor motor.

A plain single-phase motor is equivalent to a capacitor motor in which the capacitor impedance

approaches infinity. With this modification the equivalent circuit of Fig. (2.2.8) reduces to that of Fig. (2.2.9).

Showing I_x' on this diagram in the direction indicated for the capacitor motor, it now takes a negative value. Hence it is evident that the angle between I_x' and I_y is always larger than 90 degrees. This implies that efficiency of a plain single-phase motor is lower than that of a properly designed capacitor motor and that there is always some instant of time in each cycle in which the instantaneous torque is negative.

Based on the above principles, the characteristics of the machine can be predetermined which will be dealt with in detail under "performance calculation".

2.3 A correlation of the cross-field and revolving field concepts:

The revolving field theory of single-phase induction motor operation resolves the total flux crossing the air-gap into two components rotating in opposite direction but constant in magnitude. The cross-

field theory resolves the total flux into two components of varying magnitude but constant direction with reference to the stator. C.T.Button has made an effort (41.02) to consider the single-phase induction motor as it actually is.

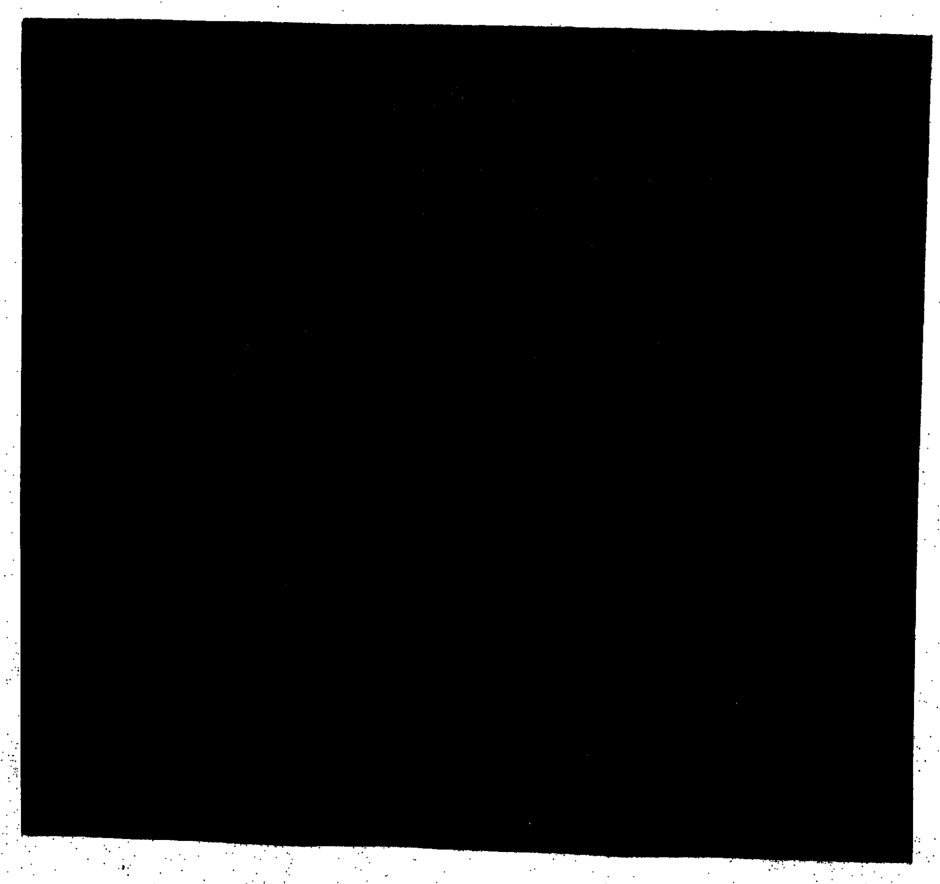


Figure (2.3.1)

Let us consider a two-pole motor with sinusoidal distribution of flux density along the air-gap.

Then the flux density along the x-axis [Fig. (2.3.1)] will be uniform. Let us consider the single coil turning in the field and assume that the coil has no magnetic core. The flux through the coil will be,

$$\phi_{s1} = \Phi_M \sin \omega t \cos \theta \quad .. \quad (2.3.1)$$

$$= \Phi_M \sin \omega t \cos (S \omega t + \alpha)$$

$$= \frac{\Phi_M}{2} \Big[\sin \left\{ (S+1) \omega t + \alpha \right\}$$

$$+ \sin \left\{ (1 - S) \omega t + \alpha \right\} \Big]$$

$$= \frac{\Phi_M}{2} \Big[\sin \left\{ (2-s) \omega t + \alpha \right\}$$

$$+ \sin (s \omega t - \alpha) \Big] \quad .. \quad (2.3.2)$$

Voltage in the coil $= \dfrac{d \phi_{s1}}{dt}$ (times a constant which is here neglected)

$$= \frac{\Phi_M}{2} \Big[(2-s) \omega \cos \left\{ (2-s) \omega t + \alpha \right\}$$

$$+ s \omega \cos (s \omega t - \alpha) \Big] \quad .. \quad (2.3.3)$$

It is seen that this expression for voltage is precisely what we would have if the single-phase field were replaced by two rotating fields of constant magnitude, $\Phi_M / 2$ = half the maximum value of the single-phase field, and each rotating in opposite directions with a velocity of ω radians per second. This would be the voltage in a rotor turn consisting of two diametrically opposite rotor conductors, if this turn were open circuited at some point, and no current flowed in this turn nor in any other rotor conductors.

Referring again to expression (2.3.3), the first component of voltage may be regarded as that due to the backward rotating flux vector (of the revolving field theory), and the other component is due to the forward rotating field. Only under open circuit rotor conditions or at standstill are these two flux components equal. The two voltage components are, then, as follows:

[illegible]

$e_f = \Phi_f \, s \omega \cos (s\omega t - \alpha)$ (constant omitted)

For convenience, [illegible] . . . (2.3.4)

and $e_b = \Phi_b \, (2 - s) \omega \cos \{(2 - s)\omega t + \alpha\}$ [illegible] (2.3.5)

effect [illegible].

The rotor current due to e_f will be

$\frac{e_B}{Z_B}$, and lagging behind the voltage e_B by an angle whose cosine is $\frac{R_B}{Z_B}$. The inphase component of this current is,

$$\frac{\phi_B R_B}{Z_B \, 2} (2-s)\,\omega \cos\{(2-s)\,\omega t + \alpha\} \quad .. \quad (2.3.6)$$

The wattless component of the current due to e_B will be

$$\frac{\phi_B X_B}{Z_B \, 2} (2-s)\,\omega \sin\{(2-s)\,\omega t + \alpha\} \quad .. \quad (2.3.7)$$

The flux per square inch in the x-axis is the product of the mmf. and the permeance per square inch. Now, if the permeance per square inch is constant, each increment of mmf. multiplied by the area it encloses projected in a plane perpendicular to the x-axis would produce a proportional increment of flux in that axis. For convenience, we may then refer to the product of mmf. and its enclosed area thus projected, as a 'magnetising effect'.

For the integral, with α varying from zero to π, the second factor within parentheses in (2.3.9) becomes zero.

In a two-pole motor, two rotor bars diametrically opposite to with the connecting end rings may be considered as a single-turn coil. If the total number of bars or conductors in the rotor is N_b, there will be $(N_b / 2)$ turns (or single-turn coils) in the rotor. Since the angular conductor density is $(N_b / 2\pi)$, if equation (2.3.7) is multiplied by $\sin\theta\,(N_b / 2\pi)\,d\alpha$ and integrated from zero to π, this will include the projected mmf. of every turn in the rotor. The cross-field magnetising effect of the current component given by equation (2.3.7) is thus determined as follows:

$$\int_0^\pi \frac{\phi_2\, X_2}{Z_2\; 2}\,(2-s)\,\omega\,\sin\left\{(2-s)\,\omega t+\alpha\right\}\times\sin\theta\;\frac{N_b}{2\pi}\,d\alpha \qquad (2.3.8)$$

$$=\int_0^\pi \frac{\phi_2\, X_2\, N_b\,(2-s)\,\omega}{2\pi\, Z_2\; 2}\,\sin\left\{(2-s)\,\omega t+\alpha\right\}.\sin\left\{(1-s)\,\omega t+\alpha\right\}d\alpha$$

$$=\int_0^\pi \frac{\phi_2\, X_2\, N_b\,(2-s)\,\omega}{4\pi\, Z_2\; 2}\left[\cos\omega t-\cos\left\{(3-2s)\,\omega t+2\alpha\right\}\right]d\alpha \qquad (2.3.9)$$

For the integral, with α varying from zero to π, the second factor within parentheses in (2.3.9) becomes zero,

and the magnetising effect in the x-axis due to the rotor current of equation (2.3.7) is

$$\frac{\phi_s X_s N_b (2-s)\omega}{4 Z_s^{2}} \cos \omega t \qquad .. \qquad (2.3.10)$$

The corresponding integrated magnetising effect due to the in-phase current component of the expression (2.3.6) is

$$- \frac{\phi_s R_s N_b (2-s)\omega}{4 Z_s^{2}} \sin \omega t \qquad .. \qquad (2.3.11)$$

The cross-magnetising effect of the slip-frequency rotor current is similarly determined as follows, considering first the reactive component:

$$\int_0^{\pi} \frac{\phi_r X_r}{Z_r^{2}} s\, \omega \sin (s\omega t - \alpha) \sin \left\{(1-s)\omega t + \alpha\right\} \frac{N_b}{2\pi} d\alpha \qquad (2.3.12)$$

$$= \int_0^{\pi} \frac{\phi_r X_r N_b \omega s}{4\pi Z_r^{2}} \left[\cos \left\{(2s-1)\omega t - 2\alpha\right\} - \cos \omega t\right] d\alpha$$

$$- \frac{\phi_y X_y N_b \omega s}{4 Z_F^2} \cos \omega t \qquad .. \qquad (2.3.13)$$

Similarly, the magnetising effect of the slip-frequency rotor current in phase with the forward flux is

$$\frac{\phi_y R_2 N_b \omega s}{4 Z_F^2} \sin \omega t \qquad .. \qquad (2.3.14)$$

The total magnetising effect or effective rotor mmf. in the x-axis is the sum of equations (2.3.10) (2.3.11), (2.3.13) and (2.3.14). The rotor current due to ϕ_B is primarily responsible for positive cross-field and the rotor current due to ϕ_F subtracts from it. Since

$$X_F = (2 - s) X_B$$

we have now a double frequency component in the cross-field. This double frequency component does not come in when we analyse by the cross-field theory.

The condition at synchronous speed for the

flux variation through the rotor is shown by Fig. (2.3.2). Vector F S is the backward rotating flux, and rotates at twice synchronous speed(with respect to the rotor). Vector O F is the forward rotating component and is fixed

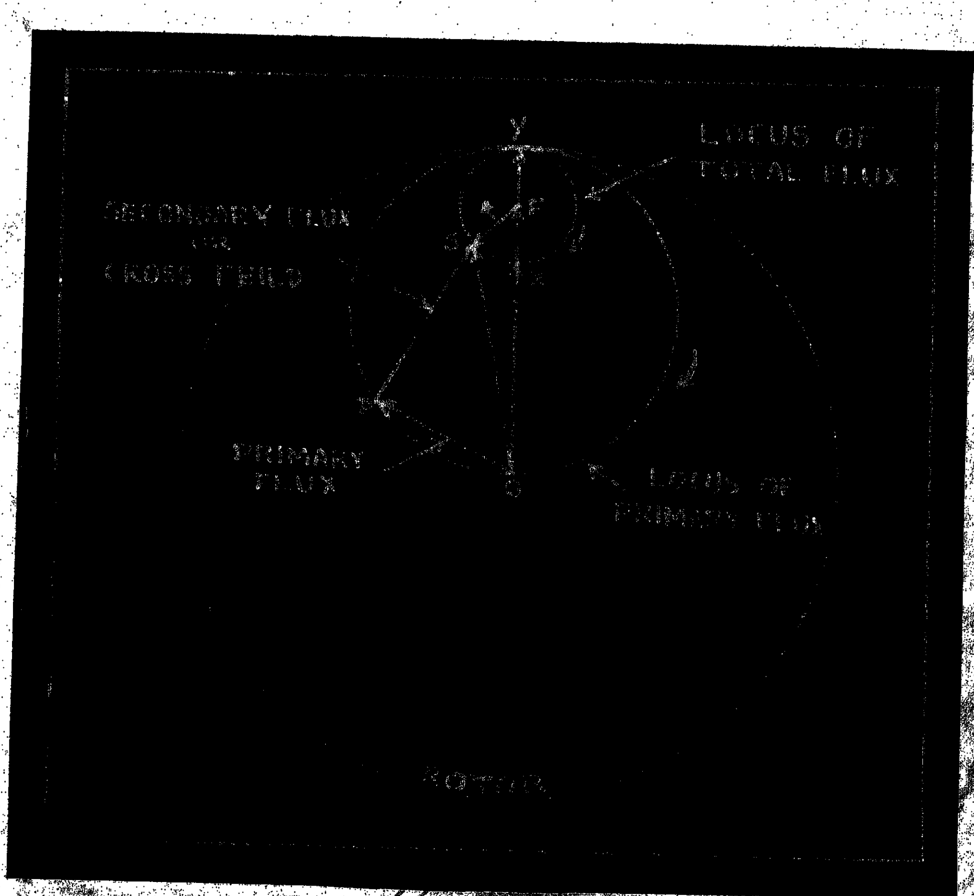


Figure (2.3.2).

with respect to rotor at synchronous speed. OX is the maximum value of the cross-field.

Fig. (2.3.3) shows the total flux locus

with respect to the rotor at a given slip. The locus of the total flux traversing the rotor describes a hypotrochoidal curve with respect to it.

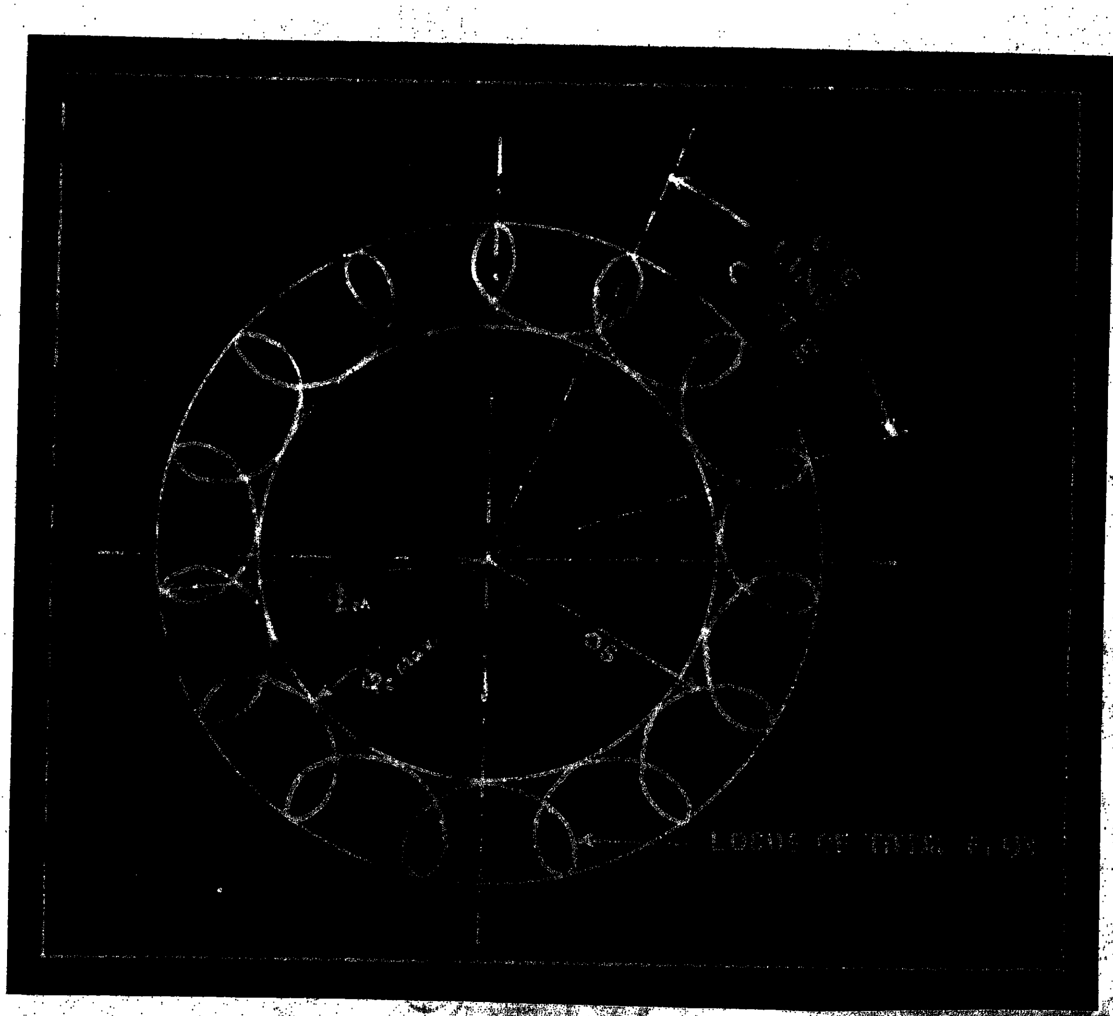


Figure (2.3.3)

These are the actual conditions that exist in a single-phase induction motor. Based on these

principles expressions for the stator current, and torque have been derived by Button which can be shown to be in good agreement with those derived from either the cross-field theory or the double revolving field theory.

Also, Arnold, it is said, has given a rigorous proof of the equivalense of these two theories in 1909 in a book of his.

2.4 Comparison of the Two Theories:

It can be proved that the current-voltage equations obtained by means of the revolving field theory are equivalent to those obtained from the cross-field theory. In other words, the results arrived at by both lines of reasoning are identical and the final equations obtained through the use of either method can be expressed in the language of the other by mathematical transformation.

It might be questioned why two approaches should be used to attain the same end; it might further be questioned as to whether one of these theories does not have important advantages over the other. In view of these natural questions V.J.Morrill enunciates the following as what should be expected from a good motor theory (41.03);

1. A good theory should present an accurate picture by means of which mathematical expressions for the current, torque etc. may be obtained.

2. It should furnish the simplest possible picture concerning the important phenomena consistent with the accuracy desired.

3. The theory should furnish means for readily considering the effects of minor phenomena when such considerations becomes necessary or desirable.

4. It should, if possible, present a picture readily susceptible to high-handed simplification for the determination of limiting conditions such as no-load, standstill, balanced operation etc.

5. The theory should preferably not change form or require a new mathematical analysis when slight normal modifications of structure are made.

6. Finally, if with no extra complication, the theory can show the relation between the motor in hand and motors of other types this is desirable, particularly in an operating design department where motors of many types and connections must be handled simultaneously.

Keeping these views in mind, we shall now try to compare the two theories:

1. In the matter of <u>accuracy</u> the revolving field theory and the cross-field theory are equivalent because both give correct expressions for current, torque etc.

2. The <u>simplicity</u> of the one theory as compared with the other is perhaps a matter of personal opinion. In the case of a plain a.c. commutator motor, the cross-field theory seems the simpler; in the case of induction motors the revolving field theory seems simpler.

3. When it is desired to consider minor phenomena such as the effect of stator harmonics, the revolving field theory appears to have some real advantages.

The effect of stator harmonics is readily determined with the revolving field theory by first calculating for each harmonic its magnetising reactance, secondary reactance and secondary resistance. Using these harmonic constants a single-phase equivalent circuit may be constructed for each harmonic and properly connected in series with the fundamental equivalent circuit as shown in Fig. (2.4.1). Using this circuit the complete characteristics, including

harmonic effects may be determined.

It is difficult to see how the cross-field theory could so simply yield results in connection with the minor phenomena.

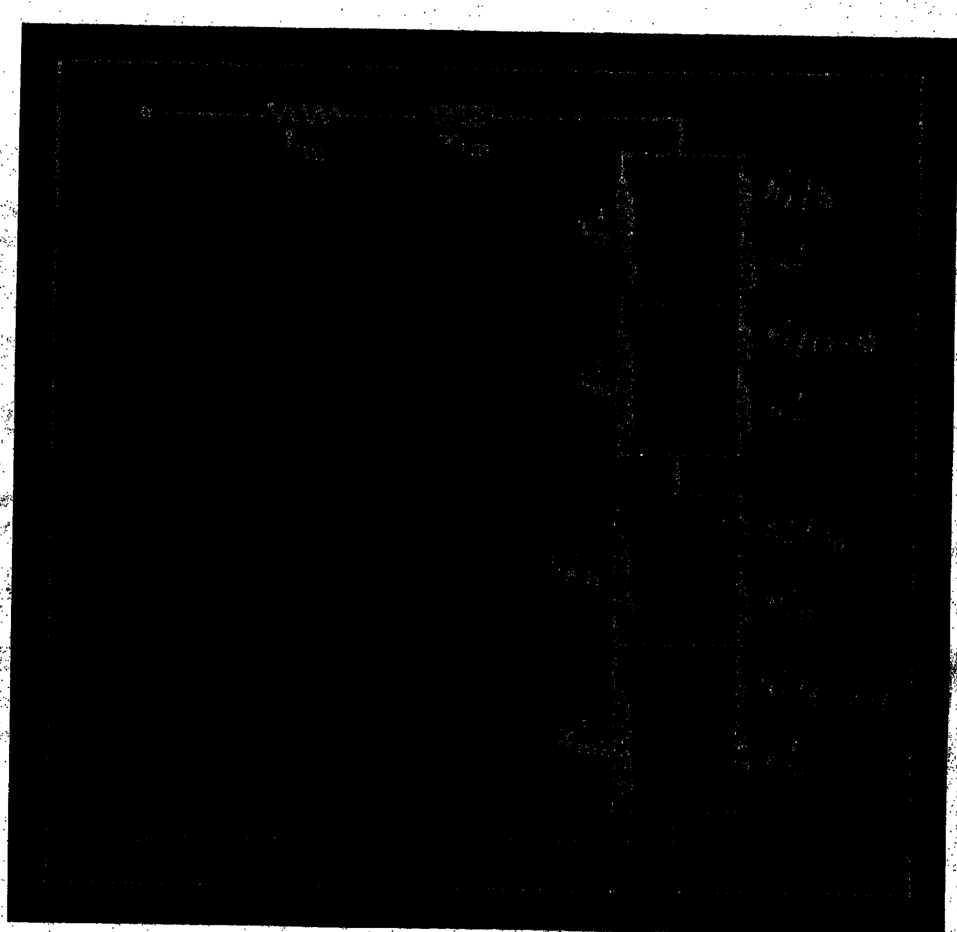


Figure ([illegible])

4. When it is desired to make high-handed simplifications to quickly determine by inspection what will happen under certain limiting conditions the revolving-

field theory really demonstrates its advantages.

At standstill the forward and backward impedances become equal and if x_m' is very large it may, without serious error, be assumed infinite and Fig. (2.4.2)(a) will apply.

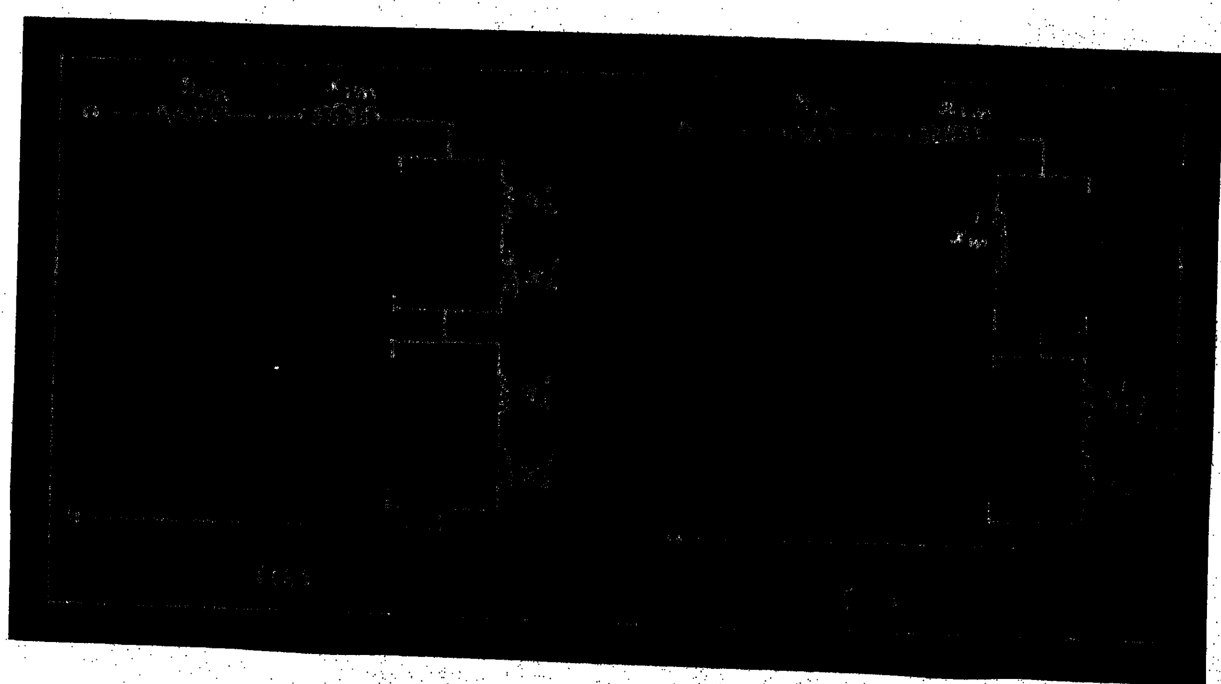


Figure (2.4.2)

At forward synchronism the slip becomes zero, and the forward-field secondary impedance becomes infinite. Since the backward slip is 2, the backward secondary impedance is usually very low with respect to x_m' and without serious error the circuit may be represented

as in Fig. (2.4.2)(b).

If it is desired to learn the no-load speed (rotational iron and mechanical losses neglected), it is merely necessary to equate the forward and backward field apparent resistances and solve for 's' . A very easy and very nearly accurate method is to assume that at no load the voltages impressed on the forward and backward fields will be the same as at synchronism. On this basis the no-load slip may be expressed as:

$$s_o \times \frac{E_{fo}^{\,2}}{r_2'} = I_o^2 \; r_m' \qquad .. \; (2.4.1)$$

therefore, $$s_o = \left[\frac{I_o}{E_{fo}}\right]^2 r_2' \; r_m' \qquad .. \; (2.4.2)$$

If it is desired to determine the no-load speed including the effect of rotational losses, it is merely necessary to add the rotational losses to the right hand side of equation (2.4.1).

In a similar way, such questions as what would happen if the secondary resistance or reactance were

zero and what would happen if x_m were made very low, can be readily answered.

5. A modification of induction motor design often resorted to is the multi-cage rotor. The equivalent circuit for a single-phase double-cage motor is as shown in Fig. (2.4.3). Branches (1), (2) and (3) can be re-

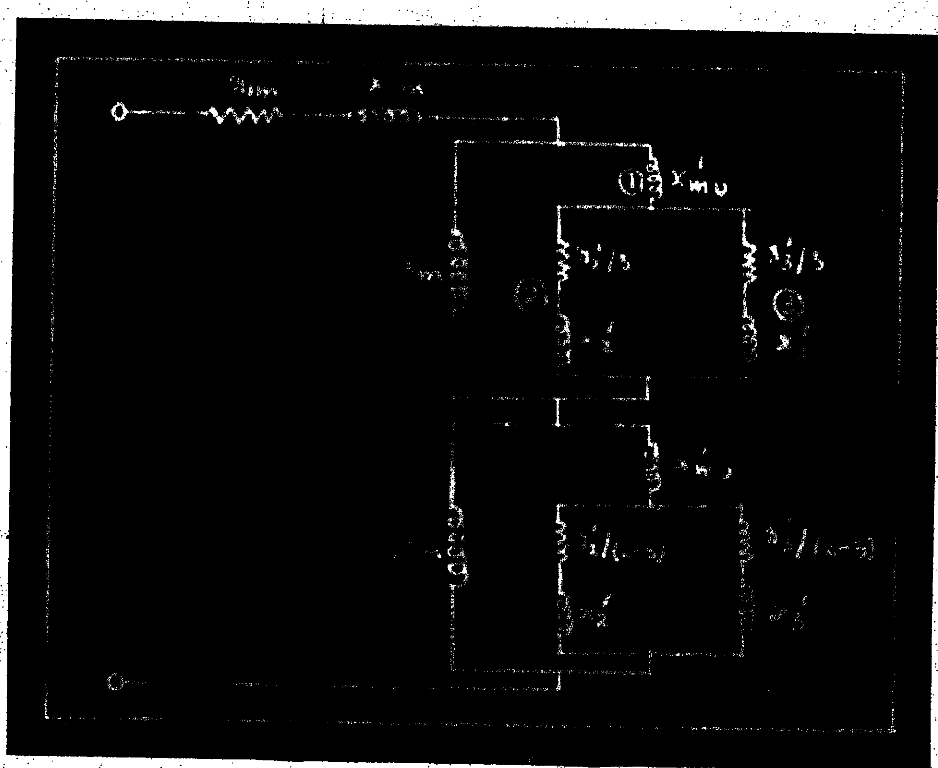


Figure (2.4.3).

duced to a simple and resistance and reactance in series after which the calculation of performance is exactly as

easy as that of a single-cage motor. The same calculation form will handle both calculations. In the case of the cross-field theory, the introduction of a double-cage rotor requires a new theoretical development.

6. When the revolving field theory is used, the current and torque equations for a balanced polyphase motor appear as a special case of the unbalanced motor and the constants and symbols are very closely related. This is advantageous in an operating department in that it permits of handling all induction motors, regardless of type, by means of the same theory. The cross-field theory on the other hand, bears little resemblance to usual polyphase motor theory. As Dr. A.E.Kennelly puts it (98.02) the relation between the polyphase induction motor and the single-phase induction motor is perhaps more readily comprehended by the mental device of assuming a double rotation of the field than in any other way. That is the physical conception of the cross-field theory appears to be rather inferior to the rotating field theory.

From the view point of generality, the revolving field theory appears to be the more general one of the two. If the two components of the revolving field are equal, we have a single-phase system; if they

are unequal, we have an unbalanced polyphase system. If one component vanishes, we have a balanced polyphase system and, if the angular velocity of the rotating field is equal to zero, we have a direct-current system (41.04).

As already stated, the currents in the rotor bars are of two different frequencies. This has been duly taken into consideration by the double revolving field theory and the skin effect can be taken into account by suitably altering the "backward rotor" circuit $r_2'/2-s$. On the other hand, the cross-field theory completely ignores it.

Probably the only consideration of which the cross-field theory can claim an advantage over the revolving field theory is in the fact that different saturation in the two axes can be considered more easily with the cross-field theory. Even here it must not be forgotten that the fluxes in the two axes in fact do not exist separately and that in the presence of unequal saturation, the fluxes in the two axes cannot be assumed to remain independant of each other which is a basic assumption on which this method of analysis depends.

Whatever may be the relative merits of the two theories, both are useful and a knowledge of both points of view is essential. A complete understanding of design can be obtained only by a mastry of both the theories.

--

CHAPTER - III.

SPECIAL PROBLEMS.

3.1 TORQUE.

3.1.1 Experimental study:

A.L.Kimball and P.L.Alger have analysed the vibrations in a single-phase induction motor in the following manner (24.01): A 25-cycle, 1/4 h.p., single-phase induction motor was placed on a light board base resting on several layers of thick felt. On running the motor, the board base readily took up the vibrations of the motor stator, because of the small intertia of the board compared with that of the motor, and because of the yielding quality of the felt upon which it rested. At normal voltage the motor vibrated very noticeably. On raising the voltage the vibrations of the motor became much more intense. When the voltage was reduced to a low value, it was found that a certain amount of vibration still remained and that the no change in this amount resulted immediately after opening the motor circuit.

Since the no-load speed of rotation of an induction motor is practically constant, independent of

the voltage, any vibration due to mechanical unbalance should be unaffected by voltage variations. Thus, the tests showed that the motor vibration was due in part to mechanical unbalance, which persisted down to the lowest voltage, and in part to electromagnetic forces which increased with the voltage.

As the frequency of the vibration due to mechanical unblance is known to be equal to the number of revolutions per second, the above conclusions were verified by measuring the vibration frequencies. It was found that the frequency of the vibration remaining at low voltage was closely equal to the frequency of rotation. Further-more, it was found that when a rotor was given a very careful running balance, this type of vibration could be practically eliminated, thus definitely proving it to be deue to mechanical unbalance.

After obtaining a good running balance, so that the motor was almost free from vibration at very low voltages, a further study of the electromagnetic vibration was made. Placing a 25-cycle motor upon a light board resting on a felt as before, the vibration frequency

was found to be approximately twice line frequency, or 50-cycles per second. Also, preliminary measurement made with a vibration amplitude indicator gave amplitudes approximately proportional to the square of the voltage. This would be expected of a vibration of electromagnetic origin since the magnetic forces vary approximately as the square of the voltage below magnetic saturation.

To prove the existence of double frequency pulsating torque, it now remains to be shown that the double frequency vibrations are purely torsional in nature. This had been done by Kimball and Alger as follows: The motor was then suspended in such a way that it could vibrate almost perfectly freely in space, without even so small a resistance as that offered by the felt. This was accomplished by placing the motor in a cradle as shown in Fig. (3.1.1) so designed as to allow any sort of a translational or rotational motion without appreciable restraint. Its freedom of motion was facilitated by suspending it from cords attached to P and Q which were nearly at the height of the centre of gravity, of the motor, and hanging these cords from the end of a flexible cantilever.

When a rotor in good static balance was placed on the cradle as shown in Fig. (3.1.1) and tested at very low voltage, the centre line AB of the cantilever was found to be perfectly still, since the centre of gra-

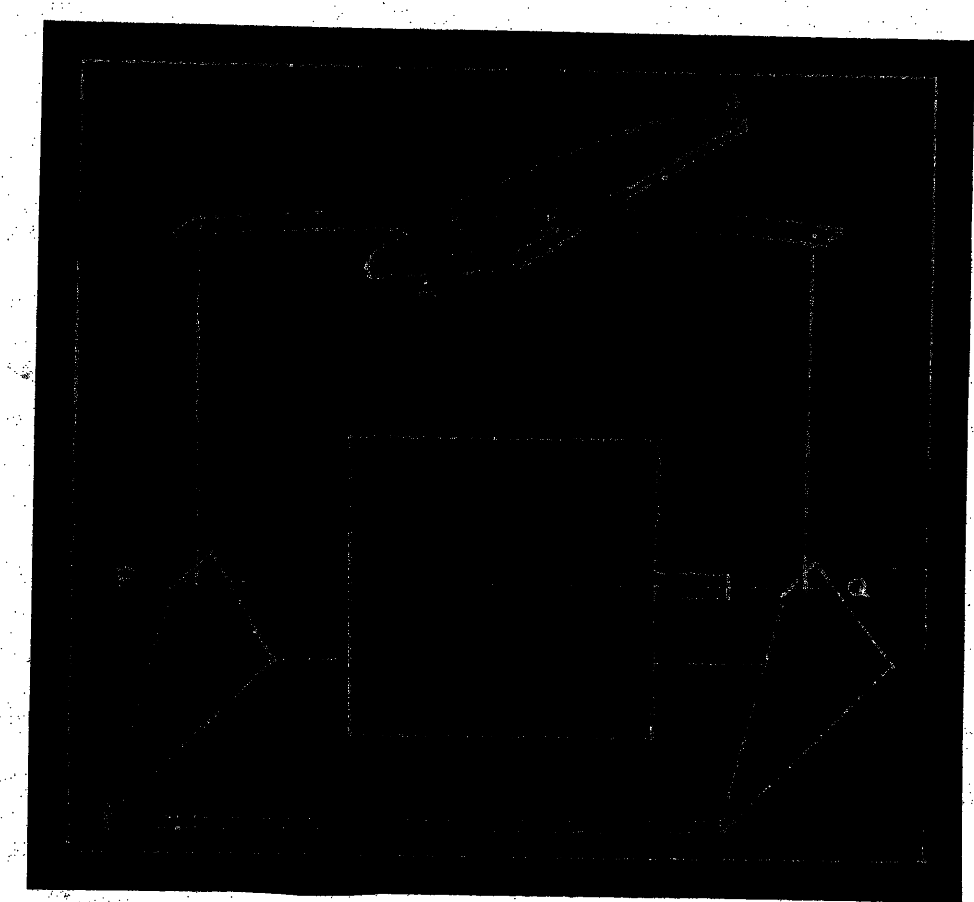


Figure (3.1.1)

vity of the motor remained fixed in space. However, in many such cases, the cantilever took up a torsional vibration with AB as a nodal line, the right and left arms

vibrating up and down. This was evidently due to dynamic unbalance, so called because it can only be detected by a test in which the motor is actually rotating. It is manifested by a tilting or wobbling motion of the shaft, the centre of gravity of rotor remaining fixed.

After a rotor was given complete running balance, it was found that all vibration of the cantilever disappeared. In short, by this method of suspension mechanical unbalance could be detected as to character and approximate magnitude. When a rotor was given no careful balance, both an up and down, and a torsional motion of the cantilever were observed.

When a carefully balanced 25-cycle motor was suspended in the cradle, the vibrations appearing as the voltage was raised were found to be always characterised by the appearance of a nodal line along the baseboard upon which no vibration could be felt. However, when the motor was placed in the cradle, this line of no vibration was found to lie centrally under the shaft, while elsewhere vibrations occurred of severity proportionate to the voltage, which increased in direct ratio with the

radial distance from this nodal line. This indicated the presence of a torsional vibration through a small angle about an axis parallel to the shaft, and since a rigid body performing such a vibration must oscillate about the centre of gravity, it can immediately be concluded that this axis coincides with the shaft itself. The vibration could be shown to be purely torsional with no transverse components, by observing that even with very high voltages producing a very strong vibration of the base, no vibration of the cantilever could be detected with the motor placed with its axis at right angles to the cantilever as shown in Fig.(3.1.1)

When the motor was turned 90 degrees so that its axis was cross-wise, a node of zero up and down vibration of the board appeared as before along the line directly under the motor shaft. The ends of the board, however, vibrated up and down, communicating their motion to the suspending cords and setting the cantilever in torsional vibration about AB as an axis.

These experiments prove the existence of double-frequency pulsating torque in a single-phase induction motor.

3.1.2 Theoretical Analysis:

The power input to a single-phase circuit is necessarily of pulsating character, as each time the incoming current or the voltage passes through zero, the power does likewise. No matter what the power factor is, a single-phase a.c. circuit always draws from the line

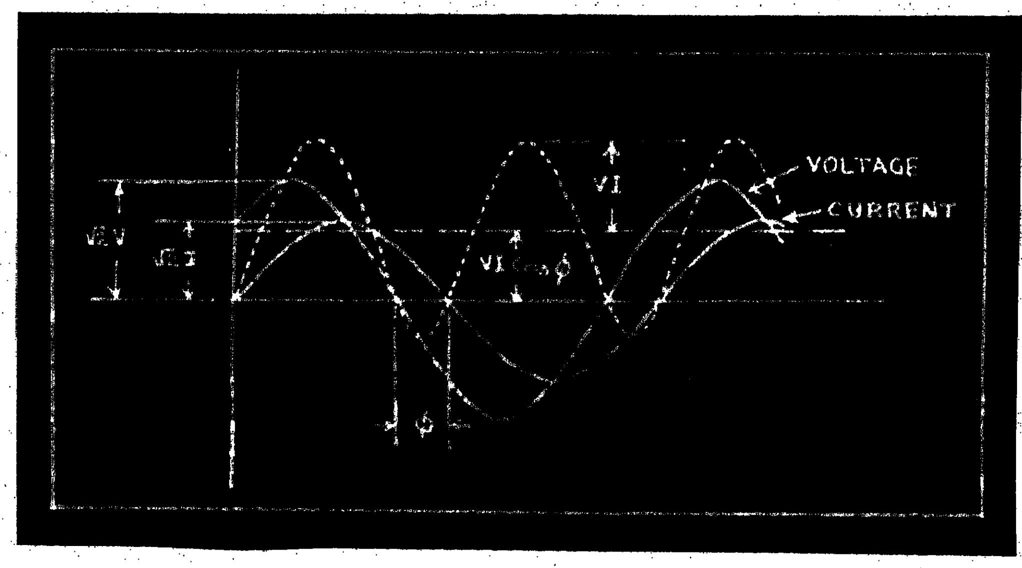


Figure (3.1.2)

a double frequency alternating power equal to the full volt amperes. The 'active' power is the average power input and is proportional to power factor. The maximum power-flow is the sum of the active (or average) power, and the alternating power, as Fig. (3.1.2) shows.

Voltage impressed on a single-phase circuit $= \sqrt{2}\ V \sin \omega t$

Current flowing in a single-phase circuit $= \sqrt{2}\ I \sin(\omega t - \phi)$

Power factor angle $= \phi$

Then, at any instant the power flowing in the line is:

$$2\ V\ I \sin \omega t \sin(\omega t - \phi)$$

$$V\ I\ [\cos \phi - \cos(2\omega t - \phi)]$$

which consists of two parts:

$V\ I \cos \phi$ is a uniform 'active' power flowing always in one direction, and equal in magnitude to r.m.s. volts × r.m.s. amperes × power factor. $V\ I \cos(2\omega t - \phi)$ is an alternating power which flows to and fro at double frequency, and whose maximum amplitude is equal to r.m.s. volts × r.m.s. amperes, independent of the power factor. The sum of the two gives the total power which pulsates at double frequency from a maximum value in the positive direction equal to (1 + power factor) × r.m.s. volts × r.m.s. amperes to a maximum value in the negative direction

equal to (1 - power factor) r.m.s. volts r.m.s. amperes, as indicated in Fig. (3.1.2).

Since the power inflow to a single-phase motor is pulsating, whereas the power taken by the load is uniform, the incoming energy must be alternately

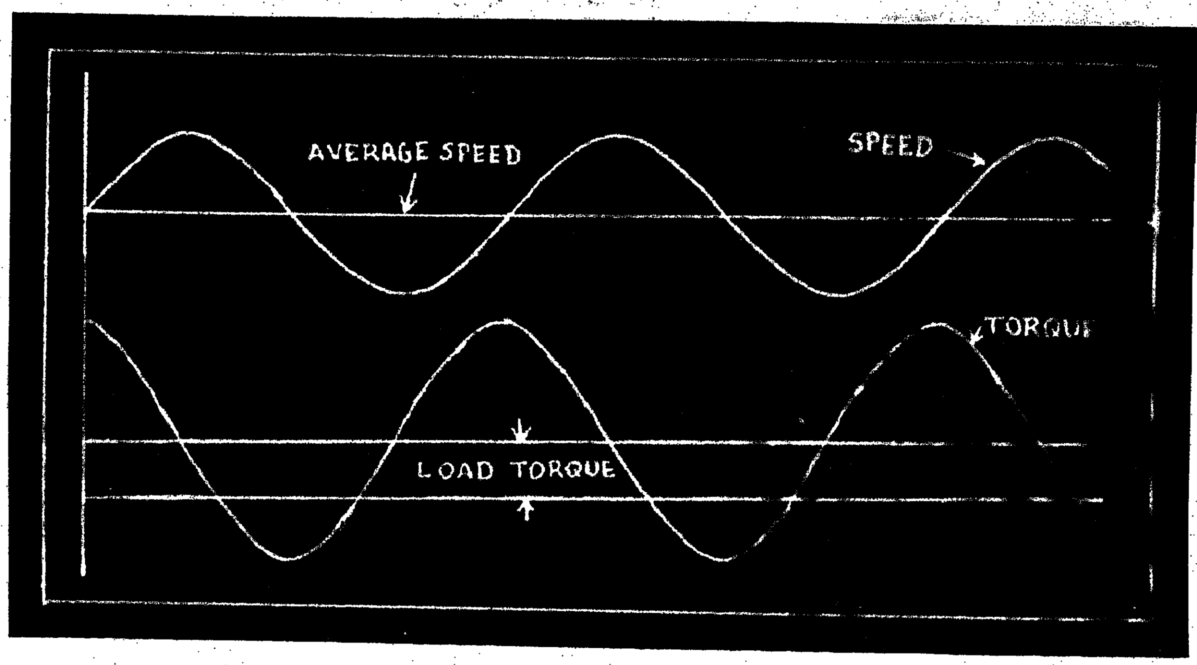


Figure (3.1.3).

stored during the peaks and supplemented by released energy during depressions. Thus, a considerable capacity for energy is required, and the energy stored must increase with the load. This energy is stored as kinetic energy

in the revolving parts, so that the torque exerted by the single-phase motor is of pulsating character corresponding to the electrical input and the teret rotor speed continually fluctuates up and down in response to the torque variations as indicated in Fig. (3.1.3).

3.1.3 Expressions for Average and Pulsating Torques:

The equivalent circuit of a single-phase induction motor, neglecting iron losses, based on the double revolving field theory is given in Fig. (2.1.3). Referring to this circuit, the equations are:

$$I_{2f}' = \frac{j\, I_m\, x_m'}{\frac{r_2'}{s} + j\,(x_m' + x_2')} \quad .. \quad (3.1.1)$$

$$I_{2b}' = \frac{j\, I_m\, x_m'}{\frac{r_2'}{2-s} + j\,(x_m' + x_2')} \quad .. \quad (3.1.2)$$

$$E = j\, x_m'(2\, I_m - I_{2f}' - I_{2b}') \quad .. \quad (3.1.3)$$

$$= j\, 2\, I_m\, x_m' \left[\frac{r_2'^2 + j\, r_2'\, (x_m' + x_2') - s(2 - s)x_2'(x_m' + x_2')}{r_2'^2 + 2j\, r_2'\, (x_m' + x_2') - s(2-s)(x_m' + x_2')^2} \right]$$

.. (3.1.4)

and $E = V - I_m (r_{1m} + x_{1m})$

Since the forward and backward fields exist in a common magnetic structure, each flux makes a torque with each current, or there are in all, four separate torques.

The torque produced by the forward revolving flux with I_{2f}' is of constant magnitude, independent of the time; as is also the torque produced by the backward field with I_{2b}'. This is true for the reason that we are considering fluxes of constant magnitude but moving in space.

The principal, or load, torque is that due to the action of the forward revolving flux and I_{2f}'. This torque in synchronous watts is,

$$T_{ff} = j\,(I_m - I_{2f}')\, x_m'\, I_{2f}'$$

$$= I_{2f}'^{\,2} \left(\frac{r_2'}{s} + j\, x_2' \right) \qquad .. \quad (3.1.5)$$

The j terms here only measure the phase displacement in space, and so may be dropped without error. Therefore, the steady synchronous watt torque is, from equations (3.1.1) and (3.1.5):

$$T_{ff} = \frac{E^2\, r_2'\, s\, \left[r_2'^{\,2} + (2-s)^2\, (x_m' + x_2')^2 \right]}{4 \left[r_2'^{\,4} + r_2'^{\,2}\, (x_m' + 2\, x_2')^2 - 2\, s(2-s)\, r_2'^{\,2}\, x_2'\, (x_m' + x_2') + s^2\, (2-s)^2\, x_2'^{\,2}\, (x_m' + x_2')^2 \right]} \qquad .. \quad (3.1.6)$$

At standstill, when $s = 1$, equation (3.1.6) reduces to:

$$T_{ff} = \frac{E^2\, r_2'}{4\,(r_2'^{\,2} + x_2'^{\,2})} \quad \text{at standstill} \qquad .. \quad (3.1.7)$$

Similarly, the synchronous torque due to the backward field and I_{2b}' is:

$$T_{bb} = j\,(I_m - I_{2b}')\, x_m'\, I_{2b}'$$

$$= I_{2b}'^{\,2} \left(\frac{r_2'}{2 - s} + j\, x_2' \right) \qquad .. \qquad (3.1.8)$$

Dropping the j terms in equation (3.1.8) and eliminating I_{2b}' by equations (3.1.2) and (3.1.4);

$$T_{bb} = \frac{E^2\, r_2'\, (2 - s) \left[r_2'^{\,2} + s^2\, (x_m' + x_2')^2 \right]}{4 \left[r_2'^{\,4} + r_2'^{\,2}\, (x_m' + 2\, x_2')^2 - 2\, s(2 - s) r_2'^{\,2}\, x_2'\, (x_m' + x_2') + s^2\, (2 - s)^2\, x_2'^{\,2}\, (x_m' + x_2')^2 \right.} \qquad .. \qquad (3.1.9)$$

When $s = 1$, equation (3.1.9) also reduces to equation (3.1.7), so that the backward and forward field torques are equal and opposite at standstill Fig. (3.1.4). As T_{ff} and T_{bb} are both invariant in time, the standstill torque is zero at every instant.

The net constant torque in synchronous watts is equal to the difference of equations (3.1.6) and (3.1.9), or to:

$$T_{ff} - T_{bb} = \frac{E^2\, r_2'\, (1 - s) \left[s(2 - s)(x_m' + x_2')^2 - r_2'^2 \right]}{2 \left[r_2'^4 + r_2'^2\, (x_m' + 2\, x_2')^2 - 2\, s(2 - s) r_2'^2\, x_2'\, (x_m' + x_2') + s^2\, (2 - s)^2\, x_2'^2\, (x_m' + x_2')^2 \right]} \quad .. \ (3.1.10)$$

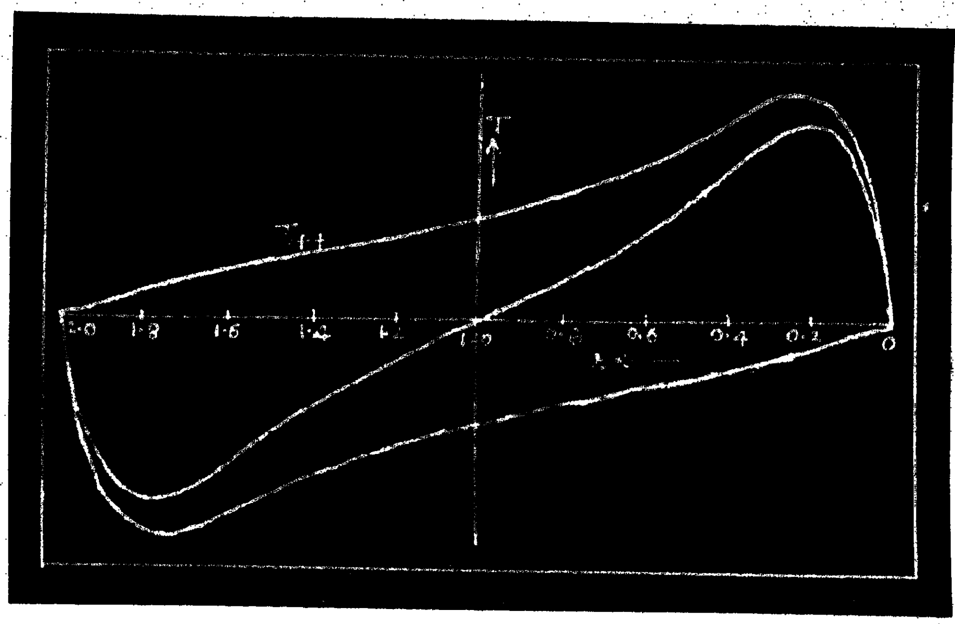


Figure (3.1.4).

Equation (3.1.10) has the same value for any particular value of 's' as it has for the same value of (2 - s), though the sign is reversed, so that the motor torque curve is symmetrical about the point of zero

speed [Figure (3.1.4)] . The output is equal to (1 -s) times expression (3.1.10).

At no load, or running light, expression (3.1.10) is equal to zero, neglecting the friction and windage losses, so that

$$s_o = \frac{r_g'^2}{2\,(x_m' + x_g')^2} \quad \text{at no load} \qquad .. \; (3.1.11)$$

To calculate the alternating power, we must take the sum of the product of the backward field voltage by I_{gf}' and the forward voltage by I_{gb}' . The phase relations of I_{gf}' and I_{gb}' with the fluxes they act upon are of no importance here, but the phase relations of the two torques they make are important.

The voltage representing the forward flux is:

$$\begin{aligned} e_f &= -j\, x_m'\,(I_m - I_{gf}') \\ &= I_{gf}'\,(\frac{r_g'}{s} + j\, x_g') \qquad .. \qquad (3.1.12) \end{aligned}$$

and that representing the backward flux is:

$$e_b = j\, x_m' \, (I_m - I_{2b}')$$

$$= I_{2b}' \left(\frac{r_2'}{2 - s} + j\, x_2' \right) \qquad .. \quad (3.1.13)$$

Since the relative speeds of I_{2f}' and e_b, and of I_{2b}' and e_f are twice synchronous speed the torques made by their interaction are double-frequency torques. The synchronous double-frequency torque is :

$$T_{2\omega} = T_{fb} - T_{bf}$$

$$= e_f \, I_{2b}' - e_b \, I_{2f}'$$

$$= \frac{2\, I_{2b}' \, I_{2f}' \, (1 - s) \, r_2'}{s\,(2 - s)} \qquad .. \quad (3.1.14)$$

At standstill, when $s = 1$, the alternating torque also reduces to zero. Evaluating equation (3.1.14) by means of equations (3.1.1), (3.1.2) and (3.1.4), it becomes,

$$T_{2\omega} = \frac{(1-s)E^2\, r_2' \left[r_2'^2 + 2j\, r_2' (x_m' + x_2') - s(2-s)(x_m' + x_2')^2 \right]}{2 \left[r_2'^2 + j\, r_2' (x_m' + 2x_2') - s(2-s)\, x_2' (x_m' + x_2') \right]^2} \quad \ldots (3.1.15)$$

The very same results can be arrived at by the cross-field analysis also.

3.2 NOISE AND VIBRATION:

Among the various applications of single-phase induction motors, domestic appliances which require fractional horse-power motors, stand foremost. And the necessity of a quiet home cannot be overstressed. This necessitates the elimination of noise, as far as possible, produced by them. Further, even in a industrial applications the noise level must be brought down to a minimum as noise has an adverse effect on human-efficiency. The study of the problem of noise can be classified as follows:

1. Characteristics of the human ear.
2. Production of noise and vibration.
3. Measurement of noise.
4. Elimination of noise.

3.2.1 Characteristics of Human Ear:

The properties of the ear are of fundamental importance in the study of noise since it is through the medium of ear that the noise is observed.(B.9) The frequency and amplitude ranges over which a normal ear receives auditory sensations are illustrated in Fig.(3.2.1) Frequencies below about 20 cycles are perceived by feeling rather than hearing, while frequencies above 20,000 cycles are not heard by most ears. The limit marked "Threshold of feeling" in Fig. (3.2.1) represents the point at which the sound intensity becomes great enough to produce a sensation of pain, while the limit marked" Threshold of audibility" represents the minimum sound audible to the normal ear. It is to be noted that the sensitivity of the ear depends upon the frequency and is maximum in the range 1,000 to 3,000 cycles.

The smallest variation in sound amplitude

that the ear is able to perceive is roughly a constant percentage of the original intensity, which is equivalent to stating that the loudness of a sound as measured by

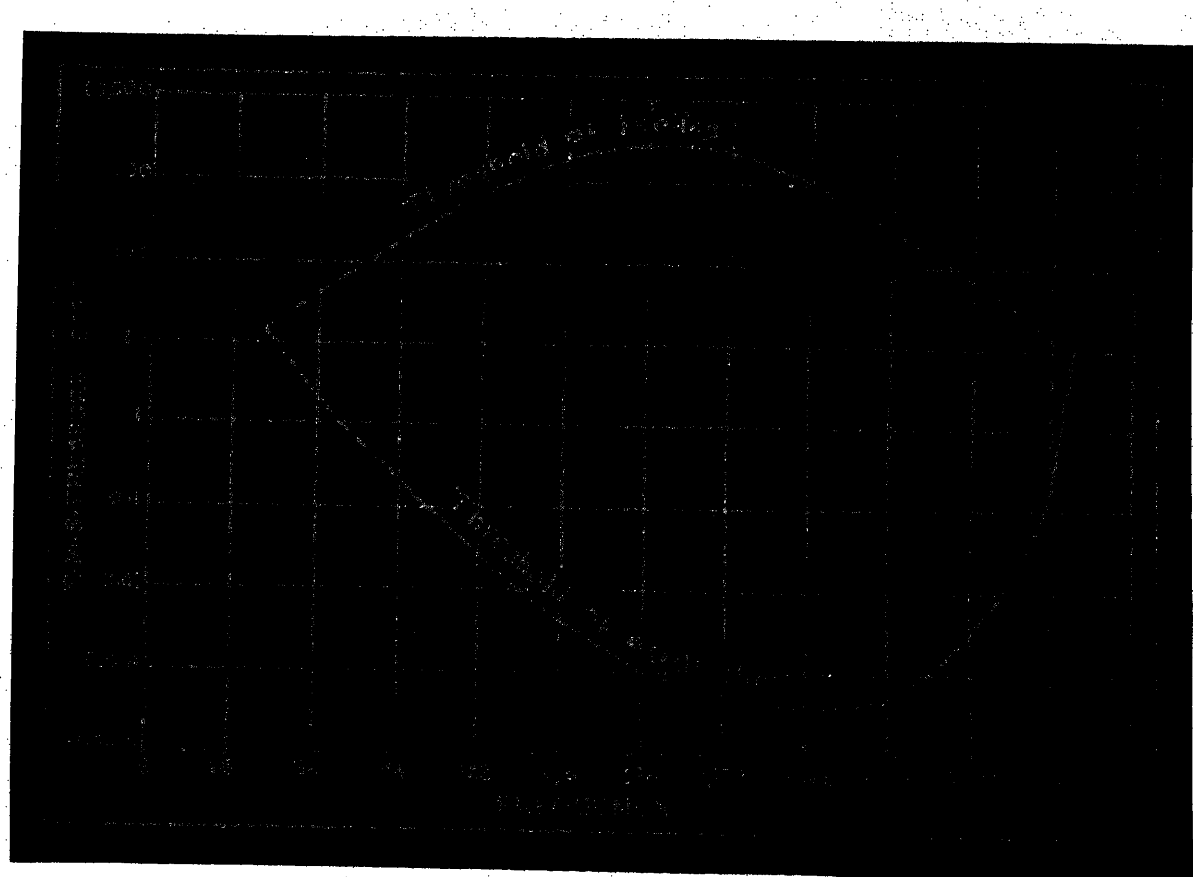


Figure (3.2.1)

the ear is proportional to the logarithm of the sound intensity. The minimum percentage of change in sound energy that is detectable, is in the order of 10 percent (0.4 db), in the middle range of frequencies at moderate

intensities. It is greater when the intensity is low or when the frequency is high or low.

3.2.2 Production of Noise and Vibration:

The main reason for the noisy operation of a motor is poor manufacture like unbalanced rotor loose bearings, excessive end play etc. Apart from these, the noise may be of electromagnetic origin also. The different electromagnetic souses of noise and vibration in single-phase motors are:

a) Pulsating torque.
b) Magnetostriction.
c) Coil vibration.
d) Magnetic forces set up in the air gap.
e) Other causes.

a) Pulsating Torque: As has already been shown, there is double frequency pulsating torque present in a single-phase induction motor. This produces torsional vibration and generates transmitted noise. Consequently, the single-phase machine is inherently noiser than its polyphase counterpart.

b) Magnetostriction: (42.01). A magnetic material, when magnetised, changes its dimensions. This phenomenon is known as "Magnetostriction". Most of the steels used in electrical machines lengthen parallel to the direction of the flux lines and contract at right angles when the intensity of the magnetisation is increased. This change in the dimensions of the sheet steel is independent of the polarity of magnetisation and hence an alternating flux causes, the core surface to pulsate at twice the supply frequency. Even though the variation in the dimensions of the core is small (about 0.0002 per cent), it is enough to set up sound waves in the surrounding medium.

c) Coil Vibration: (58.01). When the conductors in a motor carry currents, forces are set up which cause vibration of the conductors. These forces are proportional to the square of the current and if the load current is sinusoidal, the vibrations will, then, be at double frequency. However, this source of noise is not appreciable.

d) Magnetic Forces set up in the Air gap:

The air-borne noise arising from an electric motor has as its principal source, the vibration of the stator frame and yoke structure (40.01). The magnetic forces set up in the air gap of the motor cause the frame structure to be distorted periodically with time and the external surface of the frame in turn beats the air causing air-borne noise.

In addition to the fundamental air-gap fluxes produced by the current in the rotor and stator windings, harmonic fluxes are also produced. Good winding distributions generally limit the magnitude of the harmonics of low order. But, with any given slot combination and fundamental number of poles, the magnitude and orders of the tooth harmonics are definitely determined in relation to the fundamental flux. There always exist an infinite series of tooth harmonics having magnitudes and orders as shown below:

$$\text{Order of harmonic} = \frac{\text{harmonic poles}}{\text{fundamental poles}} = 2Kn \pm 1 \quad ..(3.2.1)$$

$$\text{Amplitude of harmonic wave} = A_1 \frac{1}{2Kn \pm 1} \quad ..(3.2.2)$$

The tooth harmonics go in pairs and if there are nine teeth per pole in a 4-pole motor, the largest pair of tooth harmonic are 17th and 19th harmonics. The higher-order harmonics are usually of less importance.

If the forward and backward components be used there are now six flux waves to be considered. If the subscript "1" be always associated with the stator and subscripts "N" and "M" are each associated with a member of, and represent the order of the first pair of tooth harmonics, the forward and backward components of each wave may be expressed as shown below:

$$W_{1f} = A_{1f} \cos\left(x \frac{\pi}{\tau} - \omega t\right)$$

$$W_{1b} = A_{1b} \cos\left(x \frac{\pi}{\tau} + \omega t\right)$$

$$W_{1Nf} = A_{Nf} \cos\left(N x \frac{\pi}{\tau} - \omega t\right)$$

$$W_{1Nb} = A_{Nb} \cos\left(N x \frac{\pi}{\tau} + \omega t\right) \qquad \ldots (3.2.3)$$

$$W_{1Mf} = A_{Mf} \cos\left(M x \frac{\pi}{\tau} - \omega t\right)$$

$$W_{1Mb} = A_{Mb} \cos\left(M x \frac{\pi}{\tau} + \omega t\right)$$

Similarly, the rotor fundamental flux waves and tooth harmonics can be expressed as follows:

$$W_{2f} = A_{2f} \cos \left(x_2 \frac{\pi}{\tau} - \omega s t \right)$$

$$W_{2b} = A_{2b} \cos \left[x_2 \frac{\pi}{\tau} + \omega (2 - s) t \right]$$

$$W_{2Rf} = A_{Rf} \cos \left[R x_2 \frac{\pi}{\tau} + \omega s t \right]$$

$$W_{2Tf} = A_{Tf} \cos \left[T x_2 \frac{\pi}{\tau} - \omega s t \right] \qquad .. \quad (3.2.4)$$

$$W_{2Rb} = A_{Rb} \cos \left[R x_2 \frac{\pi}{\tau} - \omega (2 - s) t \right]$$

$$W_{2Tb} = A_{Tb} \cos \left[T x_2 \frac{\pi}{\tau} + \omega (2 - s) t \right]$$

With respect to the stator, the rotor waves of (3.2.4) can be written as:

$$W_{2f} = A_{2f} \cos \left[x \frac{\pi}{\tau} - \omega t \right]$$

$$W_{2b} = A_{2b} \cos \left[x \frac{\pi}{\tau} + \omega t \right]$$

$$W_{2Rf} = A_{Rf} \cos \left[R x \frac{\pi}{\tau} - \omega \left\{ R(1 - s) - s \right\} t \right]$$

$$W_{2Tf} = A_{Tf} \cos \left[T x \frac{\pi}{\tau} - \omega \left\{ T(1 - s) + s \right\} t \right] \qquad (3.2.5)$$

$$W_{2Rb} = A_{Rb} \cos \left[R x \frac{\pi}{\tau} - \omega \left\{ R(1 - s) + 2 - s \right\} t \right]$$

$$W_{2Tb} = A_{Tb} \cos \left[T x \frac{\pi}{\tau} - \omega \left\{ T(1 - s) - 2 + s \right\} t \right]$$

The flux at every point in the air gap of the motor and at every instant of time is exactly representable as the sum of the fundamental fluxes and all the harmonic fluxes.

Using those fluxes which have been considered, we have;

$$B_\delta = \Big[W_{1f} + W_{1b} + W_{1Hf} + W_{1Hb} + W_{1Mf} + W_{1Mb} + W_{2f} + W_{2b} + W_{2Hf} + W_{2Hb} + W_{2Mf} + W_{2Mb}\Big] \quad (3.2.6)$$

The radial force density at any point in the gap due to B_δ is, according to Maxwell;

$$\frac{F}{A} = \frac{1}{72,130,000} B_\delta^{2} \text{ pounds per square inch} \quad .. \quad (3.2.7)$$

This force wave sets up vibrations in the frame structure and produces air-borne noise. The increase in noise with load is less rapid than the increase in the primary current (30.01).

e) Other causes: Inter laminar fluxes may also result in vibration of the individual laminations and this may be a source of great annoyance, if the core laminations are not tightly held together (33.01).

Some particular combinations of stator and rotor slots may set up force waves in the motor

thereby producing vibrations and noise (37.02).

3.2.3 Measurement of noise:

There are two distinctly different methods of measuring noise; the subjective methods using human ear and the objective methods using apparatus. One advantage claimed for the subjective methods is that they employ the human hearing mechanism, so that it would seem that noises of different types should be measured as equal when they produce equal interfering effects. This apparent advantage is accompanied by the disadvantage, however, that the sensation produced by a given stimulus varies widely for different individuals and for the same individual at different times, so that the average of several measurements by each of several observers is needed for a reasonably accurate results.

The chief operating advantages of the objective method are the reproducibility of the results and the ease and speed of making measurements (35.01).

To measure the motor noise in a large quiet room the set up shown in Fig. (3.2.3) can be used. The microphone should be far enough from the motor to

obtain an overall indication of the average noise emitted by the motor. It should be placed near enough, however, so that reflected waves at the microphone will be negligible in intensity compared with the direct sound from

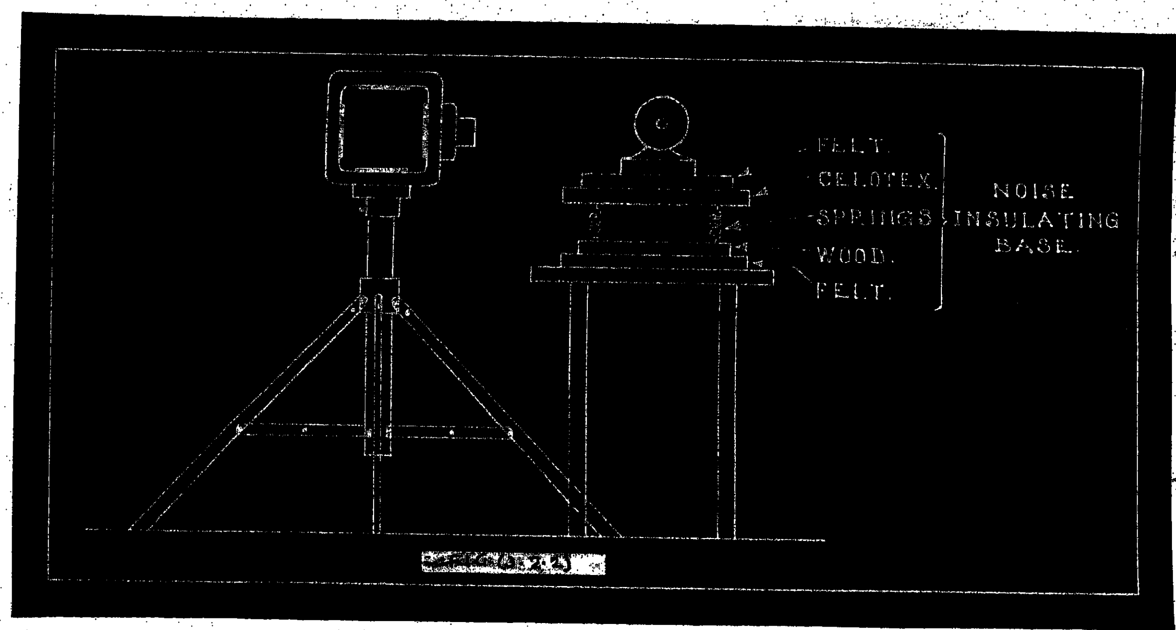


Figure (3.2.2)

the motor, and also near enough that the intensity of the signal in the microphone due to the motor noise will be substantially greater than that of the general noise of the room.

The measurement of noise as a routine test in a factory poses certain problems of its own.

Firstly, the factory surrounding is very noisy. Hence it is necessary to have a "noise proof" room or "sound proof" box. Economy drives us to have a the latter one. In constructing a sound proof box the following shall be

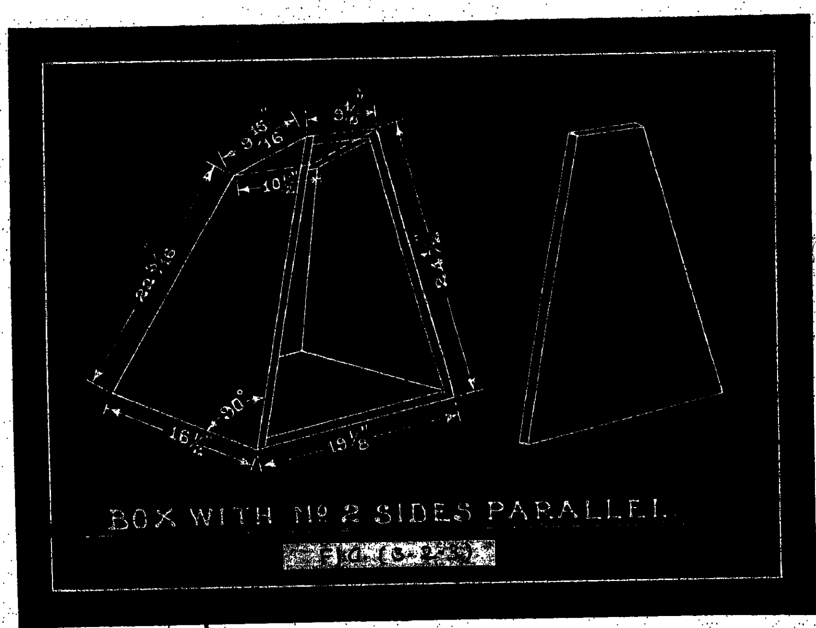


Figure (3.2.3)

the ends in view (34.01):

(i) To have sound-insulating walls to keep out room noise.

(ii) To intensify the motor noise, without distortion, to raise it above the noise level inside the box. [illegible], vacuum tube ampli- [illegible] The resonant circuit

(iii) To ensure that the errors from standing waves is a minimum.

These can be achieved by constructing the box with no two sides parallel as shown in Fig.(3.2.3) The measurement of noise can be done by having the motor and the microphone inside such a box.

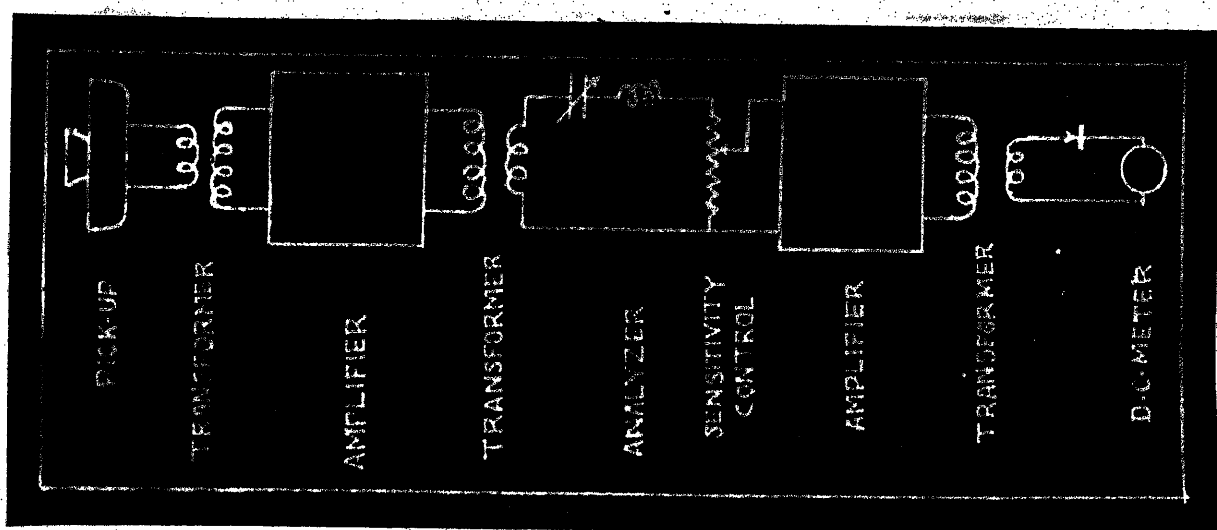


Figure (3.2.4)

The energy picked up by the microphone is then fed into the analyser shown in Fig.(3.2.4). This analyser is of the simple resonance type (20.02). Referring to Fig. (3.2.4), the pick-up feeds into a step-up audio-frequency transformer, vacuum tube amplifier, and step-down transformer. The resonant circuit

of the analyser consist of a fixed inductance and variable condenser. The voltage across the non-inductive resistance with a variable tap, is fed into a second amplifier, a step-down transformer, and a d.c. milliammeter and copper-oxide rectifier. If a sound having a frequency component corresponding to the setting of the resonant circuit impinges on the microphone a reading will be obtained on the d.c. meter. If the analyser circuit is not in resonance, it will offer such a high impedance that the particular frequency in question will not produce sufficient current in the analyser circuit to produce an appreciable drop in the non-inductive resistance.

The method of calibrating the analyser is as follows: [Figure (3.2.5)] . An electro-dynamic loud speaker capable of going to low frequencies is excited from a variable frequency sine wave source of voltage. In front of the loud speaker is placed the electro-dynamic pick-up of the analyser to be calibrated. Besides the analyser pick-up is placed another very carefully built electro-dynamic pick-up, the constants of which are known; namely for a given sound pressure the generated voltage can be calculated. This standard

microphone is connected through an amplifier to a milli-ammeter. This amplifier combined with the milliammeter, is calibrated between input volts and milliammeter readings. Since the r.m.s. sound pressure is directly proportional to the generated voltage, the pressure can

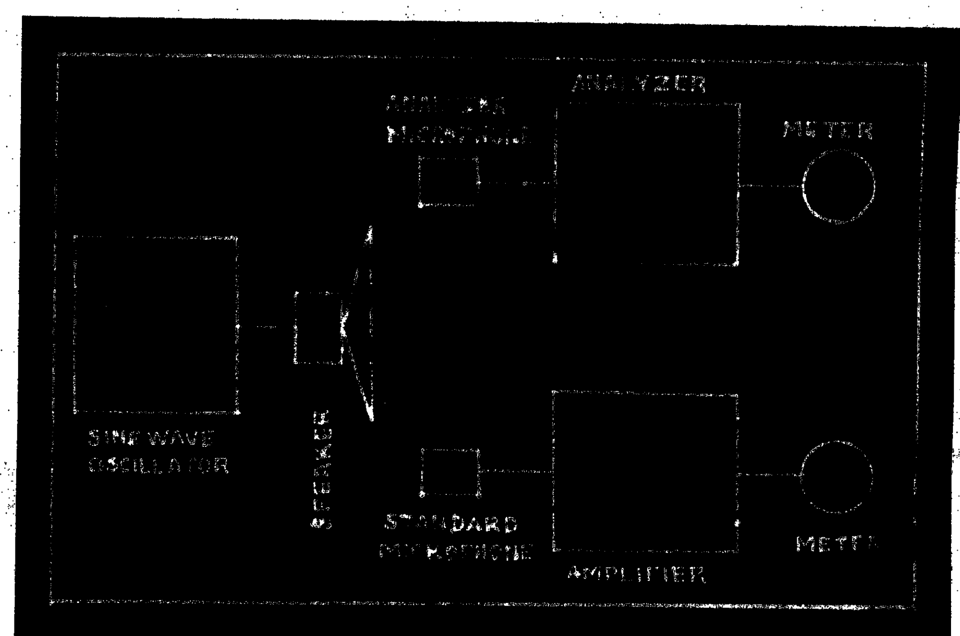


Figure (5.2.5)

be estimated directly from the reading of the milliammeter. Next a sine wave a.c. voltage of a known frequency is applied to the loud speaker element, the analyzer adjusted for a maximum reading by moving the variable condenser and the condenser setting and the meter reading noted. This gives an amplitude and frequency point on the

calibration curve of the analyzer. This is repeated for various frequencies and amplitudes until the complete calibration curves have been obtained.

Any appraisal of small-motor noise must takes into account transmittable as well as air-borne noise. One method of measuring the transmittable noise is to mount the motor on top of a box and measure the noise intensity inside the box, with the motor running. An alternative method for comparing relative transmittable noises of motors is to place a wooden board on top of the noise insulating base shown in Fig. (3.2.3), and allow the motor to run on this board.

3.2.4 Elimination of Noise;

The following are some of the methods of eliminating noise of electromagnetic origin in an induction motor; It has already been stated that certain slot combinations produce noise in an induction motor. Hence by proper choice of the slot combination the noise can be minimised. Gabriel Kron (31.01) states that the following slot combinations are liable to produce vibration and noise;

i) When the slots (of stator and rotor) differ by one or by the number of poles plus or minus one, transverse vibration and noise may occur.

ii) When the slots differ by half the number of poles, torsional vibration and noise may occur.

iii) When the slots differ by the number of poles, torsional vibration and noise may occur and also rumbling noises unaccompanied by critical vibrations.

Hence these slot combinations must be avoided.

The reduction of the strength of the harmonics reduces the noise and this can be done in two ways. (37.02). One is to design the stator punching with heavy teeth at the centre of the pole and lighter teeth toward the outside of the pole, and the other is to distribute the winding to decrease the harmonic. The method of calculating the distribution of winding is given in Chapter V. Closed slots are less noisy than open slots.

Regardless of how we wind the stator, there are always the two teeth harmonics present. The

effect of these harmonics in producing noisy operation can be eliminated by proper skewing of the rotor. If we want to get a current flow in a wound armature, we must put one side of each coil under a north pole and the other side under a south pole. The principle of skewing is based exactly on this idea. Considering the case of nine slots per pole, we have the seventeenth and nineteenth harmonics present regardless of the method of winding. Since the fundamental has four poles, the seventeenth and Nineteenth harmonic will have 68 and 76 poles, respectively, or 34 and 38 pairs of poles. It is now our object x to place one end of the rotor bar under one north harmonic pole and the other end under another north harmonic pole. Therefore, the rotor should be skewed 1/34 of the entire rotor to eliminate the seventeenth harmonic and 1/38 of the entire rotor to eliminate the nineteenth harmonic. If a 44-bar rotor is used, the skew to eliminate the seventeenth harmonic will be 1/34 times 44 equals 1.29 bars skew, and to eliminate the 19th harmonic, 1/38 times 44 equals 1.16 bars skew. If the rotor skew is held as nearly as possible to these limits, there shall be no trouble caused by the seventeenth and nineteenth harmonics.

3.3 STARTING:

3.3.1 Condition for Maximum Starting Torque:

In a single-phase, capacitor-start induction motor, while starting there are two flux systems, the main and the auxiliary, acting on the rotor. As a general case, let us consider two alternating fluxes ϕ_1 and ϕ_2 displaced in time and spaces phases by θ and ψ radians, respectively. Then, instantaneously, we have (B.10),

$$\phi_1 = \bar{\Phi}_1 \sin \omega t$$

$$\phi_2 = \bar{\Phi}_2 \sin (\omega t - \theta)$$

The perpendicular and horizontal components of ϕ_2 are, respectively,

$$\bar{\Phi}_2 \sin (\omega t - \theta) \cos \psi$$

$$\bar{\Phi}_2 \sin (\omega t - \theta) \sin \psi$$

and hence the value of the resultant field is,

$$\phi_r = \sqrt{\bar{\Phi}_1^2 \sin^2 \omega t + 2\, \bar{\Phi}_1 \bar{\Phi}_2 \sin \omega t \sin (\omega t - \theta) \cos \psi + \bar{\Phi}_2^2 \sin^2 (\omega t - \theta) \cos^2 \psi + \bar{\Phi}_2^2 \sin^2 (\omega t - \theta) \sin^2 \psi} \quad \text{.. (3.3.1)}$$

The angle which ϕ_r makes with the horizontal is given by

$$\lambda = \text{arc tan} \frac{\bar{\Phi}_1 \sin \omega t + \bar{\Phi}_2 \sin (\omega t - \theta) \cos \psi}{\bar{\Phi}_2 \sin (\omega t - \theta) \sin \psi} \quad ..(3.3.2)$$

From equations (3.3.1) and (3.3.2) it is seen that both ϕ_r and λ are periodic functions of time. Hence ϕ_r rotates at the same time varying in amplitude.

For the single-phase motor at starting, the value of ψ is 90 degrees. Hence, if flux is replaced by mmf. M,

$$M_r = \sqrt{M_1^2 \sin^2 \omega t + M_2^2 \sin^2 (\omega t - \theta)} \quad .. \quad (3.3.3)$$

$$\lambda = \text{arc tan} \frac{M_1 \sin \omega t}{M_2 \sin (\omega t - \theta)} \quad .. \quad (3.3.4)$$

The angular velocity with which M_r rotates is,

$$\frac{d\lambda}{dt} = \frac{d\lambda}{dx} \cdot \frac{dx}{dt}$$

where $x = \tan \lambda$

Now $$\frac{d\lambda}{dx} = \frac{1}{1 + \tan^2 \lambda}$$ and,

$$\frac{dx}{dt} = \omega M_1 M_2 \frac{\sin(\omega t - \theta)\cos\omega t - \sin\omega t \cos(\omega t - \theta)}{M_2^2 \sin^2(\omega t - \theta)}$$

Hence,

$$\frac{d\lambda}{dt} = \omega M_1 M_2 \frac{\sin(\omega t - \theta)\cos\omega t - \sin\omega t \cos(\omega t - \theta)}{M_1^2 \sin^2\omega t + M_2^2 \sin^2(\omega t - \theta)} \quad .. \ (3.3.5)$$

If the flux is proportional to the mmf., then the current induced in the rotor is proportional to

$$M_r \frac{d\lambda}{dt}$$

and the torque is proportional to

$$M_r^2 \frac{d\lambda}{dt}$$

or to

$$\omega M_1 M_2 \left[\sin(\omega t - \theta)\cos\omega t - \sin\omega t \cos(\omega t - \theta)\right]$$

$$= \omega M_1 M_2 \left[\tfrac{1}{2}\left\{\sin(2\omega t - \theta) - \sin\theta\right\} - \tfrac{1}{2}\left\{\sin(2\omega t - \theta) + \sin\theta\right\}\right]$$

$$= \omega M_1 M_2 \sin\theta \quad .. \ (3.3.6)$$

if the negative sign is ignored. It is desirable that the angle of phase displacement should approach 90 degrees as far as possible, because under these conditions expression (3.3.6) is a maximum. In a capacitor-start motor this is effected by the insertion of the proper value of capacitance in series with the auxiliary winding.

3.3.2 Determination of the Auxiliary winding constants:

In determining the auxiliary winding constants any one of the following views may be aimed at:

a) Conditions for maximum starting torque.
b) conditions for maximum starting torque per ampere line current.

M.S.Thacker and H.V.Gopalakrishna (49.01) have analysed this problem in the following manner: depending upon the voltage the capacitor is able to withstand, a certain number of turns and distribution of the starting winding is assumed, fixing the reactance, X_s. The current in the starting winding may be arbitrarily fixed up thereby fixing the locked-rotor impedance of the starting winding, Z_{ss}.

Substituting these quantities in the expression for starting torque and making the angle between the current in the main winding and that in the auxiliary winding equal to $\pi/2$, the expressions for the capacitive reactance and the total resistance of the starting winding are got as:

$$X_c = X_s + \frac{Z_{se}}{Z_M} R_M \qquad .. \qquad (3.3.7)$$

and

$$R_s = \frac{Z_{se}}{Z_M} X_M - R_c \qquad .. \qquad (3.3.8)$$

The capacitor resistance, R_c is treated as a known quantity.

To find out the auxiliary winding constants to give maximum starting torque per ampere of line current, the expression for starting torque per ampere is differentiated with respect to Z_{se} and ϕ, the angle between I_s and I_m, and equated to zero. The resulting equations are:

$$X_c = \frac{Z_{se}}{Z_M^2} \left[R_M^2 \sqrt{Z_M^2 - Z_{se}^2} + Z_{se} X_M \right] + X_s \qquad .. \qquad (3.3.9)$$

$$R_s = \frac{Z_{se}}{Z_M^2} \left[X_M \sqrt{Z_M^2 - Z_{se}^2} - Z_{se} R_M \right] - R_a \quad .. \; (3.3.10)$$

These two equations completely define the auxiliary winding.

In these equations the total resistance of the auxiliary winding is considered as a variable and is determined for specific conditions. Considering the auxiliary winding resistance also as a fixed quantity, Boothby (29.01) has determined the value of the capaditive reastance to be used in series with the auxiliary winding. His analysis is given under 'Design Features and Design' and is used in the actual design of the motor taken for construction.

3.3.3 Capacitor for Starting Winding:

The popularity and efficient performaes of capacitor-start motors is largely due to the development of the electrolytic capacitor which differs in theory, construction and characteristics from the ordinary capacitors having paper or some similar dielectric.

If two electrodes be put a short distance apart in certain alkaline solutions and a

current be passed, it is found that, as time passes on, the current gets less and finally drops almost zero.(B.11) This is due to the fact that the electrolysis causes a deposit on the anode of a thin film which is an insulator and in a short time the deposition is sufficiently complete to stop the current. This principle is used in the construction of the electrolytic capacitor. A

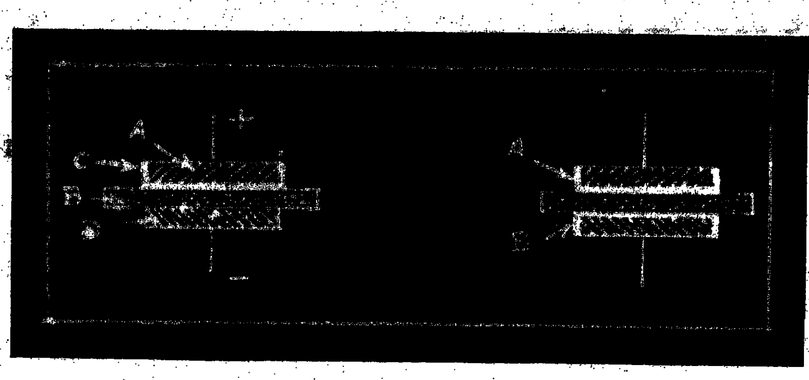


Figure (3.3.1)

simple electrolytic capacitor is illustrated in Fig. (3.3.1)(a). A and D are the electrodes and B is a chemical electrolyte, liquid or paste-like in form. C is the film of oxide formed on the plate actually A. While A is one electrode, B serves as the other electrode of the capacitor, the bottom plate D now acting only as a convenient means of maintaining contact with the electrolyte and taking no other part in the

action of the capacitor (B.11).

The film of oxide C is of microscopical thickness, much thinner than any separate dielectric material, and so a much hgiher value of capacitance can be obtained from a given size of capacitor.

An important point about the electrolytic capacitor is that the resistance of the oxide film, or its dielectric strength, acts in one direction only. If direct current be applied with the positive to the oxide-coated electrode, the oxide acts as a non-conductor and the arrangement functions as a capacitor, but if the connections are reversed, the oxide film becomes a conductor and there is no capacitor action. Thus the capacitor shown in Fig. (3.3.1)(a) is unsuitable for use with a.c. motors because of the alternating nature of the current. For alternating current applications the arrangement shown in Fig. (3.3.1)(b) is used where both plates are "formed", or coated with oxide film, so that the film A acts as a dielectric for one half a cycle, and the film B for the other half of the cycle.

If the oxide film breaks down at any point, the electrolyte decomposes setting free oxygen

which combines with the material of the plate to form fresh oxide. Because of this the life of the electrolytic capacitor is limited as contrasted with the practically infinite life of a solid dielectric capacitor.

In order to make a compact unit, the modern dry-type electrolytic capacitor is formed by winding two sheets of aluminium foil into a cylindrical shape. The two sheets of aluminium foil are separated by a guaze, or a combination of gauze and paper impregnated with an electrolyte, usually ethylene glycol or a derivative (E.1). On each of the two layers of foil, an anodic film is produced by electrochemical means. It is then rolled up and fitted into a metal can and insulated. A safety vent is usually provided to prevent explosion.

Motor-starting capacitors are rated on the basis of 20 three-second periods per hour, or an equivalent duty cycle.

—

C H A P T E R - IV.

WINDINGS AND CONNECTIONS.*

4.1 Concentric Windings:

Single-phase induction motors are generally wound with concentric coils. A comparison of this with the more familiar diamond-coil lap winding (B.1) shows that they are identical. A diamond-coil lap winding with eight slots per pole is shown in Fig. (4.1). An 'exactly equivalent' concentric type of winding is shown in Fig. (4.2). Comparing these two winding arrangements; in both, slots 1, 2, 3, and 4 carry A phase current upward; slots 5, 6, 7 and 8 carry B phase current upward; slots 9, 10, 11 and 12 carry A phase current downward; and slots 13 14, 15, and 16 carry B phase current downward. In other words, the direction of current flow through the active conductors of every slot of the winding of Fig.

---

* References: (B.1) and (B.13)

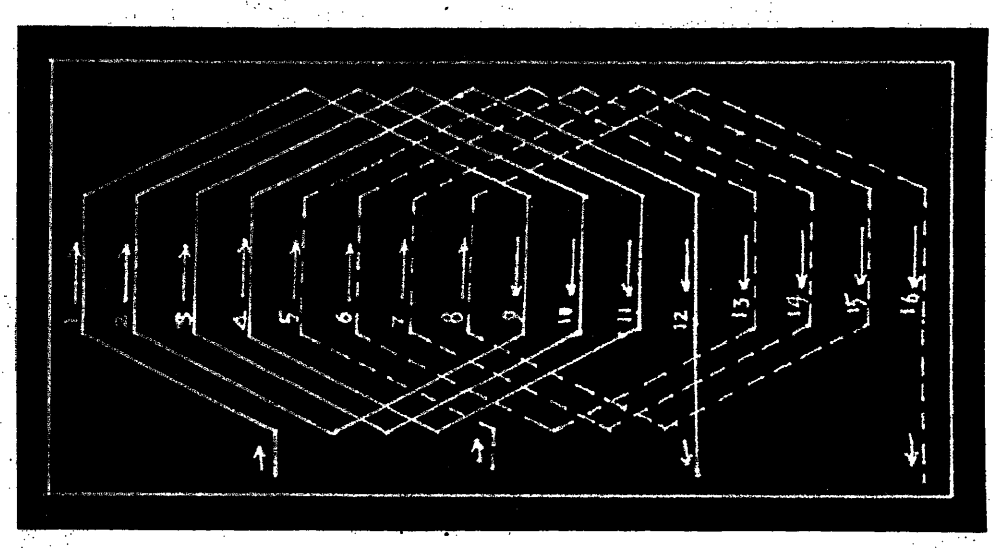


Figure (4.1)

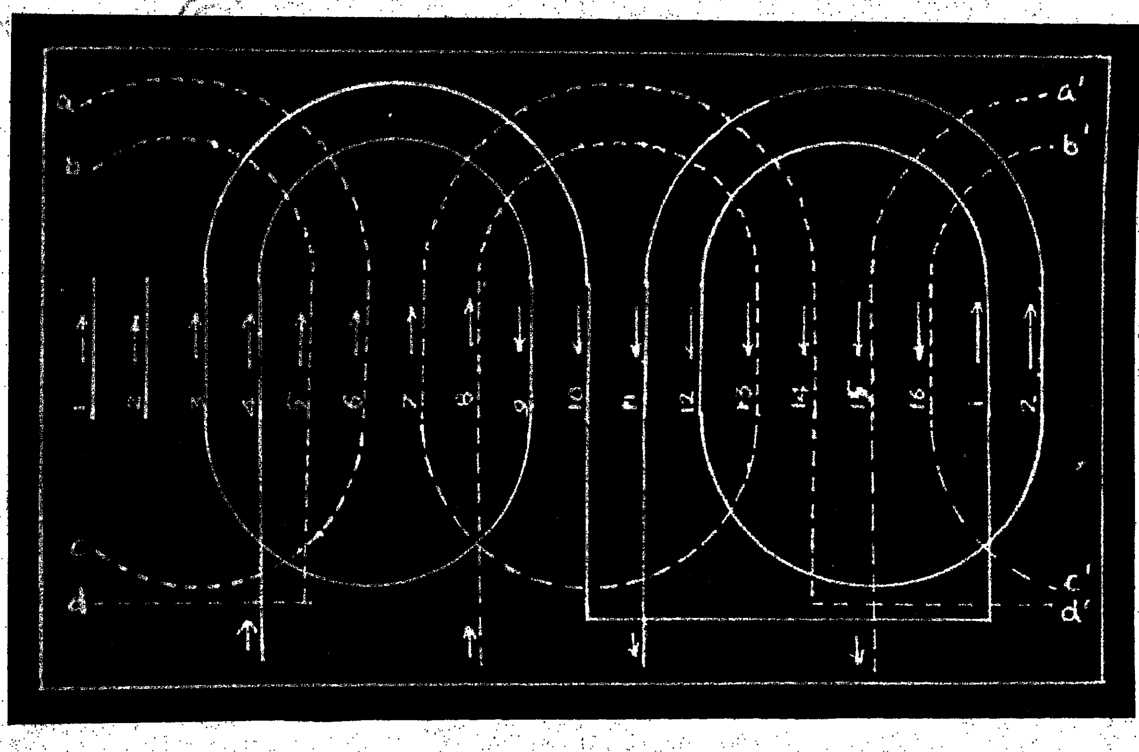


Figure (4.2)

(4.8) is identical with the direction of current flow in every slot of the winding of Fig.(4.1); the difference between these two winding arrangements is only in the end connections. The strength, location and distribution of the useful magnetic fields in the motor depend wholly upon the total number and arrangement of ampere-conductors in the slots; in no respect do these factors depend upon how the end connections are made between these conductors. Therefore, one winding is said to be <u>exactly equivalent</u> to a second winding if, with the same current flowing in the external leads of either winding, there are exactly the same number of ampere-conductors in every slot of the second winding.

It is always possible to find a concentric winding that is exactly equivalent to a progressive, or diamond-coil, winding, as has just been done. The reverse of this statement, however, is not always true; for, a concentric winding is the more flexible arrangement. Concentric windings are used in single-phase induction motors because of this greater flexibility.

In the diamond-coil, all the coils have the same pitch or "throw" , and the centre of

each coil is displaced - usually by one slot - from the centre of the neighbouring coil. In the concentric type of winding, every coil in any given pole group has a different throw. But the centres of all the coils in a single pole group coinside; ie., the coils are concentric with one another.

4.2 Different types of Stator Diagrams:

Eventhough it is possible to give the complete specification of all the details of a winding on a single drawing, it is convenient to break this

SLOT NUMBER		1	2	3	4	5	6	7	8	9	10	11	12	13	14	15	16	WIRE SIZE (GAUGE)	INSULATION	STRANDS PER CONDUCTOR
MAIN WDG.	STRANDS	72	72	72	72	x	x	x	x	72	72	72	72	x	x	x	x	21	S.C.C.En.	2
AUX. WDG.		x	x	x	x	43	43	43	43	x	x	x	x	43	43	43	43	19	S.C.C.En.	1

Figure (4.3)

information down to a few different kinds of diagrams without overlooking the fundamental principles. These diagrams are:

a) Distribution Chart: A typical winding distribution chart is of the form of Fig. (4.3), which

specifies the size of wire used in each winding, the insulation covering on the wire, the number of strands per conductor, the total number of strands in each and every slot, and the end connections of the coils in a group. In short, the distribution chart gives all the information necessary for winding the stator coils and connecting them in groups, except for the coil perimeters and the winding method. The winding method may also be given on this chart if desired.

b) Stator connection Diagram: After the stator coil groups are wound, the next step is to connect the groups together. A group is simply the combination of all the coils in a given winding under one pole. How to connect the groups together is shown in Fig. (4.4). In this diagram, each group is represented by a single, solid, white arc. The connections of the ends of these groups are shown in the figure.

c) Wiring Diagram: The wiring diagram shows the internal connections of all windings to one another and also the connections in the windings to auxiliary devices such as starting switch, resistor, reactor, capacitor or thermal protective device. If no leads other

than those shown in the stator connection diagram are necessary, a winding diagram is unnecessary.

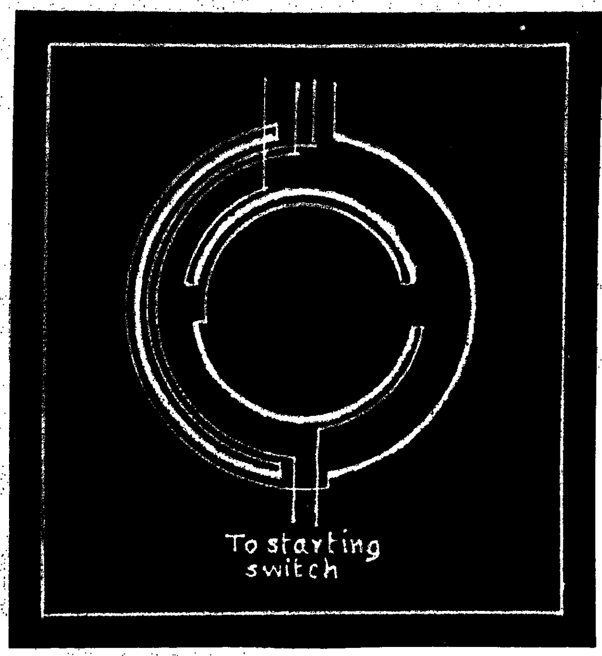


Figure (4.4)

d) Line-connection Diagram: This shows the permissible connections of the motor leads to the line. If there are but two line leads, a line-connection diagram is not needed.

4.3 Stator Windings:

Three types of windings are used for the stators of single-phase motors. They are:

a) Hand or form winding,

b) Mould Winding.

c) Skein winding.

a) Hand or Gun Winding: Coils can be wound directly in the stator punchings by hand alone, or by means of a gun, one turn at a time (B.1). For example, with the winding shown in Fig. (4.2), the winder starts with a single wire and winds the inner coil (4 and 9) until this coil is completed. He then progresses to the next coil, which is wound in the two adjacent outside slots (3 and 10), and so on, if there are more coils in the group, until all the coils in a pole group are wound, each coil being wound in the same direction. The winder then carries the wire over to slot 1 and winds in the opposite direction, all the turns in the coil spanning slots 1 and 12 and then winds the last coil from 2 to 11, still continuing in the same direction as 1 - to - 12 coil and bringing out the finished lead from slot 11. Usually the turns are counted mentally.

Since the sharp edges of the slot openings make may cut or scrape the insulation off the wire, it is usual factory practice to employ winding

guides. These guides are arranged so as to cover up the shorp edges of the slots to protect the wire so that it can be wound into the slots more rapidly. Also, rods are provided to insert in the slots to keep the wires from "climbing the core" , ie., to keep the end connections from covering up the unwound slots, in order to provide room for the coils which are later to be wound.

Inasmuch as the wire tends to cut or chafe the winder's hand, a "gun" is provided to facilitate insertion of the wire in the slots. Gun winding, if the proper guns are provided, is a cheap and fast method, and end extensions are cut to down to a minimum. But the cost of making them to wind only a few motors would be prohibitive. It is not used generally if the wire size is larger than No. 16 or if there are more than 80 turns per slot.

b) Mould Winding: The concentric coils are wound on a stepped block, or mould, provided with as many steps as there are parts to the coil. If these are tappered, as shown in Fig. (4.5), a considerable advantage is gained because each individual turn has a different perimeter, and the turns do not interfere with

one another when the coil is being inserted in the slots. With this method, all the coils for a single group are wound in succession with a single strand of wire, or with two strands of wire, if there are two strands per conductor. If only a few jobs of this type are done, wire



Figure (4.5)

finish nails can be driven into the bench, and the coils wound around these finish nails. In order to determine the perimeter of the mould or around the finished nails, a single wire is looped around the stator teeth (in the centre of the slot) in the same position in which the finished coil lies. As for the hand winding, guides to

cover the sharp edges of the slots are necessary while feeding the wires into the slots. The end extensions of the mould winding are usually somewhat larger than those of the hand winding. The single-phase mould winding can also be made as a distributed winding with equal coils.

c) Skein Winding: The skein winding used often for auxiliary windings consists of as many skeins of wire as there are poles. Each skein of wire is looped a number of times through the slots to form a pole. The number of loops may be different in the individual slot pairs. The total number of turns per pole is equal to the number of turns in the skein times the number of loops.

Fig.(4.6) shows the steps necessary to put the skein into the slots of one pole of a four-pole machine with 36 slots. The skein is placed into the slots 3 and 7 [(Fig. (4.6)(a)] a few wires at a time. Then the skein is pulled towards the winder, moving the end winding on the sides opposite to the leads close to the core. Care is taken that the slot cells do not move together with the skein, otherwise the insulation may be scraped. In the next step, the skein is given half-a-turn [Fig. (4.6)(b)] and the entire skein is passed thro'

the stator core. Then the wires of slot 3 are fed into slot 8, and those of slot 7 are fed into slot 2 [Fig.(4.6)(c)]. After the end windings have been pulled tight to the core, the skein is given again half-a-turn, but in a direction opposite to the first twist [Fig. (4.6)(d)] and the entire skein is passed through the stator core. The wires of slot 8 are now fed into slot 1, those of slot 2 are fed into slot 9, and the coil group is ready for shaping. [Fig. (4.6)(e)] .

A skein winding becomes somewhat difficult to handle, if the size of the wire is larger than No. 20 and the weight of the skein is more than 2 or 3 ounces. In order to determine the length of the skein, a single wire is looped in the slots in the same manner that the skein will be looped. Now a trail skein can be made and wound in the slots. A correct length of the skein is important.

A skein can be made either by using an adjustable skein reel or by driving 2 nails, at the correct distance apart, in a board and winding the wire around the nails. The start and finish leads must be at the same end of the skein. Before removing

the skein, short pieces of tape should be wrapped around the wires, at intervals, to avoid tangling of the wires and to separate both sides of the skein. These pieces of tape are removed as the skein is placed in the slots. When the skein is long, 4 instead of 2 nails can be used; the 2 middle nails prevent the tangling of wires.

In the method of making a skein winding described above, it is necessary to pass the entire skein through the core of the stator as many times as there are single coils minus one. Another method makes it unnecessary to pass the entire skein through the core. The principle of this method is to pass one side of the skein through the slots, by forming loops in it, until the last single coil is reached and then to use the other side of the skein to finish the coil group. This is explained in Fig. (4.7) which shows one pole group, as in Fig. (4.6) . In using this method, the lead end of the skein must be put in first and the leads should be made long enough so that they can be brought to the front of the core through the last slots (1 and 9). In Fig. (4.7)(a) a loop is made with the right-hand leg of the skein, passed into the stator core, and fed into the slots 2 and 8 [Fig. (4.7)(b)] . Then, since the last single

coil is reached, the strands of the third coil are pulled over and fed into slot 9 and the rest of the coil is fed into slot 1 Fig. (4.7)(c) . In general the loops are all made by the same leg of the skein.

4.3.1 Windings with Dissimiliar Coils and Consequent-Pole Windings: Windings with dissimiliar coils on

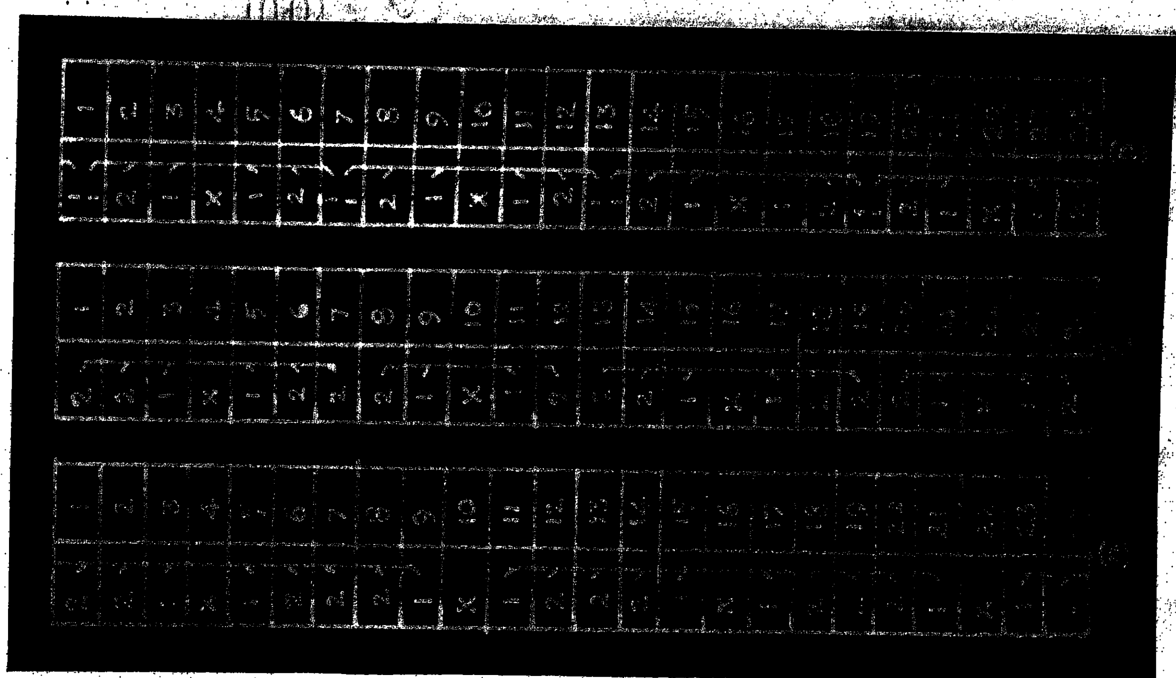


Figure (4.8).

adjacent poles are often used in single-phase motors to avoid the use of split coils. Fig. (4.8)(a) shows a conventional balanced-coil arrangement requiring two coil sides in slots 1, 7, 13, and 19. However, by the use

of unequal coils, as shown in Fig. (4.8)(b), the split coils can be avoided. An extension of the same idea is the arrangement in Fig. (4.8)(c) which uses only one coil per pair of poles, and which connects all coils for the same magnetic polarity; this is a consequent-pole winding. All three of these arrangements are exactly equivalent. Dissimiliar coils are easier to wind because there are no split coils, which are usually tighter in the slots owing to the additional insulation required. Consequent-pole windings are used in single-phase ceiling fans.

4.4 Varnish Impregnation:

Electric motors are usually varnish-impregnated for one or more of the following reasons:

i) Bonding of the windings into a rigid mass to prevent chafing and, in the case of rotating members, to prevent loss of balance.

ii) Removal of moisture from the insulation and addition of permanent barrier against re-entry of moisture, abrasive dirt, and dust.

iii) Reduction of temperature rise.

iv) Lengthening the life of the insulation by reducing the rate of oxidation, thermal decomposition, and dehydration.

v) Increasing the dielectric and mechanical strength of the insulation, as well as its resistance to certain chemicals.

Moisture resistance and dielectric strength of a film of baked insulating varnish are approximately proportional to the film thickness. For good bonding and good heat dissipation, the varnish must penetrate the windings thoroughly during the dipping process. Penetration can be improved greatly by lowering the viscosity and percentage of solids in the varnish by addition of solvents, but the film produced is thin, and numerous dips and bakes are required to build up an adequate film.

Selection of the insulating varnish for any particular motor, in general, is based upon a compromise between tensile strength and heat life of the film. Highest strength varnishes tend to be inherently brittle and are, therefore, subject to cracking by vibration or by repeated expansions and contractions due to

temperature changes. Air-drying varnishes, particularly those with shellac spirit base, can be used in emergencies when time does not permit use of baked varnish, but baked varnishes are invariably better.

a) Air-drying Varnishes: By comparison with baking varnishes, air-drying varnishes have low strength and high porosity because their films do not flow well enough to seal up the voids left by the drying out of the solvent. Fastest drying of these have a shellac spirit base and may either be clear or black. Black, asphalt-base varnishes are available, but these have only fair resistance to oil. A number of oleoresinous varnishes, both black and clear, are available; these dry by loss of solvent and by oxidation, and are more oil-resistant than asphalt-base varnishes. Synthetic-base air-drying varnishes are also used to some extent.

b) Baking Varnishes: Oleoresinous - These dry partly by polymerization and partly by oxidation, dependant upon the drying oils they contain. Linseed-oil varnishes dry almost entirely by oxidation; tung-oil varnishes by both oxidation and polymerization. Drying by oxidation causes a hot surface to form while the

varnish is still wet underneath. This is a disadvantage of this type of varnish, particularly in deep oils.

Oleoresinous black varnishes are either dyed or modified with black asphalt called gilsonite. The latter is cheap, a good insulator, and readily soluble in ordinary varnish solvents; however, the oil resistance of the varnish is lowered by the addition of gilsonite.

Oleoresinous varnishes deteriorate and become more brittle through a continuation of the same oxidation and polymerization reactions by which they dry. Thus, quick-drying oleoresinous varnishes can be expected to lose toughness at high temperatures more rapidly than the slow-drying oleoresinous varnishes. Synthetic resins are often added to oleoresinous varnishes to prolong their life at high temperatures, or to improve their resistance to some specific chemical.

e) Thermosetting Varnishes: These are heat-hardening, clear, synthetic varnishes which represent a vast improvement over ordinary baking varnishes, which depend upon oxidation for hardening, compared with oleoresinous

varnishes, these have considerably more flexibility after proper baking and will retain their flexibility longer at higher temperatures. Moreover, they are generally superior in dielectric strength and have almost unsurpassed resistance to oil, acid, alkali and moisture. Mostly they consist of thermo-setting resins of the phenolaldehyde (bakelite) or alkyd types. These types may even be mixed together and modified by the addition of other synthetic or natural resins so that almost any desired property may be obtained. Good thermo-setting varnishes will not corrode copper and have little effect on wire with synthetic coatings, provided the apparatus is not immersed in the varnish more than six hours before baking.

d) Silicone Varnishes: A series of these varnishes have been developed for apparatus that has to operate continuously at temperatures of 130° to 175° C, with occasional peaks of 250° C. Although these do not have high strength at these high temperatures, they do retain their flexibility, adhesion, and continuity of film, and hence make very suitable impregnances for stationary electrical equipment.

C H A P T E R - V.

DESIGN FEATURES AND DESIGN.*

E.M.F.Equation: Considering a full-pitch coil of one turn, as the coil moves from position A to position B [Fig. (5.1)], the flux linking with it changes from ϕ to zero, ϕ being flux per pole (B.15). Hence the change of flux linkage is ϕ and the average emf. induced in it is

$$E_{av} = \frac{\phi}{t} \times 10^{-8} \text{ volts} \quad .. \quad (5.1)$$

where t is the time required to move a distance equal to AB. t being one-quarter of the periodic time T,

$$\frac{1}{t} = \frac{4}{T} = 4f \quad .. \quad (5.2)$$

Therefore, $$E_{av} = 4 f \phi \times 10^{-8} \text{ volts} \quad .. \quad (5.3)$$

---

* The design method closely follows Kuhlmann (B.14).

If K_f be the form-factor of the flux wave-form, then

$$E_{eff} = 4 K_f f \phi \times 10^{-8} \text{ Volts} \quad .. \quad (5.4)$$

With a distributed winding of total turns T_{ph}, the total induced voltage is,

$$E_{eff} = 4 K_f K_d K_p f \phi T_{ph} \times 10^{-8} \text{ Volts} \quad .. \quad (5.5)$$

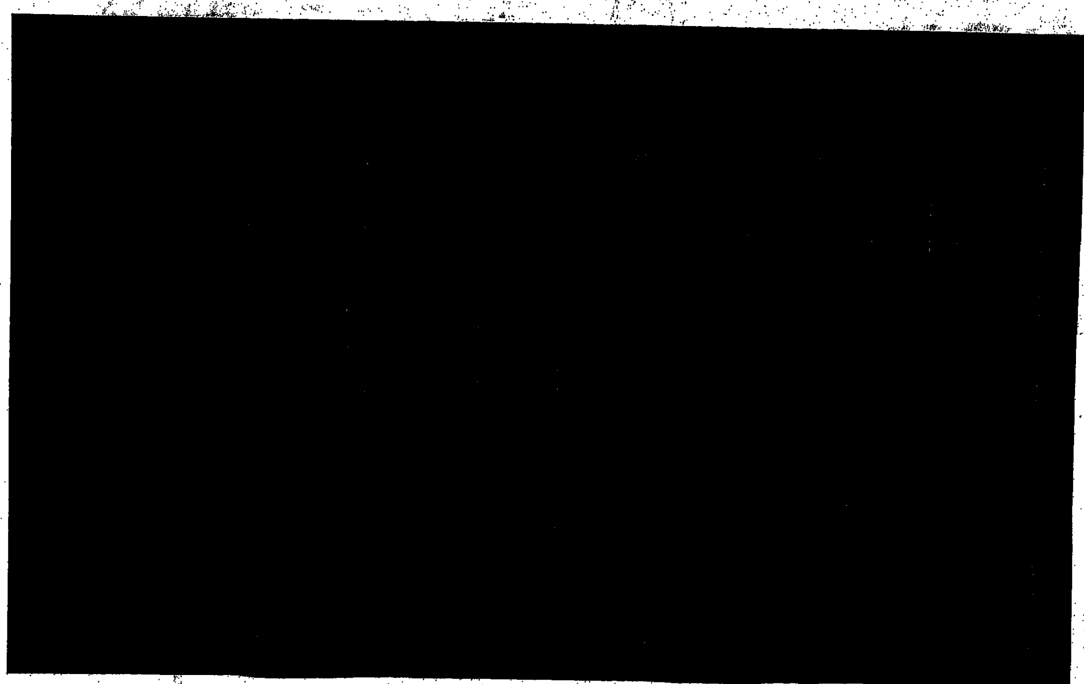


Figure (5.1).

where K_d and K_p are the distribution factor and pitch factor respectively.

For the design of electrical

machinery, it is often convenient to use a hypothetical total flux for the machine, instead of the flux per pole. To determine this hypothetical total flux, the flux density in the air gap is assumed to have maximum value over the entire pole pitch, that is, the shape of the field form is



Figure (5.2).

assumed to be rectangular as shown in Fig. (5.2). The ratio of the area under the true field form to the areas of the hypothetical rectangular field form is called the field form distribution factor, f_d . The hypothetical total

flux,

$$\phi_t = \frac{\phi P}{f_d} \quad .. \quad (5.6)$$

From formula (5.5),

$$\phi = \frac{E \times 10^8}{4 K_f K_d K_p f T_{ph}} \quad ..$$

$$\text{and} \quad \phi_t = \frac{E P \times 10^8}{4 K_f K_d K_p f f_d T_{ph}} \text{ lines} \quad ..(5.7)$$

If N is the number of conductors in series per phase and N_s, the synchronous rpm. then,

$$T_{ph} = \frac{N}{2}$$

$$\text{and} \quad f = \frac{N_s P}{120}$$

Making these substitutions,

$$\phi_t = \frac{E \times 60 \times 10^8}{N_s N K_f K_d K_p f_d} \quad .. \quad (5.8)$$

The form factor K_f, winding dis-

tribution factor K_d , and flux distribution factor f_d depend only upon the number of slots and the shape of the air-gap flux distribution curve and are not affected by changes in the number of conductors per phase or the coil throw. These factors can, therefore, be combined into one factor, called the winding constant,

$$C_w = K_f K_d f_d \quad .. \quad (5.9)$$

Then,

$$\phi_t = \frac{E \times 60 \times 10^8}{N_s N K_p C_w} \text{ lines} \quad .. \quad (5.10)$$

Output Constant: If E is the terminal voltage per phase, the output of an induction motor,

$$hp = \frac{E I m \times eff. \times Pf.}{746} \quad .. \quad (5.11)$$

where m = number of phases.

The total flux,

$$\phi_t = \pi D l B_g \quad .. \quad (5.12)$$

The total ampere-conductors on the stator,

$$I \times N K_p = \pi D Q \qquad .. \qquad (5.13)$$

Substituting equations (5.10), (5.12), and (5.13) in equation (5.11), the output equation becomes,

$$h.p. = \frac{D\ l\ B_g\ \pi\ D\ Q\ N_s\ C_w \times eff. \times pf.}{44.76}$$

$$= \frac{D^2\ l\ N_s\ B_g\ Q\ C_w \times eff. \times pf.}{4.54 \times 10^{11}}$$

$$\frac{D^2\ l\ N_s}{h.p} = \frac{4.54 \times 10^{11}}{B_g\ Q\ C_w \times eff. \times pf.} \qquad .. \qquad (5.14)$$

The magnetising current lags the voltage by 90 degrees and must be small, if reasonable operating characteristics are to be obtained. The reluctance of the air gap is always greater than that of the remainder of the magnetic circuit. To avoid excessive magnetising currents moderate densities are, therefore, required. The density in the stator teeth is directly proportional to that in the air-gap. High tooth density produces high core-

losses and increase the magnetising current. The flux density in the air gap of induction motors generally lies between limits 25,000 and 45,000 lines per square inch. The high values are for large-capacities, high-speed motors. For general purpose motors, air-gap densities from 30,000 to 40,000 lines per square inch are most satisfactory.

The value of ampere-conductors per inch of stator gap circumference depends upon the size of the motor, the voltage of the stator winding, the type of ventilation and the permissible leakage reactance. It varies between 250 to about 1,000 for small and large motors respectively.

Choosing proper values for B_g and Q , a series of constants can be derived for various ratings and speeds which can be used to calculate the stator diameter and length. Therefore, equation (5.14), becomes,

$$\frac{D^2 \, l \, N_s}{h.p.} = C \quad .. \qquad (5.15)$$

For fractional-horse power motors, it is more satisfactory to use output in watts instead of horsepower in the above equation.

Therefore

$$C = \frac{D^2\ l\ N_s}{\text{Watts output}} \quad .. \quad (5.16)$$

Kuhlmann has given a graph connecting output constants and watts output divided by synchronous r.p.m. which is shown in Fig. (5.3). These values of the output constants are only approximate to provide a starting point when laying new design.

Diameter and Length: The product $D^2 l$ can be calculated by equation (5.16) with the help of the output constants of Fig. (5.3). The diameter and length must be so selected that satisfactory operating characteristics can be obtained with minimum cost.

The operating characteristics of induction motors vary with the ratio of the length of the stator core to the pole pitch at the gap circumference. For best power factors l/τ, should be equal to from 1.0 to 1.25, and for best efficiency, about 1.5. For minimum cost l/τ should be equal to from 1.5 to 2.0. For small motors, l/τ is usually greater than 1.0 as otherwise the resulting small diameter will necessitate too small a number of stator slots.

Stator Tooth and Yoke Densities: For a given total flux, the dimensions of the slots determine the tooth density. For high tooth densities, the losses in the teeth are high, and a large number of ampere-turns are required to send the flux through the teeth. The maximum value of the stator tooth densities for the minimum section should generally not exceed,

B_{ts1} = 100,000 lines per sq. inch for 60 cycles.

B_{ts1} = 120,000 lines per sq. inch for 25 cycles.

The depth of stator laminations below the slots depends upon the flux density in the yoke. The iron losses in the yoke and ampere-turns required to send the flux through the yoke determine the density. The flux density should not exceed,

B_{ys} = 95,000 lines per sq. inch for 60 cycles.

B_{ys} = 110,000 lines per sq. inch for 25 cycles.

Generally B_{ys} is equal to from 50,000 to 85,000 lines per square inch for 60 cycles and 60,000 to 100,000 lines per square inch for 25 cycles.

Air Gap Length: Even with low air-gap densities and short air-gap lengths, the gap ampere-turns are larger than the ampere-turns for the remainder of the magnetic circuit. The air-gap density and length, therefore, determine the magnetising current. To get as small a magnetising current as possible, therefore, the length of the air-gap should be as small as mechanical construction will permit. For fractional-horsepower motors, the air-gap lengths can be determined approximately by the following emphirical equation,

$$\delta = 0.005 + 0.00035\ D + 0.001\ l + \frac{0.003\ v}{1000} \quad .. \quad (5.17)$$

Rotor Windings: Squirrel-cage windings are built up of bar conductors, short-circuited at each end by end-rings. The bars are either round or rectangular in shape and are of either copper or aluminium. The end-ring is generally of the same material as that used for the bars. Because of the large temperature ranges from no-load to full load, the best possible connection between bars and end-ring is necessary to avoid high contact resistance at the joints. The cast squirrel-cage winding is very desirable in this respect, because there are no joints.

Number and Size of Rotor Slots: For squirrel-cage motors the number of slrotor slots must be selected to avoid dead points or positions of no torque at starting. In order that the zig-zag leakage flux, which produces the locking torque, shall be as small as possible, the number of rotor slots should be so chosen that a minimum number of rotor slot openings will be opposite the centre of a stator tooth for any rotor position. The number of rotor slots must be different from that of the rotor stator. For squirrel cage rotor, the rotor slot combination of 80 or 120 per cent of the number of stator slots gives good results.

If the total rotor ampere-turns are assumed to be ten percent less than the total stator ampere-turns, the ratio of the total copper section of the rotor to the total stator copper section,

$$\frac{S_{cr}}{S_{cs}} = 0.90 \frac{A_s}{A_r} \qquad .. \qquad (5.18)$$

For a current density of 2,500 amperes pr sq. inch., in the stator winding and 4,000 amperes per sq. inch in the bars of the squirrel-cage winding, the ratio of the total rotor copper section to the total stator copper

section,

$$\frac{S_{cr}}{S_{cs}} = 0.9 \times \frac{2500}{4000} = 0.562$$

The total rotor copper section should never be less than 50 percent of the total stator copper section. It is

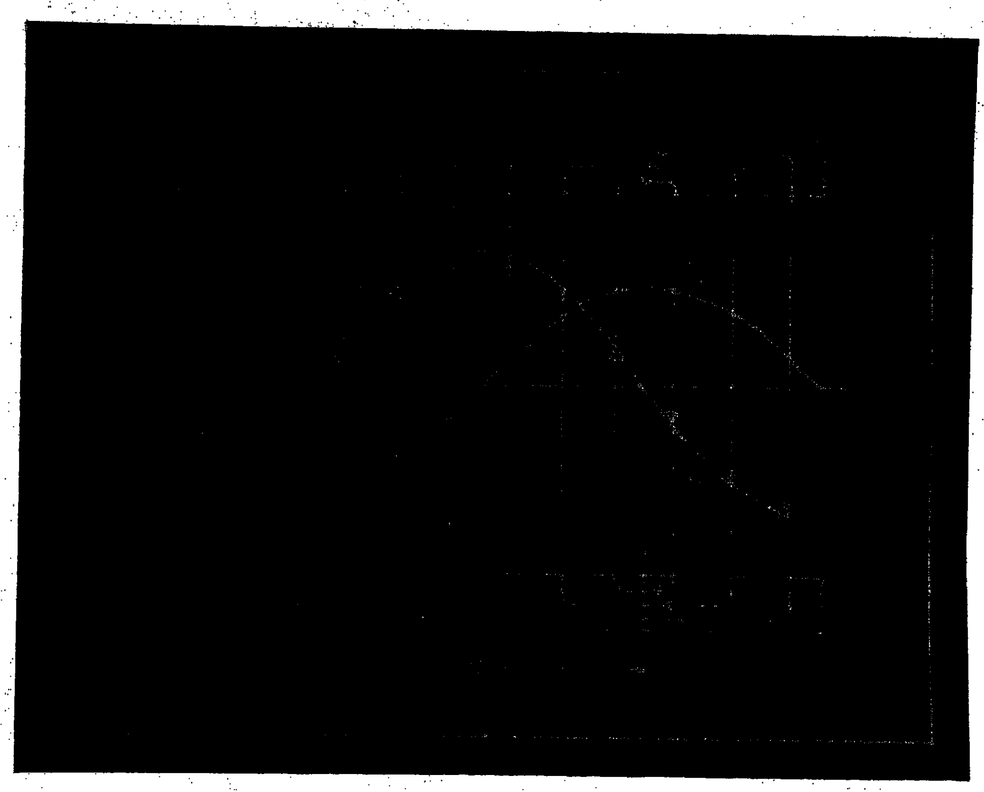


Figure (5.4)

generally from 60 to 80 percent for squirrel-cage windings.

The distribution of the current in the bars and end rings of a squirrel-cage winding is

shown in Fig. (5.4). The current in each bar divides in the end-ring, one-half returning through a bar a pole pitch to the right and the oher half through a bar a pole pitch to the left. Let the maximum value of the current in each bar be I_{max}. The maximum current in the ring is equal to the average bar current, $(2/\pi)\ I_{max}$ multiplied by the number of bars in half pole pitch (5.4). Hence, the maximum value of the current in the end ring is

$$\frac{2}{\pi}\ I_{max}.\ \frac{N_b}{2P}$$

and the effective value of the current in the end ring is

$$\frac{I_b\ N_b}{\pi\ P}$$

$$= \frac{0.32\ I_b\ N_b}{P} \qquad .. \qquad (5.19)$$

The section area of each end-ring

$$s_{er} = \frac{0.32\ I_b\ N_b}{P\ A_{er}} \qquad .. \qquad (5.20)$$

and the total bar section,

$$S_{cr} = \frac{I_b\ N_b}{A_r} \quad .. \quad (5.21)$$

Substituting for $I_b\ N_b$ from equation (5.21) in equation (5.20),

$$s_{er} = \frac{0.32\ S_{cr}}{P} \cdot \frac{A_r}{A_{er}} \quad .. \quad (5.22)$$

The ventilation is generally better for the end rings than for the bars, and the current density can be made equal to the current density in the bars or slightly higher.

Rotor slot depths equal to 4 times the width are used for squirrel-cage windings, but more often the depth of the slot is from 1.5 to 2.0 times the width.

ACTUAL DESIGN.

It is proposed to design and construct a 3/8 H.P., 220 Volts, 1460 r.p.m. , 50 cycle, single-phase, capacitor-start induction motor.

Stator: The watts output $= \frac{3}{8} \times 746 = 280$ Watts.

The motor will have 4 poles and the synchronous r.p.m. is 1500, the output constant from Fig. (5.3) is 230, and

$$D^2 l = \frac{280 \times 230}{1,500} = 43$$

Gap diameter of the stampings chosen for the construction is 3.75 inch.

$$\text{Therefore,} \quad l = \frac{43}{3.75^2} = 3.05 \simeq 3 \text{ inches.}$$

The core dimensions selected are,

$$D = 3.75 \text{ in., and } l = 3.0 \text{ in.}$$

The stator has 24 slots and the tooth width is 0.234 in., The total tooth section is

$$S_{ts} = w_{ts} \times l \times S_s \times 0.9$$

$$= 0.234 \times 3 \times 24 \times 0.9$$

$$= 15.2 \text{ sq. in.}$$

Assuming a stacking factor of 0.9 .

For a tooth density of 90,000 lines

per sq.in., the total flux,

$$\phi_t = B_{ts} \times S_{ts}$$

$$= 90{,}000 \times 15.2$$

$$= 1{,}370{,}000 \text{ lines.}$$

The winding constant cannot be calculated until the distribution of the winding is known. For the usual winding distributions, C_w will be between 0.75 and 0.85 . Let us assume a winding distribution factor of 0.85 .

The total number of conductors in series for the main winding, assuming the induced voltage to be equal to 95 percent of applied voltage,

$$N_m = \frac{P\, E_t \times 0.95 \times 45 \times 10^6}{f\, \phi_t\, C_{wm}\, f_d}$$

f_d , the flux distribution constant, is equal to 0.637 for sine-wave flux distribution.

$$\text{Therefore,}\quad N_m = \frac{4 \times 220 \times 0.95 \times 45 \times 10^6}{50 \times 1{,}370{,}000 \times 0.85 \times 0.637}$$

$$= 1{,}010 \;.$$

The turns in series per pole,

$$t_p = \frac{N_m}{2P} = \frac{1{,}010}{2 \times 4} = 126.5$$

The winding arrangement chosen for the main winding is shown in Plate (I) . For sinusoidal distribution the number of turns for each coil will be as follows:

Coil 1 - 6 sin of 1/2 coil span = sin 5/6 x 90 = 0.965

Coil 2 - 5 sin of 1/2 coil span = sin 3/6 x 90 = 0.706

1.671

$$\text{Number of turns in coil } 1 - 6 = \frac{0.965}{1.671} \times 126.5 = 73$$

$$\text{Number of turns in coil } 2 - 5 = \frac{0.706}{1.671} \times 126.5 = 53$$

Total .. 126 turns.

The winding distribution factor for concentric type single-phase windings is a weighted mean chord factor and is calculated by multiplying the chord factor of each coil per pole group by the turns in the coil and dividing the sum of these products by the total number of turns.

The winding constant is then,

$$(\sin 5/6 \times 90) \times 73 = 0.965 \times 73 = 70.4$$

$$(\sin 3/6 \times 90) \times 53 = 0.706 \times 53 = 37.4$$

$$C_{wm} = \frac{107.8}{126} = 0.855$$

The total number of conductors now, $N_m = 126 \times 8$

$= 1,008$

Since there is a change in the total number of conductors and winding constant, the value of the total flux has to be recalculated.

New value of ϕ_t is given by,

$$\phi_t = \frac{4 \times 220 \times 0.95 \times 45 \times 10^8}{5 \times 1,008 \times 0.855 \times 0.637}$$

$= 1,370,000$ lines.

The slight increase in the value of winding constant has been compensated by a slight decrease in the value of the total number of conductors and hence the value of total flux remains unaltered.

The efficiency and power factor of a single-phase induction motor are usually much lower than those of

a polyphase induction motor. We shall assume an efficiency of 62 percent and power factor of 60 percent. Then the input current,

$$I = \frac{\text{Watts output}}{E_t \times \text{eff.} \times PF}$$

$$= \frac{280}{220 \times 0.62 \times 0.60}$$

$$= 3.44 \text{ amperes.}$$

Assuming a current density of 2,800 amperes per sq.in., and a one-circuit winding, the section area of the stator conductor for the main winding,

$$S_{sm} = \frac{I}{A \times \Delta_{sm}}$$

$$= \frac{3.44}{1 \times 2{,}800} = 0.00123 \text{ sq. in.}$$

The nearest standard wire is SWG 19, with section area 0.00126 sq.in. The actual current density with this conductor,

$$\Delta_{sm} = \frac{3.44}{0.00126} = 2{,}730 \text{ amperes per sq.in.}$$

The insulation between core and coils consists of empire cloth of 7 mils thickness and leatheried of 10 mils thickness. Super enamelled wire is used.

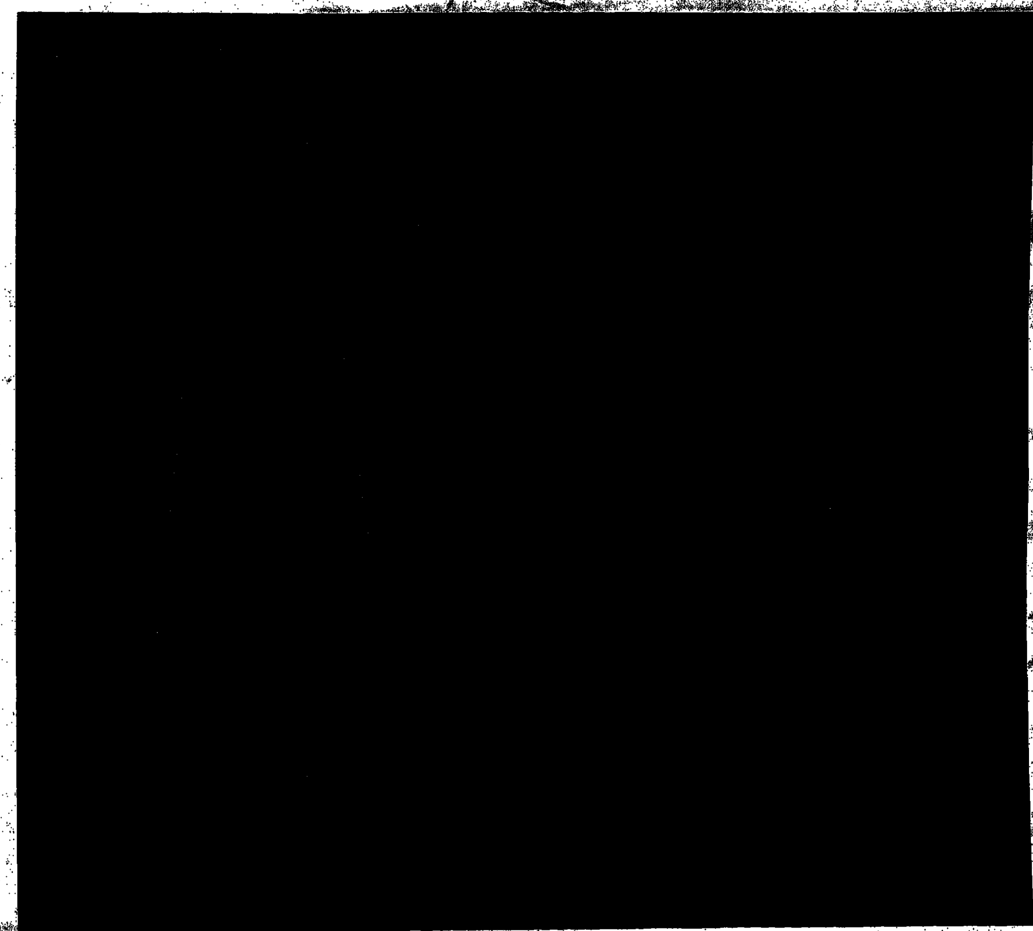


Figure (5.5)

The dimensions of the stator slot are shown in Fig. (5.5)(a). The slot area is 0.535 sq.in. Then the space factor in the slots having the maximum number of main winding turns,

$$= \frac{73 \times 0.00126}{0.315} = 0.292$$

This space factor can easily be achieved. If it is more than 0.35 considerable difficulty will be experienced in placing the conductor inside the slots.

The double radial depth of the stator,yoke, d_{ys} is measured directly and is equal to 0.95 in. The flux per pole,

$$\phi = \frac{\phi_t f_d}{p}$$

$$= \frac{1,370,000 \times 0.637}{4}$$

$$= 218,000 \text{ lines.}$$

The density in the stator yoke,

$$B_{ys} = \frac{\phi}{d_{ys} \times l \times 0.9}$$

$$= \frac{218,000}{0.95 \times 3 \times 0.9}$$

$$= 85,000 \text{ lines per sq. in.}$$

This flux density is well within the limits.

Rotor: For fractional-horsepower motors the air-gap length can be determined approximately by the following emperical equation,

$$\delta = 0.005 + 0.00035\ D + \frac{0.003\ v}{1{,}000}$$

$$= 0.005 + 0.00035 \times 3.75 + \frac{0.003 \times 1{,}400}{1{,}000}$$

$$= 0.0135 \text{ in.}$$

Therefore the outside diameter of the rotor is,

$$3.75 - (2 \times 0.0135)$$

$$= 3.723 \text{ in.}$$

The rotor punching has 34 slots, which with the 24 stater slots meets all the requirements of a quiet motor.

$$S_{cs} = N_s\ m_s\ A\ S_s$$

$$= 1{,}008 \times 1 \times 1 \times 0.00126$$

$$= 1.27 \text{ sq. in.}$$

Taking the ratio of total rotor copper section to total stator copper section as 0.8 , the total rotor copper section

$$S_{cr} = 1.27 \times 0.8 = 1.015 \text{ sq. in.}$$

Section area of each rotor bar

$$S_b = \frac{1.015}{34} = 0.03 \text{ sq. in.}$$

But the area of the rotor slot is 0.0385 sq. in. Therefore the rotor slots must not be completely filled.

Using equation (5.22) and assuming the current density in the end ring to be equal to the current density in the rotor bars, the end-ring section is given by

$$s_{er} = \frac{0.32 \times 1.015}{4} = 0.0813 \text{ sq.in.}$$

The end ring is cast from copper and is of square section, 0.285 in. x 0.285 in. The outside diameter of the ring is 3.07 in. and that of the inside is 2.5 in.

The minimum width of the rotor tooth (measured directly),

$$w_{tr} = 0.14 \text{ in.}$$

The section area of the rotor teeth,

$$S_{tr} = w_{tr}\, l\, s_r \cdot 0.9$$

$= 0.14 \times 3 \times 34 \times 0.9$

$= 12.8$ sq. in.

The stator leakage flux factor is taken equal to 0.95, and therefore, the rotor tooth density,

$$B_{tr} = \frac{\phi_t \times 0.95}{S_{tr}} = \frac{1,370,000 \times 0.95}{12.8}$$

$= 101,000$ lines per sq.in.

The radial depth of the rotor yoke,

$$\frac{t}{2} \; d_{yr} = 0.625 \text{ in.}$$

The rotor yoke density,

$$B_{yr} = \frac{\phi \times 0.95}{d_{yr} \, l \times 0.9} = \frac{218,000 \times 0.95}{1.25 \times 3 \times 0.9}$$

$= 61,400$ lines per sq. in.

The air-gap density,

$$B_g = \frac{1,370,000 \times 0.95}{\pi \times 3.75 \times 3}$$

$= 36,800$ lines per sq. in.

<u>Machine Constants</u>: The ratio of stator slot opening to air-gap length,

$$= \frac{0.25}{2.54 \times 0.0135} = 7.3$$

From the curve of Fig. (5.6), $y = 2.8$.

The stator tooth pitch at the air-gap surface,

$$t_{1s} = \frac{\pi \times 3.75}{24} = 0.49 \text{ in.}$$

The width of stator tooth at the air-gap surface,

$$w_{ts1} = 0.49 - 0.0984 = 0.3916 \text{ in.}$$

The air-gap coefficient for thestator slot,

$$k_s = \frac{t_{1s}}{w_{ts1} + (y\delta)} = \frac{0.49}{0.3916 + (2.8 \times 0.0135)}$$

$$= 1.14$$

The rotor slots are completely closed and therefore,

$$k_r = 1$$

The air-gap coefficient,

$$k = k_s\, k_r = 1.14 \times 1$$

$$= 1.14$$

For single-phase induction motors the saturation factor F_s, which is the ratio of the total ampere-turns for the magnetic circuit to the air-gap ampere-turns only, will usually lie between the limits 1.10 and 1.35 . When the magnetic densities in the teeth and yoke are low, the low value applies, and when high, the higher value applies. For this motor, F_s is chosen equal to 1.2 .

The length of the half mean-turn for each of the coils per pole of a concentric type winding,

$$= \frac{4.2\,(D + d_s)}{S_s} \text{ slots spanned } + 1$$

In this expression 4.2 is used instead of π to take into account the extension of the coil beyond the stator core. The sum of the products of one-half mean-turn of each coil and turns per coil divided by the turns per pole is the weighted one-half mean-turn of the winding. Plate I shows the winding distribution for the motor, and the length

of the half mean-turn is calculated as follows:

$$\left[\frac{4.2\ (3.75 + 0.865)}{24} \times 5 + 3.0\right] 73 = 515$$

$$\left[0.81 \times 3 + 3.0\right] 53 = 288$$

$$L_{sm} = \frac{803}{126}$$

$$= 6.36 \text{ in.}$$

The resistance of the stator main winding,

$$r_{1m} = \frac{L_{sm}\ N_m \times 0.692}{A\ s_{sm} \times 10^6} = \frac{6.36 \times 1{,}008 \times 0.692}{0.00126 \times 10^6}$$

$= 3.52$ ohms at 25 degrees C.

$= 3.52 \times 1.15 = 4.05$ ohms at 65 degrees C.

The rotor bars for this motor are to be skewed one stator slot pitch or 0.49 in. The length of the rotor bar is, then,

$$l_b = \sqrt{3.0^2 + 0.49^2} = 3.04 \text{ in.}$$

Allowing 1/8" in. clearance on either side ,

$l_b = 3.29$ in.

The inside diameter of the end ring is 2.5 in., and the outside diameter, 3.07 in. Therefore the ratio of inside to outside diameters of end ring is 0.815 . For this value of K_{ring} , which takes into account the non-uniform distribution of current in the end ring, from Fig. (5.7) is 0.95 .

The rotor resistance in terms of the stator main winding,

$$r_2 = \frac{N_m^2 \, C_{wm}^2 \, s \, r}{10^6} \left[\frac{l_b}{S_b \, N_b} + \frac{0.64 \, D_{er}}{p^2 \, s_{er}} \; K_{ring} \right]$$

$$= \frac{1{,}008^2 \times 0.855^2 \times 2 \times 0.692}{10^6} \left[\frac{3.29}{0.03 \times 34} + \frac{0.64 \times 3.07}{16 \times 0.0813} \times 0.95 \right]$$

$$= 4.78 \text{ ohms at } 25^\circ \text{ C} .$$

$$= 4.78 \times 1.15 = 5.5 \text{ ohms at } 65^\circ \text{ C} .$$

The rotor resistance determined from the locked rotor test

will be higher than the calculated value and is the effective resistance of the rotor winding at starting. For normal operating speeds the rotor resistance is very nearly equal to the direct-current resistance.

Kuhlmann (B.14) gives the following leakage reactance equations based on practical design experience which give sufficiently close results for the design of most fractional horsepower induction motor.

The slot leakage reactance,

$$x_s = 2\pi f\ N_m^2\ C_{wm}^2 \times 10^{-8} \left[\frac{6.38\ l}{S_s}\right]\left[F_{ss} + \frac{S_s}{S_r}\ F_{sr}\right] \text{ ohms.}$$

The stator and rotor slot factors, F_{ss} and F_{sr}, are calculated as shown in Figs. (5.8) and (5.9).

The zigzag leakage reactance for stator and rotor in terms of main winding,

$$x_z = 2\pi f\ N_m^2\ C_{wm}^2 \times 10^{-8} \left[\frac{2.13\ l}{S_s\delta}\right]\left[\frac{(w_{tsi} + w_{tri})^2}{4\ (t_{1s} + t_{1r})}\right] \text{ ohms.}$$

The end connection leakage reactance,

$$x_e = 2\pi f N_m^2 C_{wm}^2 \times 10^{-8} \left[\frac{(D + d_s)\text{av. coil span}}{S_s P} \right] \text{ohms.}$$

The skew leakage reactance,

$$x_{sk} = x_m \frac{\theta_{sk}^2}{12} K_p \quad \text{ohms ,}$$

where θ_{sk} is the rotor bar skew expressed in radians and is equal to . divided by rotor slots per pole times number of bars skew, and K_p is the stator leakage flux factor which can be taken equal to 0.95 ,

The magnetising reactance,

$$x_m = 2\pi f N_m^2 C_{wm}^2 10^{-8} \frac{0.645\ l}{k\ P\ F_g} \quad \text{ohms .}$$

The total leakage reactance of the stator main winding plus rotor in terms of the main winding of the stator,

$$X_{1m} = x_s + x_z + x_e + x_{sk} \quad \text{ohms .}$$

The open-circuit reactance, the reactance of the stator main winding with secondary open,

$$X_o = x_m + \frac{X_{1m}}{2} \quad \text{ohms.}$$

The leakage flux factors,

$$K_r = \frac{X_o - X_{1m}}{X_o} \quad \text{and} \quad K_p = \sqrt{\frac{X_o - X_{1m}}{X_o}}$$

The constant term for the various reactances,

$$= 2\pi f \, N_m^2 \, C_{wm}^2 \, 10^{-8}$$

$$= 2\,\pi \times 50 \times 1{,}008^2 \times 0.855^2 \times 10^{-8}$$

$$= 2.325$$

For the stator slot,

$$\frac{W_{s2}}{W_{s3}} = \frac{7}{12} = 0.583$$

From Fig. (5.8), $\phi = 0.55$, and

$$F_{ss} = \phi \frac{d_1}{W_{s3}} + \frac{d_r}{W_{s1}} + \frac{2\, d_3}{W_{s1} + W_{s2}}$$

$$= 0.55 \frac{20.5}{12} + \frac{0.5}{2.5} + \frac{2 \times 1.5}{9.5}$$

$$= 1.446$$

For the rotor slot,

$$\frac{d_1}{W_{s3}} = \frac{5.5}{3.5} = 1.57 \quad \text{and} \quad \frac{W_{s2}}{W_{s3}} = 1$$

From Fig. (5.9), $\phi = 0.65$, and

$$F_{sr} = \phi + \frac{d_4}{W_{s1}} + \frac{2\,d_3}{W_{s1} + W_{s2}}$$

$$= 0.65$$

d_4 being zero and d_3 negligible. Therefore, the slot leakage reactance,

$$x_s = 2.325 \left[\frac{6.38 \times 3}{24}\right]\left[1.446 + \frac{24}{34} \times 0.65\right]$$

$$= 3.53 \text{ ohms}.$$

The zigzag leakage reactance,

$$x_z = 2.325 \left[\frac{2.13 \times 3}{24 \times 0.0135}\right]\left[\frac{(0.3916 + 0.346)^2}{4\,(0.49 + 0.346)}\right]$$

$$= 7.46 \text{ ohms}.$$

The end connection leakage reactance ,

$$x_e = 2.325 \left[\frac{(3.75 + 0.885)\, 4}{24 \times 4} \right]$$

$$= 1.41 \text{ ohms.}$$

The magnetising reactance,

$$x_m = 2.325 \left[\frac{0.645 \times 3.0 \times 2.94}{0.0135 \times 1.14 \times 4 \times 1.2} \right]$$

$$= 179 \text{ ohms.}$$

The skew angle, $\theta_{sk} = \frac{\pi}{6} = 0.524$ radians.

The skew leakage reactance,

$$x_{sk} = 179 \cdot \frac{0.524^2}{12} \cdot 0.95$$

$$= 3.9 \text{ ohms.}$$

The leakage reactance,

$$X_{1m} = 3.53 + 7.46 + 1.41 + 3.9$$

$$= 16.3 \text{ ohms.}$$

The open circuit reactance,

$$X_o = x_m + \frac{X_{1m}}{2} = 179 + \frac{16.3}{2}$$

$$= 187.15 \text{ ohms.}$$

The leakage flux factors,

$$K_r = \frac{187.5 - 16.3}{187.15} = 0.912$$

$$K_p = \sqrt{K_r} = \sqrt{0.912}$$

$$= 0.955$$

The weight of the stator teeth,

$$G_{st} = S_{ts} \times \text{depth} \times 0.278$$

$$= 15.2 \times 0.885 \times 0.278$$

$$= 3.74 \text{ lbs.}$$

The loss per pound for the tooth density, 90,000 lines per square inch, for armature grade, 24 guage electric sheet steel is (3.9 watts per pound at 60 cycles x 0.82) 3.2 watts (B.3), and the loss in the stator teeth due to the fundamental frequency flux ,

$$W_{st} = 3.74 \times 3.2$$

$$= 11.95 \text{ watts.}$$

The weight of the stator yoke,

$$G_{sy} = \frac{\pi}{4} (6.5^2 - 5.53^2)\ 3.0 \times 0.9 \times 0.278$$

= 7.21 lbs.

For armature-grade, 24 guage, electric sheet steel, the loss per pound for the stator yoke density is (3.5 watts per pound at 60 cycles x 0.82) 2.77 watts (B.3), and the loss in the yoke due to the fundamental frequency flux,

$$W_{ey} = 7.21 \times 2.77$$

$$= 20.0 \text{ watts.}$$

Taking a multiplying factor of 2.2 to account for loss due to harmonics, the total core loss,

$$W_e = (11.95 + 20.0)\ 2.2$$

$$= 70.3 \text{ watts.}$$

The bearing friction and windage losses are assumed to be 4 per cent of the watts output. Therefore,

$$W_{fw} = 280 \times 0.04$$

$$= 11.2 \text{ Watts.}$$

Auxiliary Winding: For the capacitor-start motor, the starting torque is calculated by the equation given by

C.R. Boothby (20.01) with the correction by Trickey to take into account the effect of magnetising current.

$$T_s = \frac{1.88\ P\ E^2\ a\ r_2}{f} \quad \frac{R_a X_{1m} - R_m (X_{1a} - X_c)}{\left[R_m^2 + X_{1m}^2\right]\left[R_a^2 + (X_{1a} - X_c)^2\right]} K_r \text{ oz. ft.}$$

In this equation R_a is the auxiliary winding resistance plus the resistance of the capacitor.

The derivative of this equation with respect to X_c set equal to zero and solved for X_c gives the capacitive reactance required for maximum starting torque as,

$$X_c = X_{1a} + \frac{R_a}{R_m} (Z_{1m} - X_{1m}) \quad \text{ohms.}$$

The value of X_c required for maximum starting torque for given main winding constants varies directly with X_{1a} and R_a, which in turn vary directly with square of 'a', the ratio of effective auxiliary winding turns to main winding turns. The curves of Fig. (5.10) show how maximum torque, capacity, starting current and current density in the auxiliary winding vary with the ratio 'a' for given main winding constants and assumed auxiliary winding conductor.

To obtain a small capacitor and low starting

current 1.55 is selected for the ratio 'a' . Then,

$$N_a = \frac{a\ N_m\ C_{wm}}{C_{wa}} = \frac{1.55 \times 1{,}008 \times 0.855}{0.855}$$

$$= 1{,}560 .$$

The winding arrangement and distribution are shown in Plate I and are exactly similar to those of the main winding. The number of turns per pole for a one-circuit winding,

$$t_p = \frac{A\ N_a}{2P} = \frac{1 \times 1{,}560}{2 \times 4}$$

$$= 195$$

For sinusoidal distribution the turns per coil are calculated as follows:

$$\text{Sin}\ \frac{5}{6} \times 90 = 0.965 \text{ turns} = \frac{0.965}{1.671} \times 195 = 113$$

$$\text{Sin}\ \frac{5}{6} \times 90 = 0.706 = \frac{0.706}{1.671} \times 195 = 82$$

$$\underline{1.671} \quad \text{Turns per pole} \quad .. = \underline{195}$$

The winding constant for the auxiliary winding is, then,

$$\left(\sin \frac{5}{6} \times 90\right) 113 = 0.966 \times 113 = 109$$

$$\left(\sin \frac{3}{6} \times 90\right) 82 = 0.706 \times 82 = 58$$

$$C_{wa} = \frac{167}{195} = 0.857$$

The final ratio of effective conductors,

$$a = \frac{1,560 \times 0.857}{1,008 \times 0.855} = 1.55$$

Since N_a is not altered and there is very slight change in C_{wa}, 'a' is practically unchanged.

The length of the half mean-turn is calculated as follows:

$$\left[\frac{4.2\ (3.75 + 0.885)}{24} \times 5 + 3\right] 113 = 796$$

$$\left[\frac{4.2\ (3.75 + 0.443)}{24} \times 3 + 3\right] 82 = 42.6$$

$$L_{sa} = \frac{838.6}{195} = 4.3 \text{ in.}$$

After a few trial calculations, S.W.G. 23 wire is chosen

for the auxiliary winding. The section area of this conductor is 0.000452 sq. in. The resistance of the auxiliary winding,

$$r_{1a} = \frac{4.3 \times 1,560 \times 0.692}{1 \times 0.000452 \times 106} = 10.3 \text{ ohms at } 25^\circ \text{ C}$$

For starting torque calculations, the d.c. rotor resistance in terms of the main winding is increased by 10 percent, and the effective locked-rotor resistance,

$$r_2 = 1.10 \times 4.78$$

$$= 5.25 \text{ ohms at } 25^\circ \text{ C} .$$

The total main winding resistance,

$$R_m = r_{1m} + r_2 = 3.52 + 5.25$$

$$= 8.77 \text{ ohms at } 25^\circ \text{ C} .$$

The locked rotor resistance in terms of the auxiliary winding,

$$a^2 r_2 = 1.55^2 \times 5.25$$

$$= 12.6 \text{ ohms at } 25^\circ \text{ C} .$$

and

$$R_a = r_{1a} + a^2 r_2 = 10.3 + 12.6$$

$$= 22.9 \text{ Ohms} .$$

The total leakage reactance in terms of the auxiliary winding,

$$X_{1a} = 1.55^2 \times 16.3$$

$$= 39.1 \text{ ohms}.$$

The ideal locked rotor reactance is given by

$$X = \frac{X_{1m}}{2} + \left[\frac{X_{1m}}{2} \cdot \frac{x_m}{x_m + \frac{X_{1m}}{2}} \right]$$ on the assumption

that $x_{1m} = x_2$ (32.01). Since x_m is very large compared to $(X_{1m} / 2)$, X may be taken equal to X_{1m} itself. Then the main winding locked rotor impedance,

$$Z_{1m} = \sqrt{X_{1m}^2 + (\tfrac{1}{2} r_{1m} + r_2)^2}$$

$$= \sqrt{16.3^2 + 8.77^2}$$

$$= 18.5 \text{ ohms at } 25^\circ \text{ C.}$$

The locked-rotor current in the main winding,

$$I_{sm} = \frac{220}{18.5} = 11.9 \text{ amperes.}$$

The capacitive reactance required for maximum starting torque,

$$X_c = X_{1a} + \frac{R_a}{R_m} (Z_{1m} - X_{1m})$$

$$= 39.1 + \frac{22.9}{8.77} (18.5 - 16.3)$$

$$= 44.85 \text{ ohms.}$$

The capacity in micro-farads,

$$C = \frac{10^6}{2\pi f X_c} = \frac{10^6}{2\pi \times 50 \times 44.85}$$

$$= 71 \text{ micro-farads.}$$

A capacitor with 70 micro-farad nominal rating is selected for which the capacitive reactance,

$$X_c = \frac{10^6}{2\pi f C} = \frac{10^6}{2\pi \times 50 \times 70}$$

$$= 45.5 \text{ ohms.}$$

The impedance of the auxiliary winding with the capacitor in series,

$$Z_{ac} = \sqrt{R_a^2 + (X_{1a} - X_c)^2}$$

$$= \sqrt{22.9^2 + (39.1 - 45.5)^2}$$

$$= 23.8 \text{ ohms.}$$

The locked-rotor current in the auxiliary winding,

$$I_{sa} = \frac{220}{23.8} = 9.25 \text{ amperes.}$$

The current density in the auxiliary winding conductor at starting is, then,

$$= \frac{9.25}{0.000452} = 20,200 \text{ amperes per sq.in.}$$

The locked-rotor current for both windings in parallel,

$$I_{st} = \frac{I_{sm} (Z_{1m} + Z_{ac})}{Z_{ac}}$$

$$= \frac{11.9 \ (18.5 + 23.8)}{23.8}$$

$$= 21.2 \text{ amperes.}$$

The starting torque,

$$T_s = \frac{1.88 \times 4 \times 220^2 \times 1.55 \times 5.25}{50} \times$$

$$\frac{22.9 \times 16.3 - 8.77\ (39.1 - 45.5)}{[8.77^2 + 16.3^2][22.9^2 + (39.1 - 45.5)^2]} \times 0.912$$

$= 119.5$ oz. ft.

Full-load torque,

$$= \frac{280 \times 112.6}{1460}$$

$= 21.6$ oz. ft.

and the percent starting torque,

$$= \frac{119.5}{21.6} \times 100$$

$= 550$

C H A P T E R - VI.

PREDETERMINATION OF PERFORMANCE CHARACTERISTICS FROM DESIGN DATA.

6.1 METHODS OF CALCULATION:

a) **Double Revolving Field Theory:** After analysing the operation of single-phase induction motor by the double revolving field theory, we arrived at equations (2.1.7), (2.1.8) and (2.1.9) which are repeated here for convenient reference.

$$V = (r_{1m} + j\ x_{1m})\ I_m + j\ x_m'(I_m + I_{2f}') + j\ x_m'(I_m + I_{2b}') \quad ..(6.1)$$

$$0 = (\frac{r_2'}{s} + j\ x_2')\ I_{2f}' + j\ x_m'(I_m + I_{2f}') \quad .. \quad (6.2)$$

$$0 = (\frac{r_2'}{2-s} + j\ x_2')\ I_{2b}' + j\ x_m'(I_m + I_{2b}') \quad .. \quad (6.3)$$

Eliminating I_{2f}' and I_{2b}' between these two equations, we get the equation connecting V and I_m as (B.6),

$$\bar{V} = \bar{I}_m \left[r_{1m} + \frac{x_m'^2 \, (r_2'/s)}{(r_2'/s)^2 + (x_2' + x_m')^2} \right.$$

$$- \frac{j \, x_m'^2 \, (x_2' + x_m')}{(r_2'/s)^2 + (x_2' + x_m')^2} \quad \frac{x_m'^2 \, (r_2'/2-s)}{(r_2'/2-s)^2 + (x_2' + x_m')^2}$$

$$\left. - \frac{j \, x_m'^2 \, (x_2' + x_m')}{(r_2'/2-s)^2 + (x_2' + x_m')^2} + j(x_{1m} + 2 \, x_m') \right]$$

Therefore, .. (6.4)

$$\bar{V} = \bar{I}_m \, (c + j \, d) \qquad .. \quad (6.5)$$

$$I_m = \frac{V}{\sqrt{c^2 + d^2}} \qquad .. \quad (6.6)$$

where,

$$c = r_{1m} + \frac{x_m'^2 \, (r_2'/s)}{(r_2'/s)^2 + (x_2' + x_m')^2}$$

$$+ \frac{x_m'^2 \, (r_2'/2-s)}{(r_2'/2-s)^2 + (x_2' + x_m')^2} \qquad .. \quad (6.7)$$

and

$$d = x_{1m} + 2\,x_m' - \frac{x_m'^2\,(x_2' + x_m')}{(r_2'/s)^2 + (x_2' + x_m')^2}$$

$$- \frac{x_m'^2\,(x_2' + x_m')}{(r_2'/2-s)^2 + (x_2' + x_m')^2} \quad .. \quad (6.8)$$

and, $\tan \phi_m = d/c$ .. (6.9)

From equation (6.2),

$$\bar{I}_{2f}' = \frac{-j\,x_m'\,\bar{I}_m}{(r_2'/s) + j\,(x_2' + x_m')}$$

$$= \frac{\bar{V}\,x_m'}{-\left[(d r_2'/s) + c(x_2' + x_m')\right] + j\left[(r_2' c/s) - d(x_2' + x_m')\right]}$$

.. (6.10)

$$I_{2f}' = \frac{V\,x_m'}{\sqrt{\left[(d r_2'/s) + c(x_2' + x_m')\right]^2 + \left[(r_2' c/s) - d(x_2' + x_m')\right]^2}}$$

.. (6.11)

Also from equation (6.3),

$$\bar{I}_{2b}' = \frac{-j\,x_m'\,\bar{I}_m}{(r_2'/2-s) + j\,(x_2' + x_m')}$$

$$= \frac{\bar{V}\,x_m'}{-[(dr_2'/2-s) + e(x_2' + x_m')] + j\,[(er_2'/2-s) - d(x_2' + x_m')]} \quad .. \quad (6.12)$$

$$I_{2b}' = \frac{V\,x_m'}{\sqrt{[(dr_2'/2-s) + e(x_2' + x_m')]^2 + [(er_2'/2-s) - d(x_2' + x_m')]^2}} \quad .. \quad (6.13)$$

The torque in synchronous watts is, then,

$$= I_{2f}'^2\,(r_2'/s) - I_{2b}'^2\,(r_2'/2-s) \quad .. \quad (6.14)$$

The torque in lb.ft.,

$$= \frac{7.04}{\text{s.r.p.m.}} \left[I_{2f}'^2\,(r_2'/s) - I_{2b}'^2\,(r_2'/2-s) \right] \quad (6.15)$$

The gross mechanical power in horse-power,

$$= \frac{(1-s)}{746} \left[I_{2f}'^2 (r_2'/s) - I_{2b}'^2 (r_2'/2-s) \right] \quad \text{h.p.} \quad ..(6.16)$$

Thus the complete performance of the machine at any particular slip can be calculated by the double revolving field analysis.

In all practical calculations, the impedance of the 'backward revolving rotor' , Z_b remains practically constant for slips of normal operating range. Hence Z_b can be calculated for normal slip and this can be kept constant throughout further calculations.

Equation (6.4) can be re-written in the form

$$\frac{\bar{I}_m}{\bar{V}} = \frac{C + D s (2 - s)}{E + F s (2 - s)} \quad .. (6.17)$$

and this can be shown to be the equation of a circle. Even though it is possible to calculate the co-ordinates of the centre point and the radius, it is simpler to determine three points on the circle from equations (6.4) and (6.9). The three characteristic points, s = 0, s = 1,

and $s = \infty$, are chosen for this purpose (B.4).

b) Apparent-Impedance Method: In calculating the performance of the single-phase induction motor, the calculation of the apparent impedances Z_f and Z_b involves considerable labour and the use of complex quantities. W.J. Morrill (41.06) has developed charts to find out these apparent impedances.

Referring to Fig. (2.1.3), the apparent resistances and reactances are ,

$$R_f = \frac{x_m'^2 \, (r_2'/s)}{(r_2'/s)^2 + (x_2' + x_m')^2} \quad .. \quad (6.18)$$

$$X_f = \frac{x_m' \left[(r_2'/s)^2 + x_2' \, (x_2' + x_m')\right]}{(r_2'/s)^2 + (x_2' + x_m')^2} \quad .. \quad (6.19)$$

$$R_b = \frac{x_m'^2 \, (r_2'/2-s)}{(r_2'/2-s)^2 + (x_2' + x_m')^2} \quad .. \quad (6.20)$$

$$X_b = \frac{x_m' \left[(r_2'/2-s)^2 + x_2'(x_2' + x_m')\right]}{(r_2'/2-s)^2 + (x_2' + x_m')^2} \quad .. \quad (6.21)$$

Both sides of the above four equations are divided by x_m' and both th numerator and denominator of each of the right hand members are divided by $x_m'^2$. The resulting equations are:

$$\frac{R_f}{x_m'} = \frac{\dfrac{r_2'}{x_m' s}}{\left[\dfrac{r_2'}{x_m' s}\right]^2 + \left[\dfrac{x_2'}{x_m'} + 1\right]^2} \quad .. \quad (6.22)$$

= per unit forward field apparent resistance.

$$\frac{X_f}{x_m'} = \frac{\left[\dfrac{r_2'}{x_m' s}\right]^2 + \dfrac{x_2'}{x_m'}\left[\dfrac{x_2'}{x_m'} + 1\right]}{\left[\dfrac{r_2'}{x_m' s}\right]^2 + \left[\dfrac{x_2'}{x_m'} + 1\right]^2} \quad .. \quad (6.23)$$

= per unit forward field apparent reactance.

$$\frac{R_b}{x_m'} = \frac{\dfrac{r_2'}{x_m'(2-s)}}{\left[\dfrac{r_2'}{x_m'(2-s)}\right]^2 + \left[\dfrac{x_2'}{x_m'}+1\right]^2} \quad .. \quad (6.24)$$

= per unit backward field apparent resistance.

$$\frac{X_b}{x_m'} = \frac{\left[\dfrac{r_2'}{x_m'\ (2-s)}\right]^2 + \dfrac{x_2'}{x_m'}\left[\dfrac{x_2'}{x_m'}+1\right]}{\left[\dfrac{r_2'}{x_m'\ (2-s)}\right]^2 + \left[\dfrac{x_2'}{x_m'}+1\right]^2} \quad .. \quad (6.25)$$

per unit backward field apparent reactance.

In equations (6.22) to (6.25) the independent variables are defined as follows:

$\dfrac{r_2'}{x_m's}$ = per unit secondary resistance at slip 's' .

$\dfrac{r_2'}{x_m'(2-s)}$ = per unit secondary resistance at slip (2-s).

$\dfrac{x_2'}{x_m'}$ = per unit secondary reactance.

There are now two independent variables in the right hand members of equation (6.22) to (6.25). It is then possible to plot each of the equations (6.22) to (6.25) in the form of a family. This has been done by Morrill and the curves are shown in Figs. (6.1) and (6.2). These curves show per unit apparent resistance and per unit apparent reactance plotted for definite values of per unit secondary reactance and as a function of the reciprocal of the per unit secondary resistance for slips of 's' or (2-s).

In order to make use of the charts and to obtain an actual value of apparent resistance or reactance, first (x_2'/x_m') is determined. If this value is not exactly the same as that of a curve, it is necessary to interpolate between two adjacent curves. Then the corresponding value of of per unit apparent resistance or reactance is read as the ordinate corresponding to the proper value of $(x_m's/r_2')$ or $x_m'(2-s)/r_2'$. The actual apparent resistance or reactance is obtained as the product of the per unit apparent resistance or reactance by x_m' . Further calculations to determine the performance at any particular slip are carried out as shown in "Performance Calculation Sheet - I".

c) Cross-Field Theory: At the end of the analysis of the single-phase induction motor operation by the cross-field

theory, we arrived at equations (2.2.7), (2.2.11) and (2.2.16). They are,

$$V = I_m Z_{1m} + j x_m (I_m - I_y) \quad .. \quad (6.26)$$

$$I_x{''} Z_2 = S x_m (I_m - I_y) - j x_m I_x' - S I_y x_2 \quad .. \quad (6.27)$$

and

$$I_y Z_2 = j x_m (I_m - I_y) + S I_x' (x_m + x_2) \quad .. \quad (6.28)$$

Simultaneous solution of these equations gives (26.01),

$$I_m = - V \frac{\left[-r_2^2 + (1 - S^2)(x_m + x_2)^2 - j\, 2r_2 (x_m + x_2)\right]}{U + j W} \quad .. \quad (6.29)$$

$$I_y = - V x_m \frac{(1 - S^2)(x_m + x_2) - j r_2}{U + j W} \quad .. \quad (6.30)$$

$$I_x' = V \cdot \frac{S x_m r_2}{U + j W} \quad .. \quad (6.31)$$

where,

$$U = - r_{1m} r_2^2 + 2r_2 x_{1m} (x_m + x_2) + r_2 x_m (x_m + 2x_2)$$
$$+ (1 - S^2) r_{1m} (x_m + x_2)^2 \quad .. \quad (6.32)$$

$$W = - r_2^2\, x_{1m} - 2\, r_{1m}\, r_2\, (x_m + x_2) - r_2^2\, x_m$$

$$+ (1 - S^2)\left[x_{1m}\,(x_m + x_2)^2 + x_2\, x_m (x_m + x_2)\right] \quad .. \quad (6.33)$$

If the primary leakage flux is ϕ_1 and the secon-

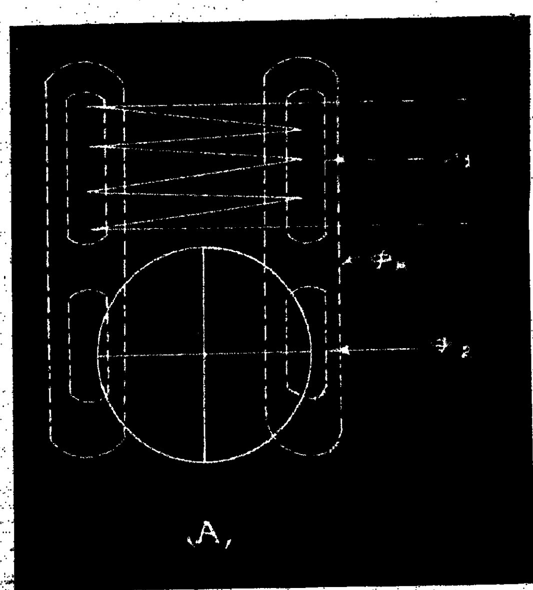


Figure (6.3)

dary leakage flux is ϕ_2 Fig. (6.3) , then,

$$\phi_M = \frac{x_m\,(I_m - I_y)}{2\pi f\; N} \quad .. \quad (6.34)$$

$$\phi_e = \frac{(x_m + x_2)\, I_x'}{2\pi f\; N} \quad .. \quad (6.35)$$

$$\phi_1 = \frac{x_{1m} \; I_m}{2\pi f \; N} \qquad .. \qquad .. \qquad (6.36)$$

$$\phi_2 = \frac{x_2 \; I_y}{2\pi f N} \qquad .. \qquad ... \qquad (6.37)$$

Substituting for I_m , I_y , and I_x' from equations (6.29), (6.30) and (6.31) in equations (6.34), (6.35) and (6.37), we get,

$$\phi_M - \phi_2 = \frac{V \, x_m \left[r_2^2 + j \, r_2 \, (x_m + x_2) \right]}{2\pi f \; N \; (U + j \; W)} \qquad .. \qquad (6.38)$$

and

$$\phi_e = \frac{S \; V \; x_m \; (x_m + x_2) \; r_2}{2\pi f \; N \; (U + j \; W)} \qquad .. \qquad (6.39)$$

The torque developed by the motor consists of two components, one component T_1 due to the interaction of the current I_y and the flux ϕ_e , and another component T_2 due to the interaction of I_x' and the transformer flux, $(\phi_M - \phi_2)$. These torque components in synchronous watts are equal to the products of the in-phase components of the currents and the fluxes with which they interact multiplied by $2\pi f N$; i.e., from equations (6.30) and (6.38),

$$T_1 \quad = \quad \frac{V^2 \; x_m^2 \; (x_m + x_2)^2 \; r_2 \; S \; (1 - S^2)}{U^2 + W^2} \qquad .. \qquad (6.40)$$

and from equations (6.31) and (6.39),

$$T_2 \quad = \quad \frac{- \; V^2 \; x_m^2 \; r_2^2 \; S}{U^2 + W^2}, \qquad .. \qquad (6.41)$$

and the total torque developed by the motor is

$$T \quad = \quad T_1 + T_2$$

$$= \quad \frac{V^2 \; x_m^2 \; r_2 \; S \; \left[(1 - S^2) \; (x_m + x_2)^2 - r_2^2 \right]}{U^2 + W^2} \; ..(6.42)$$

Power output is then calculated by multiplying torque by S.

So far we have not taken into account the core loss. One simple way of accounting this is to add the entire core loss to the stator input, adding an appropriate in-phase component of current. This is suitable for conditions of heavy load on the motor.

The magnetising reactance x_m in each axis

can be replaced by an impedance containing a resistance in which a copper loss occurs. Correct calculation of this resistance will result in a copper loss equivalent to half the core-loss (B.2), the basic idea being that approximately half the core loss occurs in each axis.

Veinott (32.01) takes into account the core loss in the following manner: The cross-field loss is considered to be half of the total iron loss and is subtracted from the power developed by the rotor. The main field iron loss is assumed to be supplied directly from the stator circuit. This method does not interfere with the equations already derived. Considering the core loss thus and based on the equations for torque and mechanical power developed already derived [Equation (6.42)], Veinott has prepared a chart to calculate the performance of single-phase induction motors. This chart is utilised to calculate the performance of the presently designed motor and is shown in "Performance Calculation Sheet - XI". In these calculations, speed being an independent variable, to start with the speed at maximum torque is taken from the graph connecting pull-out speed and (r_2/X_{1m}), which is shown in Figure (6.4). Once the output for a particular speed is calculated, the output

is assumed to be proportional to $s^2\ (1 - s^2)$ and the full-load speed is calculated.

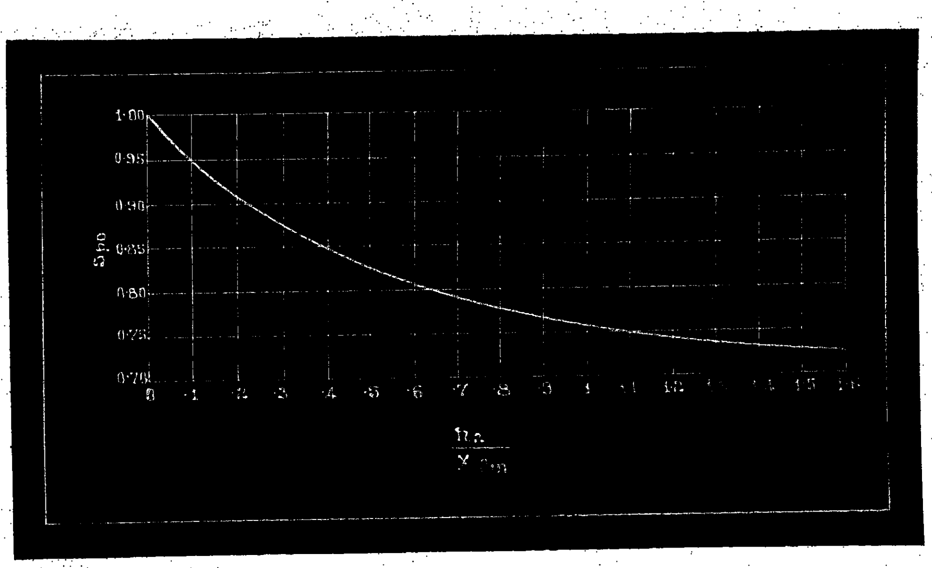


Figure (6.4).

6.2 ACTUAL CALCULATIONS:

a) Double Revolving Field Theory: Total core loss from design data is 70.3 watts. Friction and windage losses have been assumed as 11.2 watts.

Assuming 90 per cent of the applied voltage across the "forward rotor", the core loss current,

$$= \frac{70.3}{0.9 \times 220} = 0.354 \text{ amperes.}$$

Shunt resistance, r_0 to account for core loss is,

$$= \frac{198}{0.354} = 560 \text{ ohms.}$$

The performance of the motor at 5 per cent slip is calculated as follows:

1. conductance of core loss branch $= 1/r_c = 1/560$

$$= 0.001785 \text{ mho.}$$

2. Susceptance of the magnetising branch $= -j/x_m'$

$$= -j/89.5 = -j\ 0.0112 \text{ mho.}$$

3. Admittance of branch 3, [Fig. (2.1.5)(a)]

$$= \frac{(r_2'/s) - j\ x_2'}{(r_2'/s)^2 + x_2'^2} = \frac{91.8 - j\ 4.078}{8420 + 16.6}$$

$$= 0.0109 - j\ 0.000483$$

4. Admittance of "Forward Revolving Rotor" = sum of items 1, 2, and 3 $= Y_f = 0.01269 - j\ 0.01168$

5. Impedance of "Forward Revolving Rotor" =

$$Z_f = 42.7 + j\ 39.3 \text{ or } 58 \text{ ohms.}$$

6. Admittance of branch 5 [Fig. (2.1.5) (a)]

$$= \frac{(r_2'/2\text{-}s) - j\,x_2'}{(r_2'/2\text{-}s)^2 + x_2'^2} = \frac{1.395 - j\,4.075}{1.95 + 16.6}$$

$$= 0.0753 - j\,0.22$$

7. Admittance of "backward Revolving rotor" = sum of items 1, 2 and 6 = Y_b = 0.07548 - j 0.2312

8. Impedance of 'backward revolving rotor" =

Z_b = 1.285 + j 3.94 or 4.15 ohms.

9. Impedance of entire motor = $Z = Z_{1m} + Z_f + Z_b$

= 48.04 + j 51.39 or 70.4 ohms.

10. Primary current, $I_m = \frac{220}{70.4}$ = 3.13 amperes.

11. Power factor = $\frac{48.04}{70.4}$ = 0.683

12. Voltage across "forward revolving rotor" =

e_f = Item (10) x Item (5) = 182 volts.

13. Core loss current in the "forward revolving rotor"

$$= \frac{182}{560} = 0.324 \text{ ampere.}$$

14. Rotor current $I_{2f}' = \frac{182}{\sqrt{8,437}} = 1.94$ amperes.

15. Core loss in the "forward revolving rotor"

$$= (\text{Item } 13)^2 \times r_c = 0.324^2 \times 560 = 58.8 \text{ Watts.}$$

16. Copper loss in the "forward revolving rotor"

$$= I_{2f}'^2 \, r_2' = 1.94^2 \times 2.75 = 10.8 \text{ watts.}$$

17. Forward developed torque:

$$= I_{2f}'^2 \, (r_2'/s) = 1.94^2 \times 91.8$$

$$= 361 \text{ synchronous watts.}$$

18. Voltage across the "backward revolving rotor" =

$$e_b = (\text{Item } 10) \times (\text{Item } 8) = 13 \text{ volts.}$$

19. Core loss current in the "backward revolving rotor"

$$= \frac{13}{560} = 0.0232 \text{ ampere.}$$

20. Rotor current $I_{2b}' = \frac{13}{\sqrt{18.55}} = 3.02$ amperes.

21. Core loss in the "backward revolving rotor"

$= (\text{Item } 19)^2 \times r_c = 0.0232^2 \times 560 = 0.32$ Watt.

22. Total core loss = (Item 15) + (Item 21) or

59.12 watts, versus 70.3 watts, which has

been used in fixing r_c.

23. Copper loss in the "backward revolving rotor"

$= (\text{Item } 20)^2 \times r_2' = 3.02^2 \times 2.75 = 25$ watts.

24. Backward developed torque

$= I_{2b}'^2 (r_2'/2-s) = 3.02^2 \times 1.395$

$= 12.7$ synchronous watts.

25. Torque developed = (Item 17) - (Item 24)

$= 361 - 12.7 = 348.3$ synchronous watts.

26. Power developed = Torque developed x (1 - s)

$= 348.3 \times 0.97 = 337$ watts.

27. Nett watts output = (Item 26) - F and W

$= 337 - 11.2 = 326$ watts.

28. Shaft torque $= \dfrac{112.6 \times (\text{Item 27})}{(1-s)\ \text{s.r.p.m.}}$

$= \dfrac{112.6 \times 326}{0.97 \times 1{,}500} = 25.2$ oz. ft.

29. Efficiency $= \dfrac{\text{output}}{\text{input}} = \dfrac{326}{220 \times 3.13 \times 0.683}$

$= 0.693$

30. Losses from (input - output) = 470 - 326

= 144 Watts.

31. Sum of individual losses, as a check:

$I_m^2\ r_{1m} = 3.13^2 \times 4.05$	=	39.7
Rotor copper (Item 16)	=	10.8
Rotor copper (Item 23)	=	25.0
Core loss (Item 22)	=	59.12
F and W	=	11.2
		145.82 watts

versus 144 watts from (input - output) method.

Similar calculations have been made for various values of slip and the results are shown in Table I .

TABLE I.

No.	Percentage slip	Current Amp.	Power factor	Input Watts	Output Watts	Torque oz. ft.	Efficiency.
1	1.5	2.52	0.519	288	172	13.1	61.8 %
2	2.0	2.71	0.588	350	223	17.1	63.5
3	3.0	3.13	0.683	470	326	25.2	69.3
4	4.5	3.83	0.751	633	449	35.3	70.9
5	6.0	4.54	0.761	760	546	43.6	71.8
6	14.0	7.49	0.756	1250	706	61.5	56.5

The different characteristics corresponding to these values are shown in Fig. (6.5).

Calculations for drawing the circle diagram:

$s = 0$ or 2.

Substituting $s = 0$ or 2 in equation (6.4), we get

$$\bar{V} = \bar{I}_m \left[r_{1m} + \frac{x_m'^2 \, (r_2'/2)}{(r_2'/2)^2 + (x_2' + x_m')^2} \right.$$

$$\left. - \frac{j x_m'^2 \, (x_2' + x_m')}{(r_2'/2)^2 + (x_2' + x_m')^2} + j \, (x_{1m} + 2 \, x_m') \right]$$

$$= \bar{I}_m \left[4.05 + \frac{89.5^2 \, (2.75/2)}{(2.75/2)^2 + (4.075 + 89.5)^2} \right.$$

$$\left. - \frac{j (89.5)^2 \, (4.075 + 89.5)}{(2.75/2)^2 + (4.075 + 89.5)^2} + j \, (8.15 + 179) \right]$$

$$= \bar{I}_m \; (5.3 + j \, 178.5)$$

$$I_m = \frac{220}{\sqrt{5.3^2 + 178.5^2}} = 1.25 \text{ amperes.}$$

$$\tan \phi = 33.5$$

$$\phi = 88^\circ \; 18'$$

$$\cos \phi = 0.0297$$

These conditions are represented by the point P_o' in Fig. (6.6) .

s = 1

Substitution of s = 1 in equation (6.4) yields

$$\bar{V} = \bar{I}_m \left[r_{1m} + \frac{2x_m'^2 \, r_2'}{r_2'^2 + (x_2' + x_m')^2} - j \frac{2 \, x_m'^2 \, (x_2' + x_m')}{r_2'^2 + (x_2' + x_m')^2} + j \, (x_{1m} + 2 \, x_m') \right]$$

$$= \bar{I}_m \left[4.05 + \frac{2 \times 89.5^2 \times 2.75}{2.75^2 + (4.075 + 89.5)^2} - j \frac{2 \times 89.5^2 \times (4.075 + 89.5)}{2.75^2 + (4.075 + 89.5)^2} + j \, (8.15 + 179) \right]$$

$$= \bar{I}_m \; (9.05 + j \, 16.5)$$

$$I_m = \frac{220}{\sqrt{9.05^2 + 16.5^2}} \approx 11.7 \text{ amperes.}$$

$$\tan \phi = 1.82$$

$\phi = 61^0 \ 13'$

$\text{Cos}\ \phi = 0.4815$

These conditions are represented by a point P_L in Fig. (6.6).

$\underline{s = \infty}$

When's' is made equal to infinity, equation (6.4) reduces to:

$$\bar{V} = \bar{I}_m \left[r_{1m} - \frac{j\ 2\ x_m'^2}{(x_2' + x_m')} + j\ (x_{1m} + 2\ x_m') \right]$$

$$= \bar{I}_m \left[4.05 - j\ \frac{2\ (89.5)^2}{(4.075 + 89.05)} + j\ (8.15 + 179) \right]$$

$$= \bar{I}_m \quad (4.05 + j\ 16)$$

$$I_m = \frac{220}{\sqrt{4.05^2 + 16^2}} = 13.32 \text{ amperes.}$$

$\tan\ \phi = 3.94$

$\phi = 75^0 \ 46'$

$\text{Cos}\ \phi = 0.2459$

The point P_∞ in Fig. (6.6) represents these conditions.

The circle passing through these points three points is drawn. The no-load point P_o is calculated as follows:

The no-load current is taken to be approximately equal to the stator current at zero slip (B.4).

i.e., $I_o \simeq 1.25$ amperes.

The total copper losses at no-load are approximately equal to $1.5\ I_o^2\ r_{1m}$.

No-load copper losses = $1.5 \times 1.25^2 \times 4.05$

= 9.5 watts.

Core loss from design data = 70.3 watts.

Assumed windage and frictional losses = 11.2 watts.

Total no-load losses .. 91.0 watts.

The point P_o is chosen on the circle such that the input is 91.0 watts. The line through P_o parallel to the line joining P_o' and P_L is the output line. The vertical distance from any point on the circle to this line represents

the power delivered. From the circle diagram the performance of the machine is calculated and the results are shown in Table II.

TABLE II.

No.	Current Amps.	Input Watts	Output Watts.	Percentage Output.	Power Factor.	Efficiency percentage
1	2.5	440	300	107	0.80	68.2
2	2.75	495	352	126	0.82	71.0
3	3.0	550	385	137	0.83	70.0
4	3.75	691	484	173	0.84	70.0
5	4.5	836	576	206	0.84	68.9
6	6.8	1190	686	245	0.79	57.7

The different characteristics corresponding to these values are shown in Fig. (6.7) .

b) Apparent-Impedance Method: The equivalent circuit taken into consideration in the above calculations is that

of Fig. (2.1.5)(a). The apparent-impedance method of calculating the single-phase induction motor performance characteristics is based on the equivalent circuit shown in Fig. (2.1.4) . The calculations are shown in "Performance Calculation Sheet - I" and the corresponding characteristics are shown in Fig. (6.8).

c) Cross-Field Theory: The calculations based on the cross-field theory are shown in " Performance Calculation sheet - II" and the corresponding characteristics are shown in Fig. (6.9).

C H A P T E R - VII.

TESTS AND TEST RESULTS.

7.1 Test Procedures:

7.1.1 Determination of Machine Constants: The stator main winding resistance, 'r_{1m}' is determined by the drop-of-potential method. If r_t is the value of the resistance measured at temperature t, then at any other temperature T, the resistance will be (41.05),

$$R_T = \frac{234.5 + T}{234.5 + t} \; r_t$$

Other constants to be determined are X_0, X, and r_2. These can be determined from a reading of watts and amperes at full voltage with the rotor locked and a reading of no-load amperes. The circuit connections for the measurement of power and amperes under locked-rotor conditions (or at any other load) is shown in Fig. (7.1) (41.05). Let E_L, I_L and W_L be

the line voltage, line current and power input respectively. Veinott (35.02) quotes from an unpublished work of Trickey the following expression for locked-rotor current:

$$I_L = \frac{E_L}{(r_{1m} + P) + j\,Q} \qquad .. \qquad (7.1)$$

where,

$$P = \frac{r_2\, X_r}{1 + (r_2/X_0)^2} \qquad \frac{r_2\,(X_0 - X)}{X_0\left[1 + (r_2/X_0)\right]^2} \qquad .. \qquad (7.2)$$

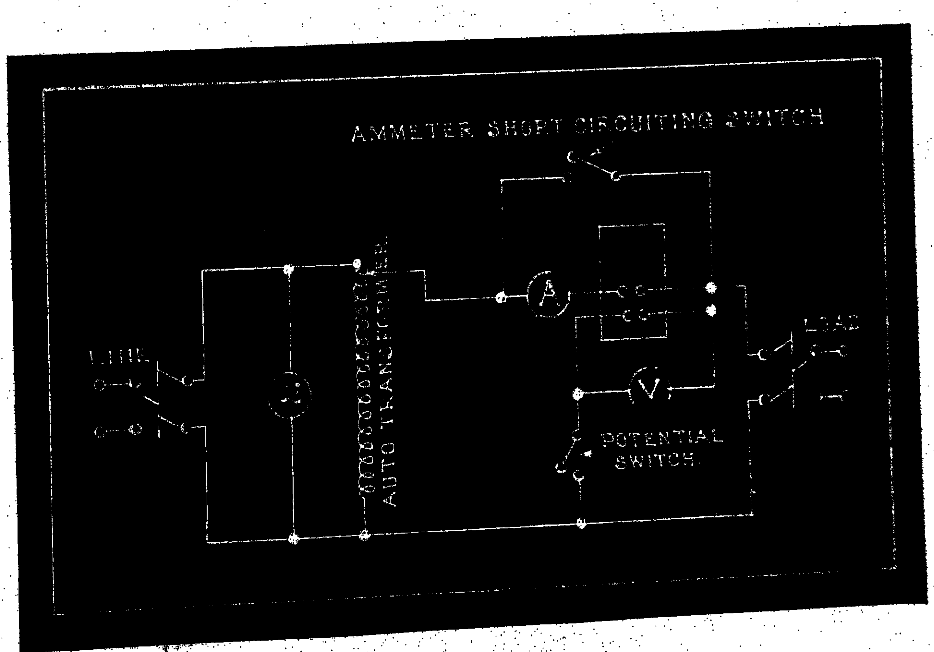


Figure (7.1)

$$Q = \frac{X \left[1 + \frac{r_2}{X} \cdot \frac{r_2}{X_0} \right]}{1 + (r_2 / X_0)^2} \quad .. \quad (7.3)$$

In terms of test results, P and Q are as follows:

$$P = \frac{W_L}{I_L^2} - r_{1m} \quad .. \quad (7.4)$$

$$Q = \sqrt{\left[\frac{E_L}{I_L}\right]^2 - \left[\frac{W_L}{I_L^2}\right]^2} \quad .. \quad (7.5)$$

From the equivalent circuit based on the double-revolving field theory, the no-load current, I_e is obtained as,

$$I_e = \frac{2 E_L}{X_0 + X} \quad .. \quad (7.6)$$

by putting $s = 0$.

Simultaneous solution of equations (7.2), (7.3) and (7.6) yields,

$$X = \frac{E_L}{I_o} - \sqrt{\left[\frac{E_L}{I_o} - Q\right]^2 + P^2} \quad .. \quad (7.7)$$

$$X_o = \frac{2\, E_L}{I_o} - X \quad .. \quad (7.8)$$

$$r_2 = \frac{P\, X_o}{X_o - Q} \quad .. \quad (7.9)$$

In equation (7.4) the value of r_{1H} is that measured immediately after the locked-rotor test. The value of r_2 calculated from equation (7.9) corresponds to conditions existing immediately after the locked-rotor test.

The flux factor K_p is calculated from the equation,

$$K_F = \frac{X_o - X}{X_o} \quad .. \quad (7.10)$$

and $K_p = \sqrt{K_F}$ .. (7.11)

7.1.2 Determination of Locked-Rotor and Breakdown Torques:

Locked-Rotor Torque: Rated voltage is applied at

rated frequency (41.05). A cord is wrapped around the pulley a number of times so that the pulley barely rotates (approximately 8 to 10 rpm.). Because of the variations in torque, the scale readings swing between a maximum and minimum value, and the minimum value of torque for one revolution of the rotor is read out.

Breakdown Torque: This is determined by allowing the motor to run light, then increasing the torque until the speed of the motor falls off abruptly.

7.1.3 Load Test: The purpose of the load test is to determine the variation of the power factor, efficiency, watts, amperes, and speed with changes in load. Starting as near breakdown torque as possible, the load is held constant at one value of torque, and the watts input, amperes, voltage, slip by stroboscopic means, and torque are readx. These readings are repeated for different settings of torque down to no load. The horsepower output is computed from the known values of torque and speed.

7.1.4 No-Load Saturation Test: The motor is run at no load with normal frequency and voltage applied until the watts input are constant. Readings are taken of volts, amperes, and watts input at rated frequencies and voltage

ranging from 125 percent voltage down to the point where further voltage reduction increases the current. The voltage adjustment is done by an auto-transformer. Immediately following this test, before temperature can change sensibly, a reading of the input watts, W_L and input amperes, I_L, at 50 to 60 percent of rated voltage is taken with the rotor locked and with only the main winding excited. This test is followed by an immediate measurement of stator resistance, R_1.

If the input current, at any voltage, is I_s, the total copper loss in the machine, at the same voltage, is (41.05)

$$\frac{I_s^2}{2} \left[R_1 + \frac{W_L}{I_L^2} \right] \quad . \quad .. \quad (7.12)$$

The copper losses so figured are subtracted from the total input at the same voltage; the resultant values are then plotted against the input voltage and the curve extrapolated to zero voltage, where the intercept represents friction and windage.

7.1.5 Temperature Run: Holding the horsepower output at the rated full-load value, the motor is run at rated

and (7.9), other constants, X, X_0 and r_2 are calculated and the results are :

$X = 10.1$ ohms.

$X_0 = 227.9$ ohms.

and $r_2 = 8.85$ ohms at 65° C .

7.2.2 Locked-rotor and Breakdown Torques:

$$\text{Locked-rotor torque} = \frac{(23.5 - 2.75) \times 3.02 \times 16}{12}$$

$= 83.5$ oz. ft.

$= 387$ percent full-load torque.

$$\text{Breakdown torque} = \frac{(14 - 2.9) \times 3.02 \times 16}{12}$$

$= 44.7$ oz. ft.

7.2.3 Load Test: Starting from about 25 percent full load and loading upto 175 percent full load, 43 sets of readings were taken and calculated. The resulting characteristics were plotted to a large scale and the mean curves

were drawn. Points close to, or on the mean curves are chosen and are tabulated as shown in Table III. These points are plotted on the predetermined characteristics (with black ink) so that the deviation of the actual performance from the predetermined performance can be easily observed.

7.2.4 No-load Saturation Test.

TABLE IV.

No.	Volts.	Amps.	Watts input.	Copper loss.
1	275	2.6	130	55.5
2	250	2.25	105	41.5
3	220	1.85	80	28.0
4	200	1.725	70	24.3
5	180	1.40	60	16.0
6	160	1.30	50	13.75
7	140	1.10	45	9.85
8	120	1.00	40	8.15
9	100	0.80	35	5.21
10	80	0.70	30	4.00
11	70	0.75	30	4.58
12	60	0.80	30	5.21

Locked-rotor test immediately following the no-load saturation test:

Volts = 120 , Amps. = 5.55, Watts = 360 ,

Resistance of stator main winding immediately after locked-rotor test:

$$= \frac{11.3}{2.45} = 4.61 \text{ ohms.}$$

The copper loss in Table IV is calculated by using the expression (7.12). The values of Table IV are plotted against voltage as shown in Fig. (7.2) and from this graph,

Core loss at normal voltage = 34.5 Watts.

Windage and Friction losses = 19.0 watts.

7.2.5 Temperature Run: The motor attained steady temperature after running at full load for 6 hours and 30 minutes continuously. The final temperature as measured by thermometer was 53.5° C., and by resistance measurement, was 57.5° C . The ambient temperature at the time of the test was 30° C .

A P P E N D I X - I.

TORQUES *

A 1. 1 Basis of Rating Single-Phase Motors:

The horsepower rating of a fractional-(and integral-) horsepower motor is based upon the breakdown torque. The value of breakdown torque to be expected by the user for any horsepower and speed shall fall within the range given in Table V.

The temperature of the motor at the start of the test for breakdown torque shall be approximately 25° C.

The minimum value of breakdown torque obtained in the manufacture of any design will determine the rating of that design. Tolerances in manufacturing will result in individual motors having breakdown torques from 100 percent to approximately 150 percent (125 percent for motors rated in millihorsepower) of the value on which the rating is based, but this excess torque shall not be relied upon by the user in applying the motor to its load. Breakdown torque range includes the higher figure, down to, but not including the lower figure.

---

* Reference: (56.01).

T A B L E - V.

50	50 - 25	50	Standard Frequencies Cycles.
3,000	1,500	1,000	Standard Synchronous Speeds, r.p.m.
2,850	1,425	950	Fractional-horse-power, Standard nominal speeds, r.p.m.
Breakdown Torque in oz. ft.			Brake h.p.rating.
2.4 - 4.4	4.8 - 8.5	7.2 - 12.4	1/20
4.4 - 7.2	8.5 - 13.8	12.4 - 19.8	1/12
7.2 -10.5	13.8 - 19.8	19.8 - 28.9	1/8
10.5 -13.8	19.8 - 25.8	28.9 - 37.8	1/6
13.8 -19.8	25.8 - 37.8	37.8 - 53	1/4
19.8 -25.8	37.8 - 48.5	53 - 69.5	1/3
25.8 -37.8	48.5 - 69.5	69.5 - 99	1/2
37.8 -53	69.5 - 99	...	3/4
53 -69.5	99 -131.2	...	1

Note: Figures pertaining to 60 cycles standard frequency and, subfractional- and integral-horsepower ranges are omitted.

A 1. 2 Locked-Rotor torque:

The locked-rotor torque of single-phase general-purpose fractional- (and integral-) horsepower motors, with rated voltage and frequency applied, shall be not less than that shown in Table VI.

T A B L E - VI.

h.p.	Minimum Locked-Rotor Torque.			
	3,000	1,500	1,000	50 cycles speed r.p.m.
1/8	..	29	39	
1/6	18	39	51	
1/4	25	55	70	Torque
1/3	31	69	88	in
1/2	44	102	120	oz.ft.
3/4	60	143	..	
1	73	..	..	

A 1. 3 Rating of the Motor Constructed:

Referring to Table V, the nominal speed of the motor, designed and constructed by the author, is 1425 rpm. The breakdown torque of the motor has been determined by test as 44.7 oz.ft. Referring again to Table V, this falls within the breakdown torque range for 1/3 h.p., rating and hence the nominal rating of the motor as 1/3 h.p. As per Table VI, a motor rated at 1/3 h.p., must have a locked-rotor torque equal to or greater than 69 oz.ft. but less than 102 oz.ft. The locked-rotor torque of the motor has been found from test as 83.6 oz.ft., which is within this limit. The locked-rotor current with both the main and the auxiliary windings connected to supply, is 12.7 amperes, which is less than 15.8 ampères as required by ASA - C.50.2 - 1955 .

APPENDIX - II.

DISCUSSION AND CONCLUSION.

The actual characteristics of the machine are markedly different from those predetermined from design data. This may be due to the fact that the machine constants, as determined from tests, are different from those calculated. The following discrepancies have been noted:

i) Increased stator and rotor resistances.

ii) Decreased leakage reactance, increased open-circuit reactance and decreased core loss.

iii) Increased maximum torque.

iv) Decreased efficiency.

v) Discrepancy in the values of current.

vi) Decreased temperature rise.

The following explanations are offered to explain the discrepancies:

i) The stator main winding resistance and the

rotor resistance are higher than calculated values. The length of the half-mean-turn of the stator main winding had to be higher than the calculated value to facilitate easy winding and this accounts for the high stator main winding resistance. Similarly, the rotor bars also had to be longer to facilitate easy bracing of the end rings to the bars and the bracing of the end rings to the rotor bars might not have been perfect which account for the higher rotor resistance.

ii) The fact that the leakage reactance is lower and the open-circuit reactance is higher than the respective designed values suggest that saturation might have been lower than expected. This view is also further supported by the value of core-loss experimentally determined, which is only about half of the designed value.

iii) In a polyphase motor the maximum torque is independent of the rotor resistance, which is effective in determining the slip at which maximum torque occures. In the single-phase motors, the secondary resistance not only determines the slip for maximum torque but also determines its magnitude. The maximum torque is reduced by increasing the secondary resistanse (B.6). Also at low

values of slip, the value of Z_b is nearly x_2' , and this is in series with the forward impedance and reduces the maximum torque. The value of maximum torque of the motor, as determined from tests, is greater than the calculated value. Probably the effect of the decrease in the leakage reactance is dominant over the effect of the increase in secondary resistance.

iv) The increased value of resistances causes the efficiency to be lower than the calculated values.

v) The low saturation causes the current to be lower than the calculated values upto about full load. After that the currents are greater than the calculated values. This suggests that upto about full load the magnetising current dominates and after that the wattful component of the current dominates.

vi) The design is based on an operating temperature of 65° C. But the temperature, determined by resistance measurement, was only 57.5° C., at the end of temperature run test at full load. This may be due to efficient cooling and may be due to the fact that the frame size is quite bigger than the one used commercially.

Discrepancies numbered (ii), (iii) and (v), all suggest that the magnetic saturation is less than expected. The magnetic characteristics of the steel used for armature stampings could not be got at the time of design. A higher flux density might have been used. If the machine had to be redesigned, this factor might be taken into account. Even though the continuous rating of the machine is only 3/8 h.p., the low temperature rise suggests that the machine may take even a load of 1/2 h.p. continuously.

R E F E R E N C E S.

BOOKS.

B.1 Fractional Horse-Power Electric Motors.
Cyril G. Veinott.

B.2 Alternating-Current Machines.
A.F.Puchstein, T.C.Lloyd and A.G.Conrad.

B.3 Electrical Engineers' Hand Book - Electric Power.
Harold Pender and William A.Del Mar.

B.4 Electric Machinery - Volume II.
Michael Liwschitz - Garik.

B.5 Alternating Current Machinery.
L.V.Bewley.

B.6 The Induction Motor.
Herbert Vickers.

B.7 Principles of Alternating-Current Machinery.
R.R.Lawrence.

B.8 Symmetrical Components.
C.F.Wagner and R.D.Evans.

B.9 Radio Engineering.
Frederick Emmons Terman.

B.10 Fractional H.P. Electric Motors.
F.G.Spreadbury.

B.11 Intermediate Electricity and Magnetism.
Hutchinson.

B.12 Fractional Horse Power Motors.
Stuart F. Philpott.

B.13 Winding Alternating-Current Machines.
Michael Liwschitz-Garik.

B.14 Design of Electrical Apparatus.
John H. Kuhlmann.

B.15 Electrical Technology.
H.Cotton.

JOURNALS.

88.01 "A New System of Alternating Current Motors and Transformers" - Nikola Tesla - AIEE Trans., Vol. 5, 1887-88, p.308.

97.01 "The Alternating Current Induction Motor" , C.P.Steinmetz. AIEE Trans.,Vol.14,1897,p.186.

98.01 "Single Phase Induction Motor". C.P.Steinmetz. AIEE Trans., Vol. 15, 1898, p.35.

98.02 Disc. on "Single Phase Induction Motors". Dr.A.E.Kennelly. AIEE Trans., Vol.15, 1898,p.106.

12.01 "Single-Phase Induction Motors". W.J.Branson. AIEE Trans., Vol.31, 1912, p.1749.

24.01 "Single-Phase Motor Torque Pulsations". A.L. Kimball, Jr., and P.L.Alger. AIEE Trans., Vol. 43, 1924, p.730.

25.01 "The Single-Phase Induction Motor". L.W.Perkins. AIEE Trans., Vol. 44, 1925, p.40.

26.01 "The Cross-Field Theory of Alternating-Current Machines". H.R.West. AIEE Trans.,Vol.45, 1926, p. 1749.

29.01 "Disc.on "The Condenser-Motor", "The Fundamental Theory of the Capacitor Motor" and "The Revolving Field Theory of the Capacitor Motor". C.R. Boothby. AIEE Trans.,Vol.48, 1929, p. 639.

29.02 "Study of Noises in Electrical Apparatus". T.Spooner and J.P.Foltz. AIEE Trans.,Vol.48, 1929, p. 747.

30.01 "Quiet Induction Motors". L.E.Hilde-Brand. AIEE Trans.,Vol.49, 1930, p.850.

31.01 "Induction Motor Slot Combinations". Gabriel Kron. AIEE Trans., Vol.50, 1931, p. 757.

32.01 "Performance Calculation on Induction Motors". C.G.Veinott. AIEE Trans., Vol.51, 1932,p.743.

34.01 "Measurement of Noise from Small Motors". C.G. Veinott. AIEE Trans., Vol.53, 1934, p.1624.

35.01 "Measurement of Telephone Noise and Power Wave Shape". J.M.Barstow., P.W.Blye and H.E.Kent. AIEE Trans., Vol.54, 1935, p.1307.

35.02 "Segregation of Losses in Single-Phase Induction Motors". C.G.Veinott. AIEE Trans., Vol. 54, 1935, p. 1032.

36.01 "An Analysis of the Shaded Pole Motor". P.H. Trickey. AIEE Trans., Vol.55, 1936, p.1007.

37.01 "Characteristic Constants of Single-Phase Induction Motors" - Part I: Air-Gap Reactance". Wayne J. Morrill. AIEE Trans., Vol. 56, 1937, p. 333.

37.02 "The Cause and Elimination of Noise in Small Motors". W.R.Appleman. AIEE Trans., Vol. 56, 1937., p. 1359.

40.01 "Harmonic Theory of Noise in Induction Motors". Wayne J. Morrill. AIEE Trans., Vol. 59, 1940, p. 474.

41.01 "The Cross-Field Theory of the Capacitor Motor". A.F.Puchstein and T.C.Lloyd. AIEE Trans., Vol. 60., 1941, p. 58.

41.02 "Single-Phase Motor Theory - a Correlation of the Cross-Field and Revolving Field Concepts". C.T.Button. AIEE Trans., Vol.60., 1941, p.507.

41.03 "Disc. on "The use of Auxiliary Impedances in Single-Phase Operation of Polyphase Induction Motors", "Performance Calculation of Repulsion Motors", "Performance Calculation on Capacitor Motors - The Revolving-Field Theory", "Single-

Phase Motor Theory - a Correlation of the Cross-Field and Revolving Field Concepts", "Design Factors Involved in the Design of Domestic Motored Appliances", "Single-Phase Induction-Motor Performance Calculation" and "The Cross-Field Theory of the Capacitor Motor". Wayne, J. Morrill. AIEE Trans., Vol. 60., 1941, p. 669.

41.04 Disc. on "The Cross-Field Theory of the Capacitor Motor". E.J.Schaefer. AIEE Trans., Vol. 60., 1941, p. 667.

41.05 "Proposed Test Code for Single-Phase Motors". AIEE, No. 502, Nov. 1941.

41.06 "The Apparent-Impedance Method of Calculating Single-Phase Motor Performance". Wayne J.Morrill. AIEE Trans., Vol. 60., 1941., p. 1037.

42.01 "Magnetostriction in Electrical Sheet Steels". F.Brailsford and R. Martingal. Jour.I.E.E., Part I., 1942, p.225.

45.01 "Symmetrical Components as applied to the Single-Phase Induction Motor". F.W.Suhr. AIEE Trans., Vol. 64., 1945, p. 651.

45.02 Disc. on "Symmetrical Components as Applied to the Single-Phase Induction Motors". Edward Bretch. AIEE Trans., Vol64., 1945, p. 958.

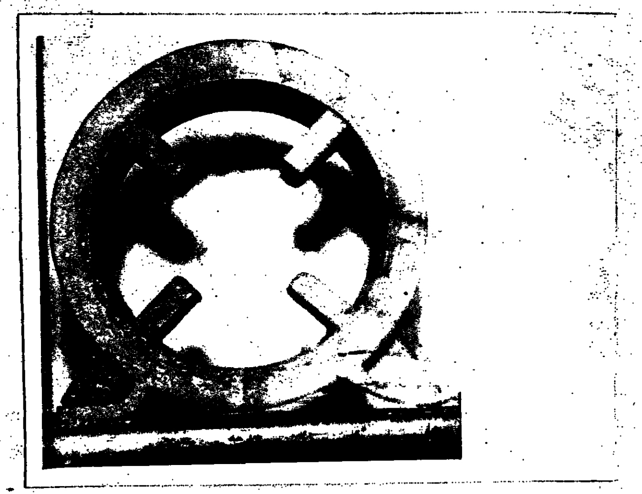
47.01 "The Equivalent circuit of the Capacitor Motor". Sheldon S.L. Chang. AIEE Trans., Vol. 66, 1947., p. 631.

49.01 "Design of Auxiliary Circuits of Single-Phase Induction Motors". M.S.Thacker and H.V.Gopalakrishna. AIEE Trans., Vol. 68, 1949, p.1373.

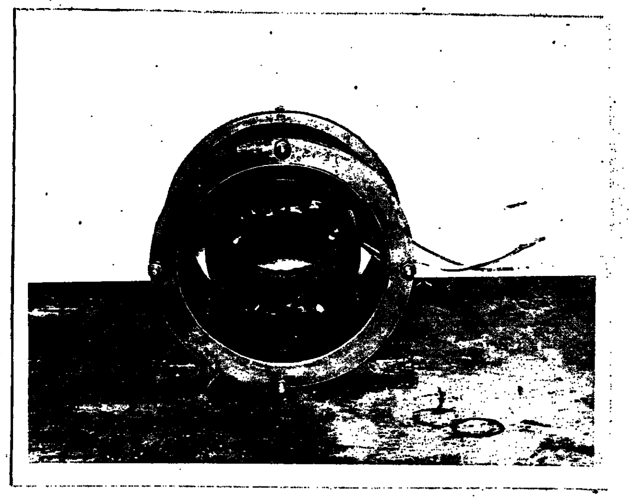
55.01 "Alternating Current Induction Motors, Induction Machines in General, and Universal Motors". ASA. C 50-2 , 1955.

58.01 "Noise in Single-Phase Induction Motors, its Measurement and Analysis". M.Maria Louis. Technology, Vol. 6, No.1., March 1958, p.59.

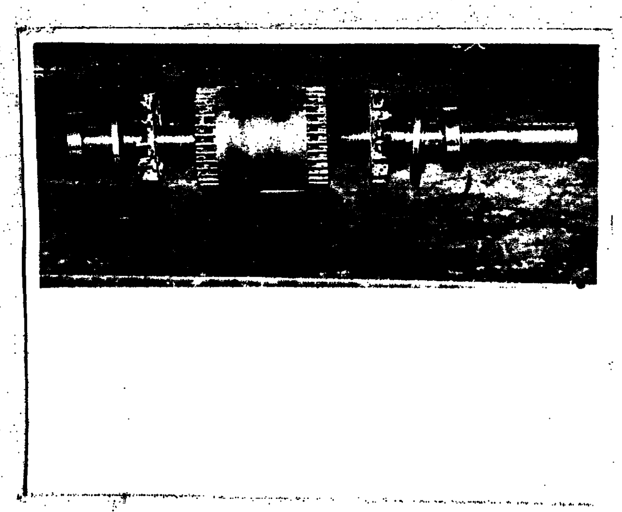
DRAWINGS



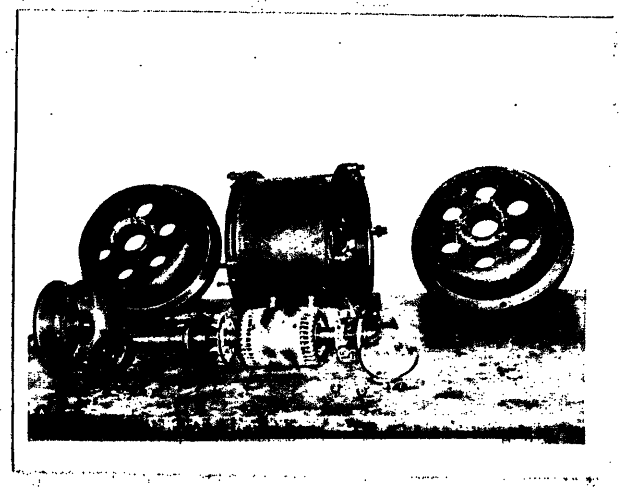
a) STATOR FRAME BEFORE MACHINING



b) FINISHED STATOR



c) ROTOR



d) COMPONENT PARTS

PLATE-II